LOW COST SOLAR POWERED

WATER PUMP

by

George Vouzas

BSc Mechanical Engineering (Athens University 1983)

Submitted to the University of Cape Town in fulfilment of the requirements for the degree of Master of Science in Engineering.

September 1985

ABSTRACT

The study describes the development of a prototype solar energy powered water pump. The system was developed in an attempt to meet the following requirements and constraints: Cheap, convenient and easy manufacture, reliability and low maintanance of the system, no auxiliary power requirements, and minimum running costs.

The literature survey indicated that a number of pumping systems have been studied in the past, with variable successes, based on numerous thermodynamic cycles. Our system operates on the combination of two constant volume and two constant pressure processes, on a working fluid which expands due to input heat from the sun, and contracts due to heat rejection to the pumped water. This expansion and contraction of the fluid is utilized to move flexible bellows, resulting in the pumping action.

The thermodynamic and heat transfer aspects of the system have been modelled and the results were compared with the experimental data. A number of working fluids were attempted and the final results show very good agreement between the theoretical and experimental results for Freon 113. Lack of detailed thermodynamic data did not allow similar comparison for Methanol. Yet, experiments on another fluid (Cyclohexane) were abandoned because the fluid was found to be incompatible with the bellows material.

The results also indicate that the pump's performance depends strongly on the utilization ratio, a parameter which we have defined as the ratio of the amount of water used for cooling, divided by the total quantity of water pumped during each cycle. It also became apparent that the choice of the working fluid influences greatly the system's performance. The results indicate that for higher boiling point working fluids, the suction depth can be increased towards the theoretically maximum of $\simeq$ 10m; however the heat input requirements are increased, which in turn will require larger collector and sophisticated tracking mechanisms.

Predictions of the pump's performance for typical summer and winter days were performed using the solar radiation data collected by the Pretoria's station (RSA). Bearing in mind that this is a non-sophisticated system, and the likely users would be "laymen", a program has been devised which with the aid of a very simple chart informs the user of simple adjustments, necessary for the pump's best performance.

In conclusion not withstanding the fact that our initial objectives have been met beyond our expectations, it is recommended that future work be undertaken along the lines indicated in chapter 5 of this thesis.

ACKNOWLEDGEMENTS

I would like to express my sincere thanks to:

Associate Professor J.Gryzagoridis, the project supervisor, for his invaluable guidance, encouragement, and friendship throughout this project.

The CSIR for their financial assistance.

Professor R.K.Dutkiewicz for suggesting the study.

Mr. L.Watkins, Mr. D.Finlayson, Mr. M.Batho, Mr. J.Mayer, and Mr. A.Warburton for their assistance in the construction of the experimental equipment.

Mr. W.Jervis and Mr. S.Venter for computational assistance.

Mr. V.Appleton for photographic assistance.

Last,but not least, all my friends for their encouragement and help.

TABLE OF CONTENTS

CHAPTER 4

CHAPTER 5

APPENDICES

LIST OF ILLUSTRATIONS

LIST OF FIGURES

LIST OF TABLES

Page

NOMENCLATURE

A: Apparent extraterrestrial solar radiation
B: Extiction coefficient
C: Concentration ratio
c_p: Specific heat
D: Number of day
f: Focus length
g: Constant for gravitational acceleration
h: Enthalpy, Heat transfer coefficient
P: Water pressure head
H_s: Solar time
I: Solar radiation
k: Thermal conductivity
L,x: Length
m: Mass
$\dot{m}$: Mass flow rate
n: Number of pipes in the cooling system, Number of adjustments per year
P: Pressure
Pr: Prantl number
Q: Heat
r: Radius
Re: Reynolds number
T: Temperature
U,u: Internal energy
V: Volume
v: Specific volume
$\dot{V}$: Volume flow rate
t: Time
W,w: Work
Y: Meters above sea level

GREEK CHARACTERS

α: Absorptivity
β: Volume coefficient of expansion, Collector's tilt
γ: Optical losses,Specific weight, Azimuth
δ: Solar declination
Δ,δ: Change of
ϵ: Emissivity
η: Efficiency
θ: Angle of incidence
θ_c: Concentrator's acceptance half angle
λ: Utilization ratio
μ: Kinematic viscosity
ν: Dynamic viscosity
ρ: Reflectivity, Density
τ: Transmisivity
φ: Latitude, Concentrator's rim angle
ω: Hour angle

SUBSCRIPTS

a: Aperture, Ambient
abs: Absorbed
add: Added
b: Bellows
c: Collector, Cover, Convection, Cycle
cool: Cooling process
cw: Cooling water
D: Direct
d: Diffuse, Disgharged water per cycle
f: Working fluid
heat: Heating process
i: Inner surface
in: Input, Inlet
l: Losses
m: Mean
n: Normal
o: Optical, Standard, Outer surface
out: Output, Outlet
p: Pipe, Pump
pl: Plate
r: Receiver, Radiation
rej: Rejected
s: Sunset
sc: Solar constant
th: Thermal
u: Useful
w: Water
z: Zenith

CHAPTER 1

INTRODUCTION

1.1. FOREWORD

The idea of using solar energy for pumping water originates as far back in history at the turn of the sixteenth century, but it was only recently that this idea started to be applied in a variety of pumping systems. With the emphasis in recent years on investigations to develop alternate energy resources, solar power has come on its own as a replacement or supplement to the more conventional energy forms. Solar power has become an atractive proposition for isolated areas where electricity is expensive, or does not exist at all, and the cost of fuel is very high due to transport. Furthermore, solar energy is an abundant resource in most of the arid regions and it is quite natural to use this resource for water pumping.

1.2. SOLAR ENERGY

1.2.1. Availability of solar energy.

Before proceeding to the description of solar powered pumping systems, some background about solar energy will be presented and specifically topics refering to the availability, the collection, and the utilization of solar energy in the form of heat, will be discussed.

The solar energy per unit time, received on a unit area of surface perpendicular to the sun's radiation, in space, at the earth's mean distance from the sun, is assumed constant and is called the "solar constant", whose value was proposed by Thekaekata and Drummond (1) to be 1353 W/m^2.

The earth revolves around the sun in a near circular orbit, the earth-sun distance varying by about 3% from the mean distance. This variation in distance produces a nearly sinusoidal variation in the intensity of the solar radiation that reaches the earth's atmosphere, which has been approximated according to J.Bush and L.Richards (2) by the following equation:

$$I = I_{SC} \cdot \left[1 + 0.033 \cdot \cos \frac{360 \cdot (D-2)}{365} \right] \qquad 1.1$$

During the earth's orbit arount the sun, a special geometry is involved, giving rise to important angles such as solar declination, solar time, incident angle of sun's rays etc. which are utilized in the calculations for the prediction of available solar energy. Some elements of this special geometry are shown in appendix A.

Not all the energy expressed by the solar constant reaches the surface of the earth, because of strong absorption by cardon dioxide, oxygen and ozone present in the atmosphere. The solar energy incident on the earth's surface is also dependent on the atmospheric content of dust and other pollutants. The above is illustrated in figure 1.1, after J.Threlkeld and E.Jordan (3) which indicates the absorption effects for a surface at sea level location, moderate atmospheric conditions, and sun's incident angle.

It is useful to distinguish solar radiation between the solar radiation which is received from the sun without change of direction, (the so called beam or direct) and the solar radiation which is received from the sun after its direction has been changed by reflection and scattering due to the atmosphere (diffuse). Generaly the calculation of the amount of the available radiation for any solar energy application, requires the knowledge of both direct and diffuse components.

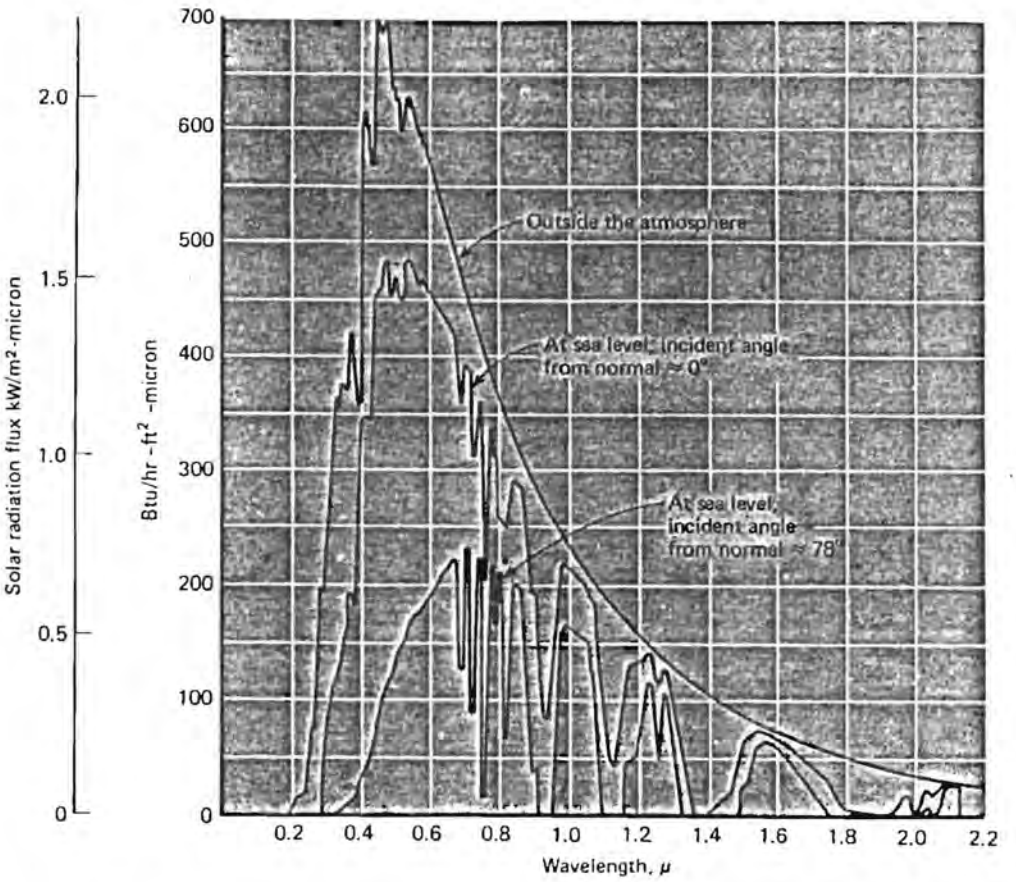

Figure 1.1 Spectral distribution of solar radiation as function of atmospheric conditions and angle of incidence.(3)

As the sun's radiation passes through the atmosphere it is attenuated in proportion to the length of its path according to an extinction coefficient B. The direct normal irradiance at the earth's surface, according to P.Lunde (4), is

$$I_{D,n} = A \cdot \exp\left(-\frac{P}{P_o} \cdot \frac{B}{\cos\theta_z}\right) \qquad 1.2$$

where P/P_o is the pressure at the location concerned relative to the standard atmosphere.

$$\frac{P}{P_o} = \exp(-0.0001184 \cdot Y) \qquad 1.3$$

Monthly values for the apparent extraterrestrial solar intensity (A) and the extinction coefficient (B), as given by J.Yellott (5), are found in the table below.

Nominal day	A (W/m^2)	B
January 21	1230	0.142
February 21	1215	0.144
March 21	1186	0.156
April 21	1136	0.180
May 21	1104	0.196
June 21	1088	0.205
July 21	1085	0.207
August 21	1107	0.201
September 21	1151	0.177
October 21	1192	0.160
November 21	1221	0.149
December 21	1233	0.142

Table 1.1 Values of apparent extraterrestrial solar intensity (A) and extinction coefficient (B).(5)

The prediction of the available solar energy at any

locality, maybe be achieved by a variety of techniques which utilize radiation data (available from maps and tables) or other meteorological measurements.

Theoretical models (see for example ref. 6,7) use atmospherical characteristics (such as visibility, atmospheric pressure and temperature, relative humidity, cloud cover etc.) in estimating the direct portion and the diffuse portion of the total solar radiation.

Models based on meteorological data (see for example ref. 8) use empirical relationships that correlate solar radiation with meteorological parameters, such as the percentage of possible sunshine and the cloud cover. Byers (9) has estimated that of the total solar energy incident at the top of the atmosphere, 33% is reflected from the tops of clouds back to outer space, 9% is lost to outer space by atmospheric scattering, 15% is absorbed by atmospheric constituents, 27% reaches the earth's surface as direct radiation, and 16% reaches the earth's surface as diffuse radiation. Thus 43% of the energy incident at the outer limit of the atmosphere reaches the earth. These calculations are based on the average cloudiness for the earth, taken as approximately 52%.

Finally, since the most common available radiation data are the daily totals of global radiation on a horizontal surface, (and the hourly totals of the same parameter for some locations), a number of empirical techniques have been

developed in order to estimate the direct and the diffuse radiation from measured total horizontal radiation. According to R.Boer (10) the main disadvantage of the above mentioned empirical techniques is their inability to model the variability of solar radiation. On the other hand, these methods have been used by solar designers for some years and provide a widely accepted method for estimating solar energy availability to solar energy powered systems. Most of these techniques are based on the method developed by Liu and Jordan (11), who used statistical characterization of the parameters. The pertinent part of their method, for our application, is explained in appendix B.

1.2.2. Collection of solar energy.

Solar energy is converted to heat energy by means of the solar collectors. A solar collector is thus a heat exchanger in which energy is transfered from a distant source of radiant energy, (the sun), to a working fluid.

Flat-plate collectors (ie. collectors where the area absorbing the solar radiation is the same as the area intercepting it) are designed for applications requiring energy delivery at moderate temperatures, up to perhaps 100 degrees Celsius above the ambient temperature. P.Hofmann et al (12) have shown the approximate operating temperature levels for flat-plate collectors as indicated in table 1.2.

Flat-Plate Design		Approximate Operating Temperature Level (ΔT Above Ambient)	
Cover	Absorber Plate	(°F)	(°C)
One glass	Flat black paint	50	30
Two glass	Flat black paint	100	55
One glass	Selective black	100	55
Two glass	Selective black	150	85

Table 1.2 Approximate operating temperature levels for flat-plate collectors.(12)

Another important characteristic of a flat-plate collector is its efficiency which is obtained by the widely accepted formula proposed by Hottel and Whillier (13):

$$\eta_c = \frac{Q_u}{A_a \cdot I} = \tau \cdot \alpha \quad -Q_l \cdot \frac{\bar{T}_{pl} - T_a}{I} \qquad 1.4$$

Focusing collectors utilize optical systems -reflectors or refractors- to increase the intensity of solar radiation on the absorbing surface. Higher energy flux on the absorber means a smaller surface area for a given total amount of energy, and correspondigly increased temperatures at which energy is delivered. Approximate values of the maximum operating temperatures for different non-tracking concentrator type collectors are reported by A.Rabl(14) as shown in table 1.3.

Tracking	Examples	Approx. Range of C	Approx. Maximum Operating Temperature
		(a)	
None Tilt fixed	CPC	1.5–2.0	Up to 100°C no vacuum Up to 150°C vacuum Up to 250°C advanced technology
None 2 tilt adjustments per year	V trough	1.5–2.0	Up to 150°C vacuum
	CPC	3.0	Up to 180°C vacuum
None Tilt adjust seasonal to daily	V trough	2–3	Up to 180°C vacuum
	CPC	3–10	100–150°C no vacuum 150–250°C vacuum Up to 350°C advanced technology

Table 1.3 Approximate maximum operating temperatures for different non-tracking concentrators.(14)

A very important characteristic of a concentrator is its concentration ratio (C), which is defined as the ratio of the aperture area over the receiver area. For a particular aperture area, the higher concentration ratio results in increasing the collector's operating temperatures because the heat losses are kept minimum due to small receiver area. Wilson and Hinterberger (15) proved that the concentration ratio is closely related to the collector's acceptance half angle (θ_c), and that the maximum theoretical concentration ratio is

$$C_{max} = \frac{1}{\sin\theta_c} \qquad 1.5$$

and proposed the design of a concentrator that can reach this limit. At the same time Baronov and Melnikov (16) proposed indepentently the design of a similar concentrator

using similar arguments and arriving to the same conclusions.

The thermal performance of a concentrator can be described in a manner analogous to the flat-plate collector and its efficiency can be as well expressed by the Hottel and Whillier equation (1.4).

Concentrators have two major disadvantages:

a. They do not collect the diffuse component of sunlight.

b. They require accurate focusing and relatively sophisticated sun tracking mechanisms, which usually are expensive and require auxiliary electrical power.

However, in cases where the tracking motion required is linear, the tracking mechanism may be a simple mechanical one.

K.Gupta et al (17) have reported on a tracking device based on a simple clockwork mechanism which consists of a falling weight, controlled by a pendulum that drives a shaft which is parallel to the earth's axis at a rate of one revolution per day. The concentrator is mounted on this shaft and it thereby tracks the sun.

E.Farber et al (18) have reported on a tracking device whose bacic principle of operation centres around the use of the sun's energy, to develop a pressure differential between

two opposing cylinders, through which, a linkage system propels the collector structure.

1.2.3. Closure

It is quite apparent from the literature that significant contributions to the utilization of solar energy have been proposed, however it is safe to conclude that for developed areas the major portion of energy demands will be provided by means other than solar. For developing or rural communities, however, the outlook is very different. Here, because the demands for the provision of energy are modest, the use of sun powered devices would make dramatic changes in the fortunes of such communities.

From the countless small tasks at present performed by manual or animal labour or not at all, water irrigation stands in the forefront. As with any other innovations, the introduction and acceptance of a solar powered device for pumping water, or use in irrigation schemes, will largely depend on economics and simplicity of the device.

1.3. PUMPING SYSTEMS

The mechanical energy needed for pumping may be produced from solar energy in a number of ways. In the solar thermal or the thermodynamic conversion schemes, solar collectors are employed to raise the internal energy of a fluid. This fluid may be either utilized directly in any of the thermodynamic cycles such as Rankine, Sterling, Brayton etc. or through a thermal interface activate a secondary working fluid. The mechanical energy produced may operate any conventional or specially designed water pump.

To illustrate the way a conventional pump works, the following example of an existing pumping system is shown below. Figure 1.2 depicts a schematic of the major components and fluid circuits of a 37-KW (50-hp) solar powered irrigation pump designed and built by Battelle (BMI)(12). Refering to figure 1.2, the operation of a typical conventional solar pump is as follows: In the morning, whenever the solar flux reaches a high enough intensity to heat the water in the collector to a usable temperature, the concentrating collector automatically begins tracking the sun. Simultaneously, a small electric motor operates two pumps; one to circulate water through the collector, boiler and preheater, and another to pump the working fluid through the various heat exchangers. As soon as the turbine develops sufficient speed to maintain the

operation, the starting motor is disconnected and the unit continues to operate on solar energy through out the rest of the day. The cycle thermal efficiency of the above described pump is relatively high (17.64%).

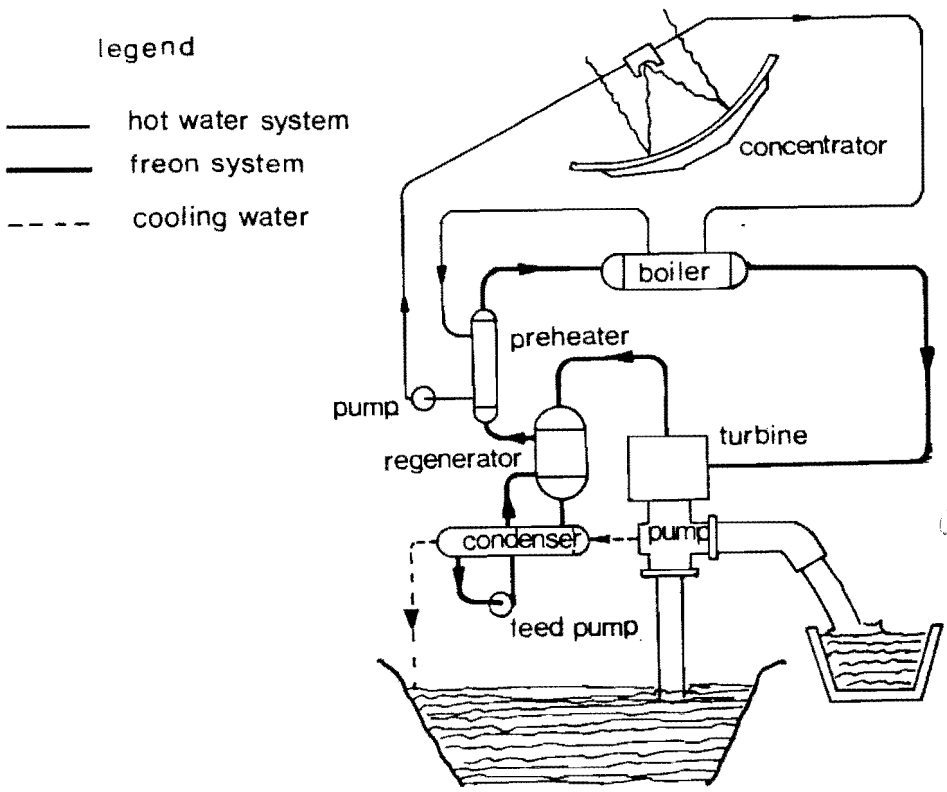

Figure 1.2 Conventional solar powered water pump.(12)

Conventional pumps can be quite powerful and they are capable of supplying water for the irrigation of big areas from deep water wells, however their main disadvantages are:

1. They are not energetic independent since they use auxiliary power to operate the circulating pumps and tracking mechanism.
2. The maintenance is not simple. Regurarly the system requires cleaning the collectors, purging

the condenser of non-condensible gases, maintaining the proper charge of working fluid in the system, lubricating where necessary, adding corrosion inhibitors and/or antifreeze to the collector's fluid, and cleaning the strainers and filters.

These disadvantages make the use of a conventional pump in isolated and rural areas problematic. To overcome these disadvantages, some specially designed solar water pumps were proposed. Up to now these pumps have achieved their goal of energetic independence and low maintenance, but only at the expense of power output.

1.4. SPECIALLY DESIGNED SOLAR PUMPS

There have been numerous special designs for solar water pumping systems. Because the present study considers a special kind of water pumps, work done previously on these pumps will be examined in detail. Basically almost all such pumps make use of the fact that fluids expand and contract upon heating and cooling respectively. The volume increase when heated at a given pressure may be utilized to displace water to a higher elevation, and the volume reduction at a lower pressure when cooled, corresponds to a suction of water from a depth.

1.4.1. The first solar operated water pump was invented by Salamon de Gaus (1576-1626) a French engineer who described his machine in 1615. Unfortunately the original reference proved impossible to locate. Bernard Foret Belidor (1697-1761) also invented a form of solar operated pump, which was shown by Mc Veigh (19) and reproduced for our purpose in figure 1.3. Belidor's pump is primed by filling the tank to the level AB. During the day, solar radiation heats the tank, causing the air to expand and force the water through the non-return valve (C), to reach the upper reservoir. On cooling, either artificially or at night, the internal air pressure falls below atmospheric, drawing water

into the pump from the lower reservoir through the non-return valve (D). No quantitative results are reported about Belidor's pump.

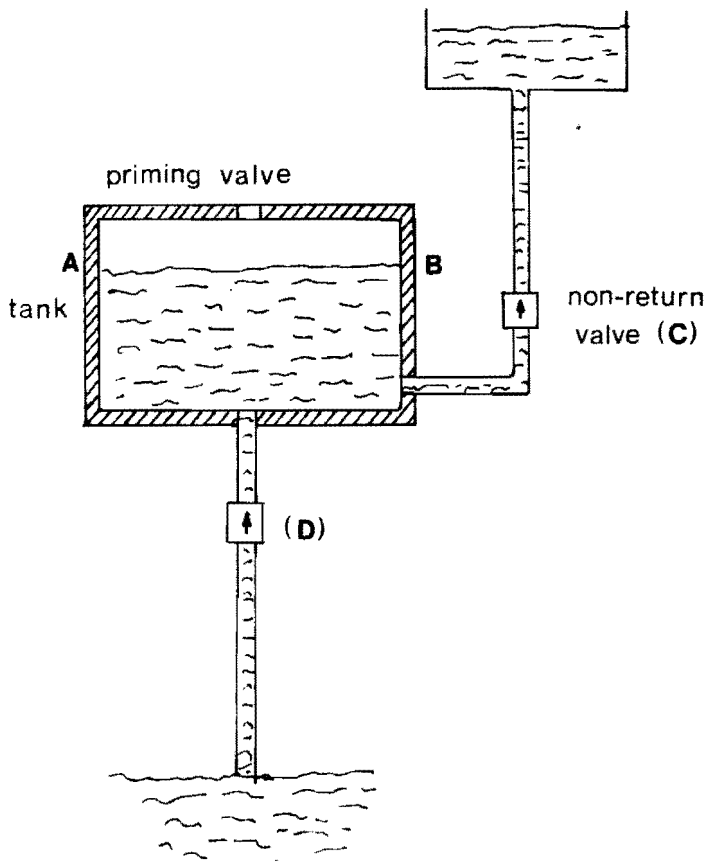

Figure 1.3 Belidor's solar pump.(19)

1.4.2. A modern version of Belidor's solar pump developed by R.Bernard (20) is depicted in figure 1.4. The system consists of a thermal device using air and water, working alternatively on a diurnal cycle utilizing the daytime solar heat and the nocturnal cooling. A tank is needed which is big enough to contain the volume of water corresponding to the user's daily requirements. In order to obtain a

sufficient high temperature, (≈130 °C) the tank is put in an insulated glasshouse.

When the sun heats up the air in the tank, it expands and part of it escapes through the inlet pipe. As the tank always contains a small residual quantity of water, (remaining after the previous operation) the water vapour produced by the solar heat helps to expel the air, which can be seen bubbling in the water at the lower end of the P.V.C. pipe.

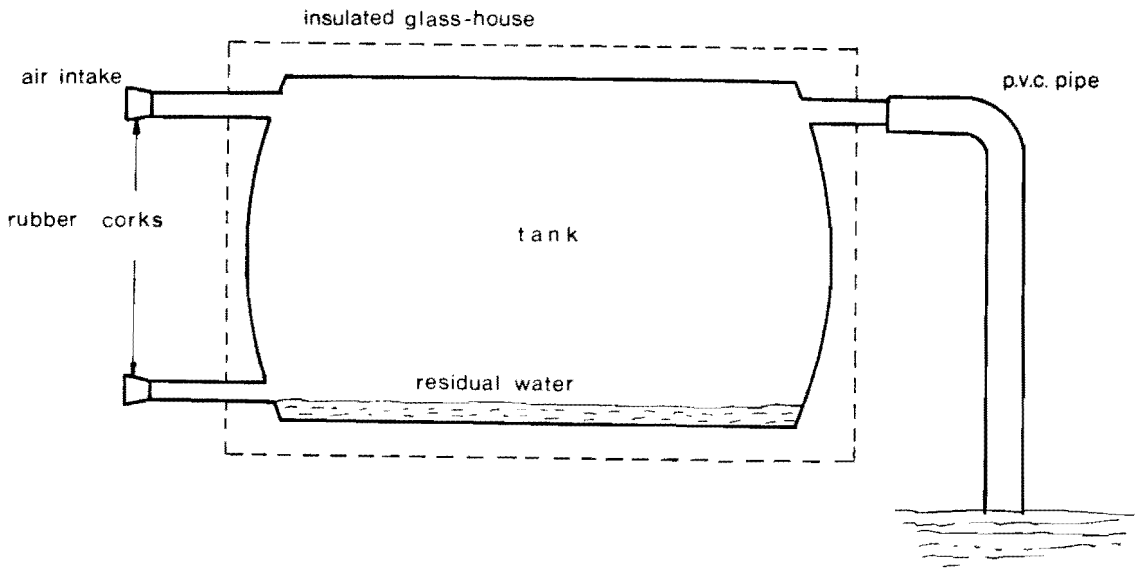

Figure 1.4 A solar pump by R.Bernand.(20)

At the end of the afternoon the tank cools off and the bubbling stops. The water is slowly drawn up the pipe due to the depression produced by the condensation of the vapour. The following morning, the user removes both corks to drain

the pumped water and stores it in another tank, or uses it directly in an irrigation system. He replaces the corks preparing the tank for a new cycle.

Maintaince problems of this system are kept to a minimum due to the fact that there are no moving parts. The efficiency of this system is reported to be very low ("fifty times lower than that of an ordinary pump") but exact figures are not reported in this paper.

1.4.3. Two types of pumps using n-pentane as the working fluid have been described by D.P.Rao and K.S.Rao (21), as described below: an air cooled and a water cooled pump.

Air cooled pump

The pump (figure 1.5) consists of a tank located inside the well, a flash tank, a working fluid recycle-tank, and a solar collector. The tank inside the well is constructed below the level of the water table so that water can fill the tank under atmospheric pressure. Water enters through a non-return valve fitted at the bottom of the tank. The flash tank serves as a storage for the working fluid as well as a separator for the liquid vapour mixture coming out of the collector.

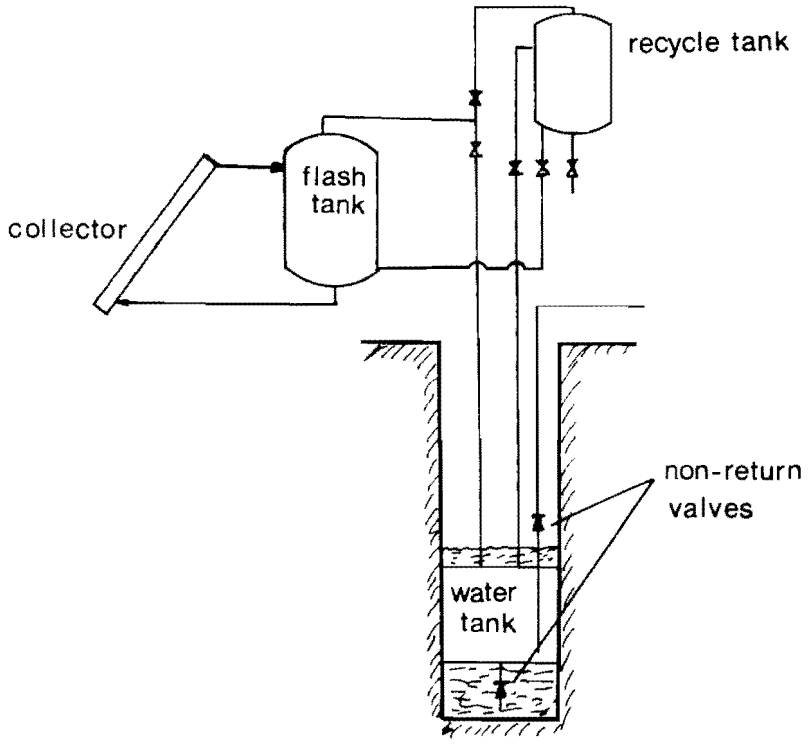

Figure 1.5 Air cooled pump.(21)

During day time the working fluid flows due to gravity into the collector from the flash tank where it is vapourized and returned to the flash tank. The vapour from the flash tank flows down into the tank located inside the well, displacing water from the tank as vapourization proceeds at a pressure corresponding to the head required to pump water. At night the collector acts as a condenser for the working fluid, rejecting heat to ambient. The condensate flows back to the flash tank from the collector under gravity. Due to heat losses to the water and the wall of the tank, some of the working liquid which is condensed in the water tank, may not return to the flash tank. This part of

the working fluid can be pumped into the recycle tank the next day before new water is pumped. The working fluid from the recycle tank can be transfered to the flash tank under gravity or pressure equilisation.

The performance of this pump was discussed by R.Soin et al (22) and its efficiency was reported to be 0.81%.

Water cooled pump

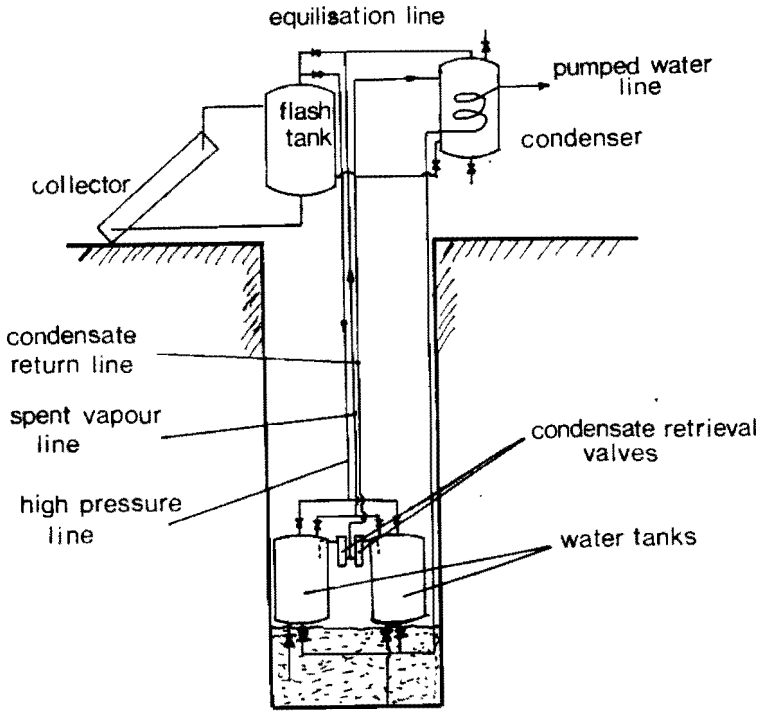

Figure 1.6 Water cooled pump.(21)

In the air cooled pump described above, the daily pumping capacity is limited by the water tank size. The water cooled pump (figure 1.6) was proposed to overcome this limitation. Besides the collector and the flash tank, there are two

water tanks located close to the water source and a condenser at the ground level. The working fluid drawn into the collector is vapourized and returned to the flash tank.

We begin by assuming that the water tanks are full of water. The vapour from the flash tank is let into one of the water tanks, thereby pumping is effected. The discharging water condenses the vapour in the shell side as it goes through the condenser coils. After the first tank is emptied, the vapour is switched over the second tank. Simultaneously the first tank is connected to the condenser. The vapour of the first tank is condensed by the water that is being pumped from the second tank. As condensation proceeds, the pressure in the first tank is reduced and water enters through a non-return valve. Thus, as the second tank is being emptied, the first one is being filled. On reversing the cycle, by manipulation of the valves, the first tank will pump while the second one draws water. In this manner continuous pumping of water can be achieved. To prevent the working fluid from going into the water line, a water seal is always maintained inside the water tanks. The working fluid which is condensed in the water tank can be pumped into the condenser at the start of each cycle.
The efficiency of this pump was reported by R.Soin et al (22) to be approximately 0.2%.

1.4.4. It is also possible to use water as the working fluid instead of n-pentane or any other low boiling point liquid. A system using water as the working fluid powered by solar energy and the burning of biomass was presented by Muthuveerappan et al (23) (figure 1.7).

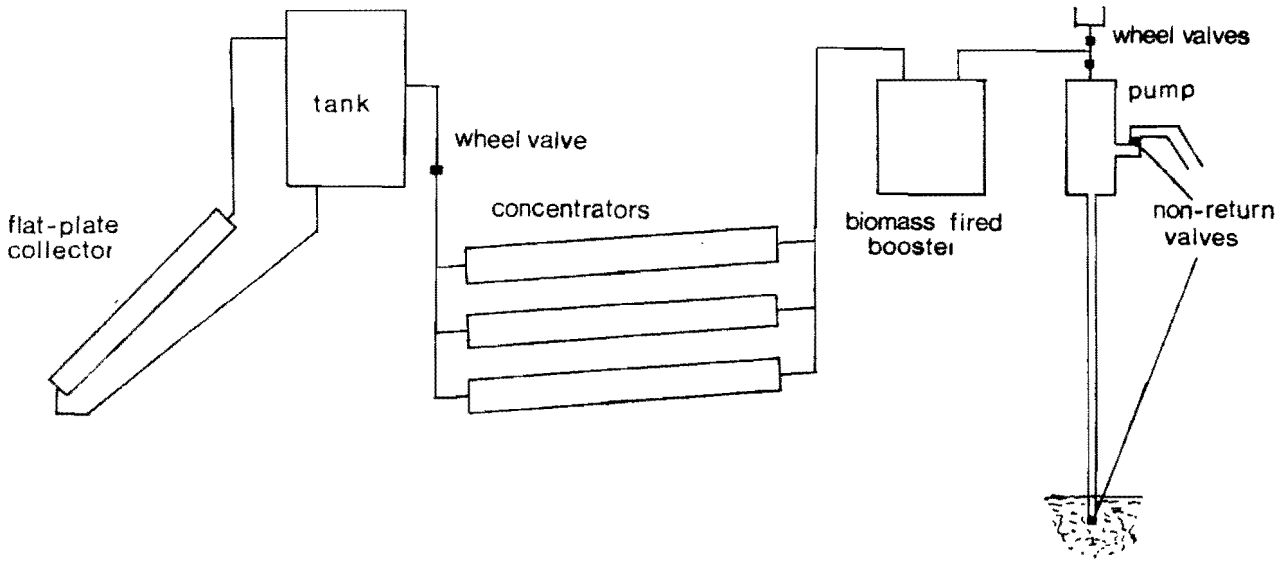

Figure 1.7 Solar and biomass powered pump.(23)

It consists of a flat-plate collector, a concentrating type collector requiring periodical tilt adjustment, a biomass fired auxiliary energy booster, and a simple pump of robust construction. The system has no moving parts except for two non-return valves. The system operates on steam supplied continuously and produced by solar energy and biomass heating.

Steam flowing at a particular velocity strikes the water surface inside the pump body and creates turbulance so as to

initiate condensation in the pump barrel. Initially the condensation creates vacuum which sucks the water into the pump body. When fresh water enters into the pump body, vacuum conditions are augmented very rapidly, which creates a rapid flow of water in the suction line. This high velocity water flow is suddenly brought to rest by the on coming steam, creating high pressure just like in the case of a hydraulic ram. The pressure opens the delivery valve and the water is delivered at a faster rate, while the water flow in the suction line is being continued due to inertia. Water flows from the pump through the suction and delivery valves till the pressure dies out. Then, the oncoming steam pushes a small quantity of hot water from the pump body through the delivery valve by virtue of its pressure. Once the hot water has been forced out, the second cycle starts by the initiation of condensation of steam.
The efficiency of the combined engine and pump is reported to be approximately 0.015%.

1.4.5. A version of the above described pump which uses a compound parabolic concentrator to evaporate the water, and the principle of a liquid piston, was designed by H.Reichmuth and J.Barnes (24) as shown in figure 1.8.

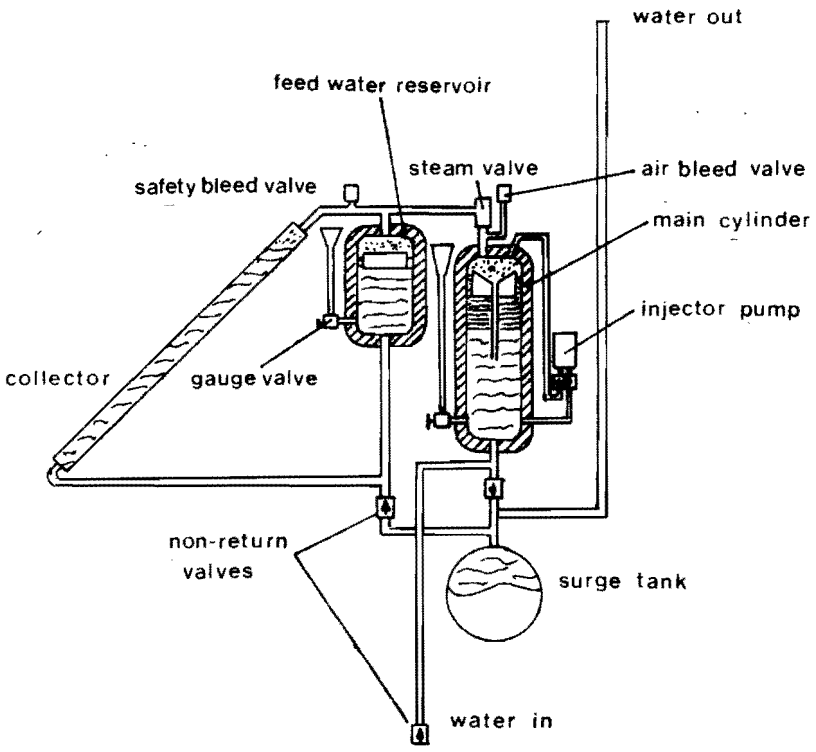

Figure 1.8 Liquid piston pump.(24)

The water is pumped in the following manner: Steam, entering the main cylinder under pressure, forces the water out to a new elevation. Since the top of the cylinder is well insulated, the steam will not condense fast enough. Therefore some means of cooling and condensing of the steam are needed. A water spray provided by an injector pump cools the inside of the cylinder. The injector pump is automatically filled with cold water from the bottom of the cylinder during the pressure portion of the stroke. The pump sprays the water into the top of the cylinder as the pressure in the cylinder drops after the flow of steam is cut off. The steam, upon condensing draws in water from a

lower point, refilling the main cylinder for another stroke. The theoretical efficiency of this system was reported to be approximately 2.5%.

1.4.6. A solar pump that operates on a thermodynamic Rankine cycle using an organic fluid (methyl alcohol) and has a liquid piston pump, has been developed and tested by H.Agrawal and S.Pal(25) (figure 1.9).

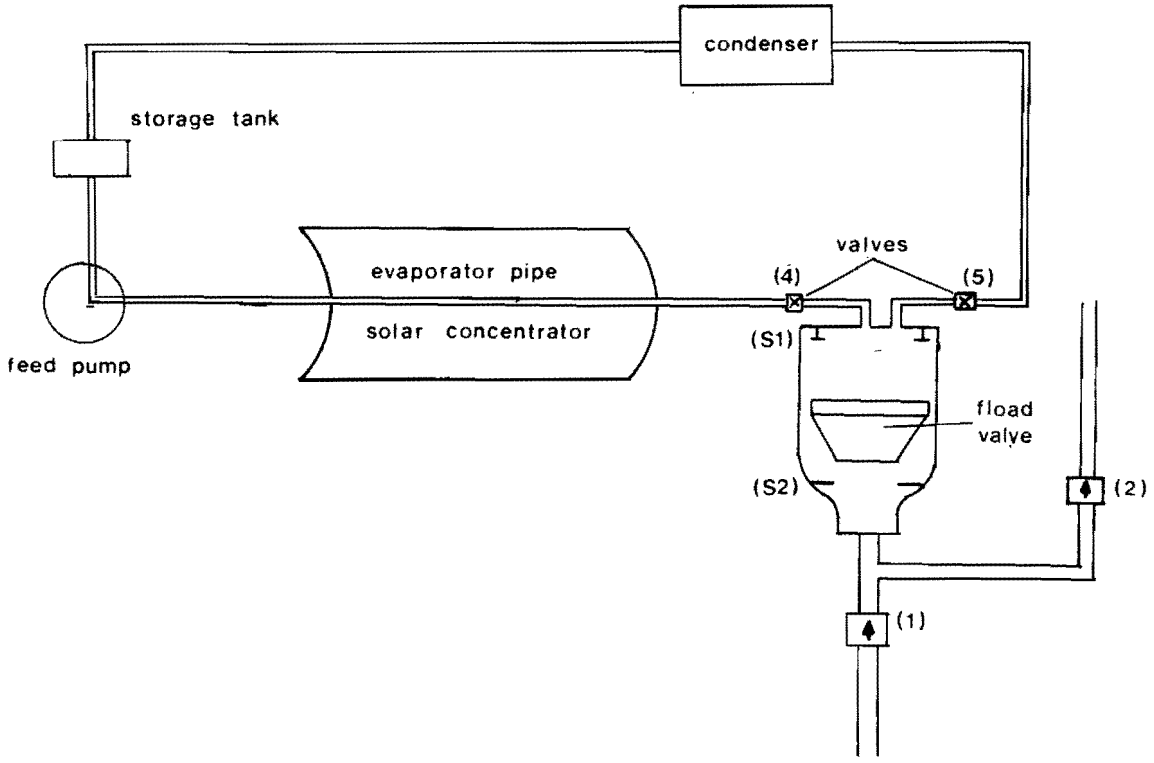

Figure 1.9 Rankine cycle pump.(25)

Superheated vapour of the working fluid is generated in a stationary compount parabolic concentrator. The vapour is

directed in the pumping section where, due to its pressure, it pushes down the liquid piston of turpentine oil that is immiscible both in water and methyl alcohol vapours. The piston's downward movement forces the water out through a non-return valve (2). During this process valve (5) is closed. When the float valve reaches the seat (S1), valve (5) opens and valve (4) closes. Thus, the vapour is exhausted to the condenser. The condensation of vapour produces a partial vacuum in the cylinder causing suction of fresh water from the water source or supply. When the float valve reaches the seat (S2), valve (5) closes and valve (4) opens. New vapour is directed in the pump section and the cycle repeats itself. No quantitative results have been reported here.

1.4.7. Another type of solar water pump is the one that uses bellows instead of a piston. A low temperature, bellows actuated solar pump, was developed by T.Bhattacharyya et al (26) and it is shown in figure 1.10. It operates on the Rankine cycle as well, using a low boiling point liquid as the working fluid.

The pump consists of an array of flat-plate collectors, a boiler drum, few airtight chambers and a condenser to be cooled by the water being pumped. Flexible bellows in the bellows chamber form the critical part of the system.

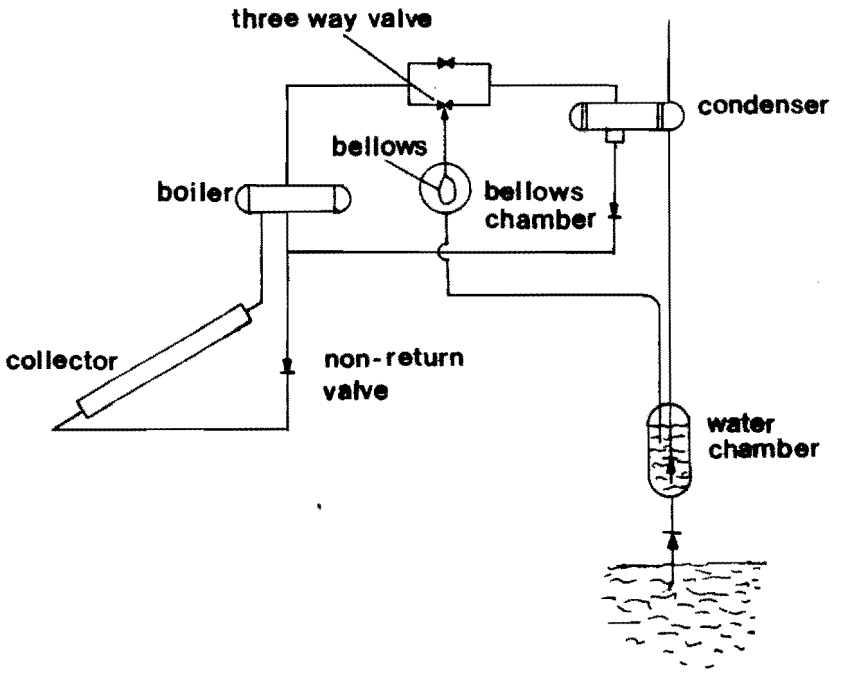

Figure 1.10 Bellows actuated pump.(26)

In principle, the heat collected by the collector array is utilized to boil the working fluid. The generated vapour is accumulated and its pressure rises according to its temperature increase. After obtaining the desired pressure in the boiler drum, the bellows chamber is alternately connected to the vapour chamber and condenser by means of a three-way valve. This causes the bellows to expand and contract in the confined chamber. This chamber is connected to the actuating water chamber, which is initially filled and equiped with suction and delivery pipelines with check valves. The suction line dips in the water supply reservoir. The expansion and contraction of the bellows cause pressurization and rarification of the trapped air in the

bellows chamber which, in turn, acts on the water in the water chamber to effect alternately delivery and suction of water.

After many cycles of operation, the condensate is returned to the vapour chamber by equilizing the pressures in the vapour chamber and in the condenser. A commercial quality rubber bladder was used as the bellows for this unit.

The overall efficiency was calculated and reported to be in the range of 1-2%.

1.4.9. Another device using bellows as a piston has been designed and tested by R.Sachdeva et al (27) and it is shown in figure 1.11. It consists of a metallic tube closed at one end; the other end of the tube is fitted with an expansion bellows. The entire space inside the tube is filled with the working fluid which is then sealed after completely purging it of air. The tube is fixed in a slightly inclined position with the bellows at the top. A concentrated source of heat is applied at a localised spot near the lower end of the tube. The working fluid being a saturated liquid will get vapourised at the lower end. The bubbles that are formed will travel a short distance upwards pushing out the liquid column because of a slight increase in pressure associated with vapourisation. This will cause an outwards movement of the bellows. A vapour film is formed on the hot inside surface which now acts as an insulator resulting in a sudden reduction of heat transfer to the fluid.

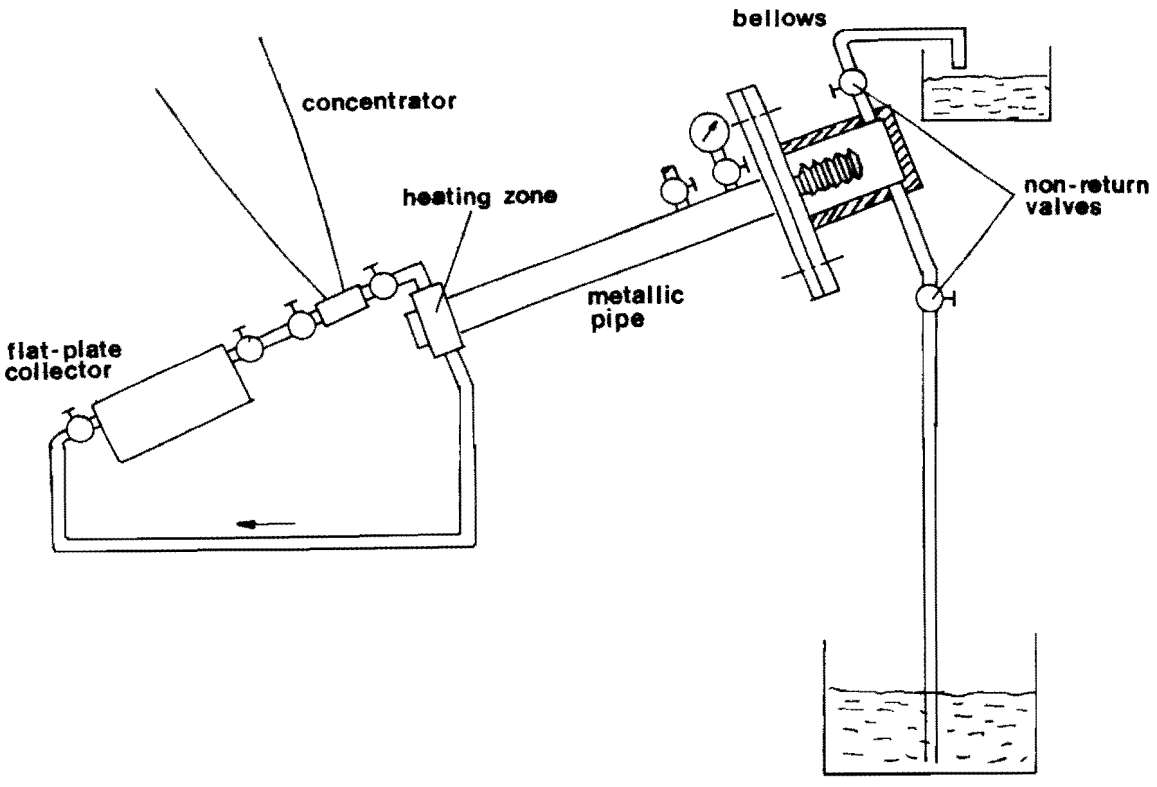

Figure 1.11 Bellows piston pump.(27)

Except for the small heating zone the rest of the tube surface is cool or kept cool. This causes sudden colapse of bubbles. The liquid column moves inwards and also the pressure decreases. Both these events will lead to the inwards motion of the bellows bringing it back to the original position. Meanwhile, the heat sourse is still active at the localised spot; the collapse of bubbles brings the liquid column in contact with the hot surface and the cycle repeats itself. The efficiency of this system is not reported in this paper.

1.4.10. Yet another design suitable for solar water pumping

is the Minto wheel as described by M.Bahadori (28) (figure 1.12).

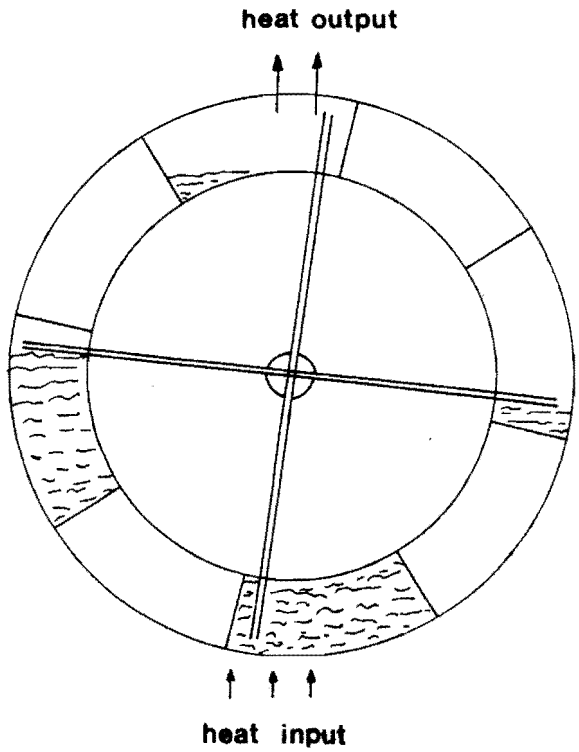

Figure 1.12 Minto wheel.(28)

The wheel consists of a series of sealed containers fastened around the wheel's rim. Diametrically opposite containers are connected by tubes. A liquid with low boiling point is sealed into the bottom containers. When a "bottom" container is heated part of the liquid evaporates and the vapour pressure forces the remaining liquid to rise into the opposite container. This shift of mass causes the "top" container to become heavier while its opposite "bottom" container becomes lighter and as result, the wheel starts turning, in the same manner as water turns a water wheel.

The Minto wheel runs very slowly and has very low

efficiency. According to P.Adams (29) who designed a Minto wheel at U.C.T. laboratory, the thermal efficiency was reported to be 0.54% and the speed 0.16 revolutions per minute.

CHAPTER 2.

DESCRIPTION OF THE SYSTEM AND APPARATUS

2.1. THE PROPOSED PUMP

Analyzing the previously described pumping systems, it can be concluded that a common characteristic of all these systems is the very low efficiency. However, low efficiency may not be the sole parameter for the acceptance of a solar energy powered pumping system. Some of the qualities that a solar pump should have in order to become attractive to potential users are:

1. Cheap, convenient and easy manufacture.
2. Reliability.
3. Easy to operate and minimum running costs.
4. Low maintenance.
5. No auxiliary energy.
6. Relative high efficiency.

Most previously mentioned pumping systems show that they have similar structure; namely they consist of a solar collector, a boiler, a water chamber, a condenser, non-return valves, piston etc. Studying these systems one can remark the following:

1. It might be possible that the basic structure, as

described previously can be simplified by combining two or more processes into one part of the apparatus, or one piece of equipment.

2. When the working fluid is in direct contact with the water it should be non-toxic and immiscible, a fact which limits the choices of working fluid; therefore, the use of a reciprocating medium overcomes the above limitation. The reciprocating medium's motion should be as frictionless as possible so that energy losses be minimized. The use of bellows serves this purpose adequately.

3. Auxiliary energy, when used, serves to power either smaller pumps to move the working fluid from one part of the system to another, or control tracking mechanisms. To eliminate any use of auxiliary energy, the design of the pump should be such that the movement of the working fluid is due to natural flow as a result perhaps of density changes, and if acceptable, the use of tracking devices should be avoided.

4. The maintenance requirements are depended on how complicated the structure of the pump is, therefore mechanical simplicity is also a paramount aspect.

The design of the proposed pump is based on the idea that the heating (in the boiler) and the cooling (in the condenser) processes occur within the same place, ie. in the receiver of the collector. Using this idea two benefits

are derived: First the size of the pump is reduced, and second the structure of the pump is simplified since pipes and links are minimized. The proposed pump is shown in photograph 2.1.

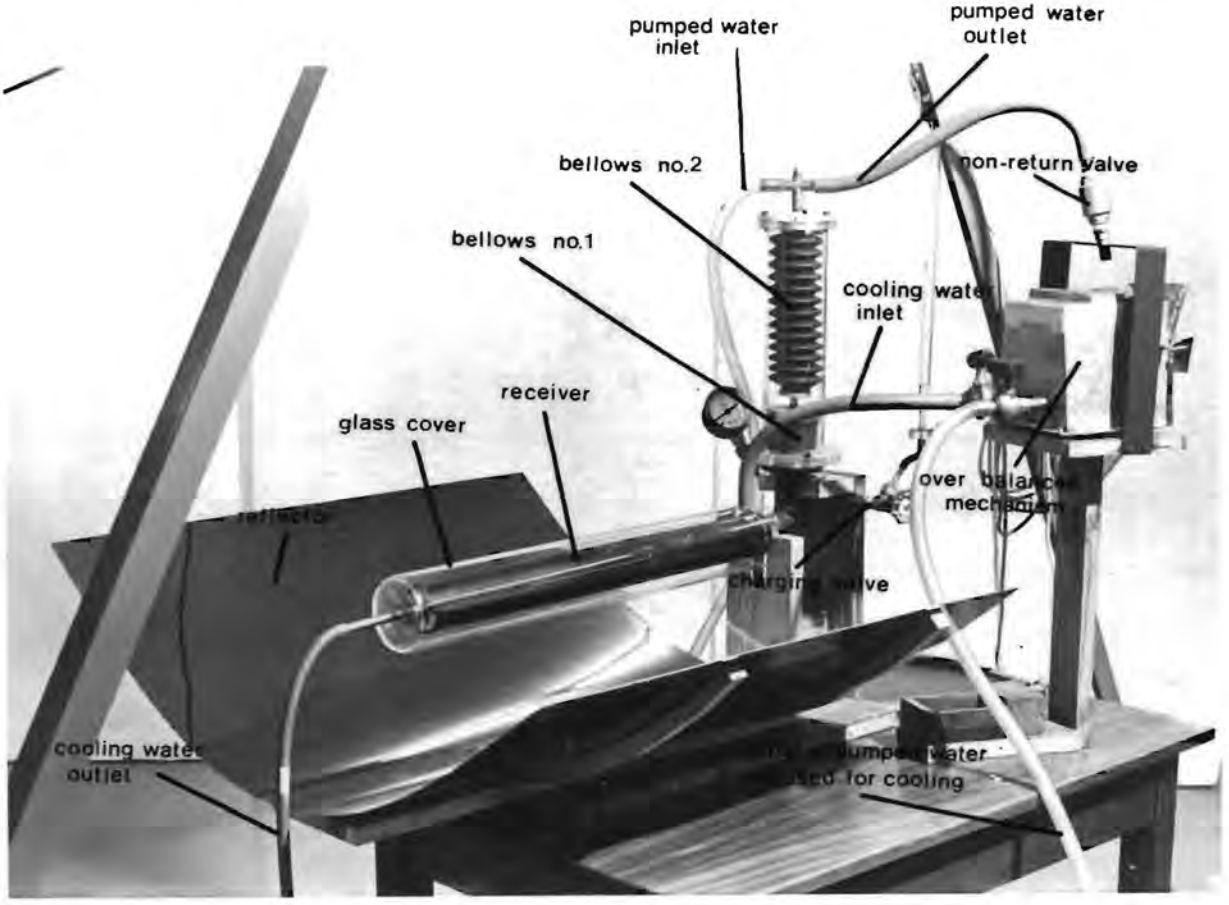

Photograph 2.1 The proposed pump.

It consists of a tubular receiver whose one end is closed, and the other one is connected to a set of identical flexible bellows in series. The bellows are contained within a perspex cylinder which serves to ensure the straight and upright movement of both sets of bellows. Non-return valves are placed at both the delivery and suction lines. The

working fluid, a low boiling point liquid is contained in the receiver. The pumped water is driven through a non-return valve into the over-balanced mechanism and from there it flows out via the cooling system located within the receiver.

The pump operates as follows: The receiver absorbs solar radiation which has been directed to its surface by the concentrator, its temperature is increased and heat is transfered to the working fluid. While the working fluid is being heated, its pressure rises according to its temperature rise. When the pressure in the receiver has increased sufficiently, bellows no.1 start expanding which in turn collapses bellows no.2 containing the water, which is pushed out through the non-return valve. The expelled water is accumulated in the over-balanced mechanism which is adjusted to operate only when the desirable quantity of water has been accumulated. This method provides also the necessary time delay, so that the cooling process does begin at the desired time during the expelling stroke of the bellows. From the over-balanced mechanism the water flows into a container which is provided with two outlet taps. These are adjusted so that the necessary quantity flows by gravity through the one tap via the cooling system to its final destination, while the rest of it flows directly to its final destination. As heat is transfered from the working fluid to the cooling water, the temperature of the working fluid is reduced and consequently its pressure is decreased below the atmospheric level. When sufficient

vacuum is achieved, bellows no.1 start contracting, sucking fresh water from its source into the bellows no.2. When all the cooling water has left the condenser part of the receiver, the working fluid heats up again and the cycle is repeated.

2.2. DESCRIPTION OF THE MODEL

The following description, with sketches and drawings of the system is based on the final model developed constructed and tested by the author.

2.3.1. Receiver

Figure 2.1 depicts the design of the receiver. Part (A) that serves as a support for the cylinder, bellows, the necessary charging and evacuating valves, thermocouples, and pressure gauge, was manufactured using brass tubing. Part (B) that serves as the absorber of solar radiation was manufactured using thin galvanized sheet metal.

A matt black paint was used as the receiver's absorbing coating, because it is cheap and readily available, and has high absorptance. (α=0.91)

As glazing cover, a glass tube was used for its excellent weatherability, low cost and high transmittance. (τ=0.88)

The cooling system is incorporated within the receiver. Among the different cooling systems that were attempted and tested, the one that proved to be the most suitable for this application, is shown in figure 2.1. Its design ensures the uniform flow of the cooling water into the four copper tubes.

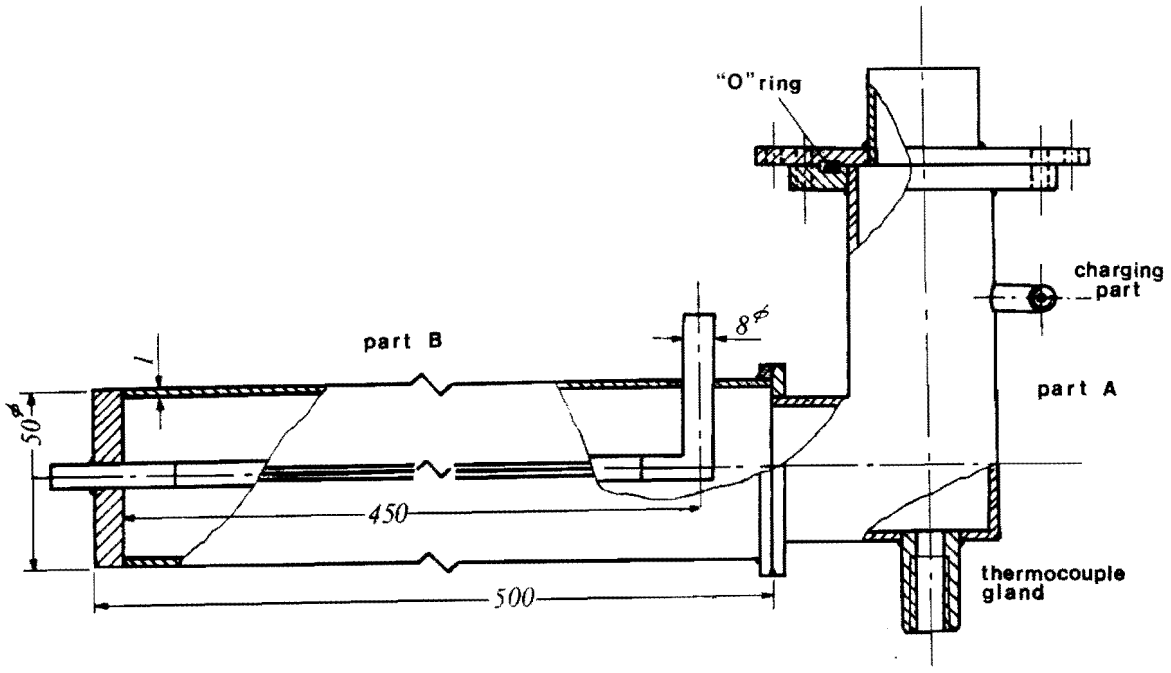

Figure 2.1.a Receiver (B) and bellows support (A).

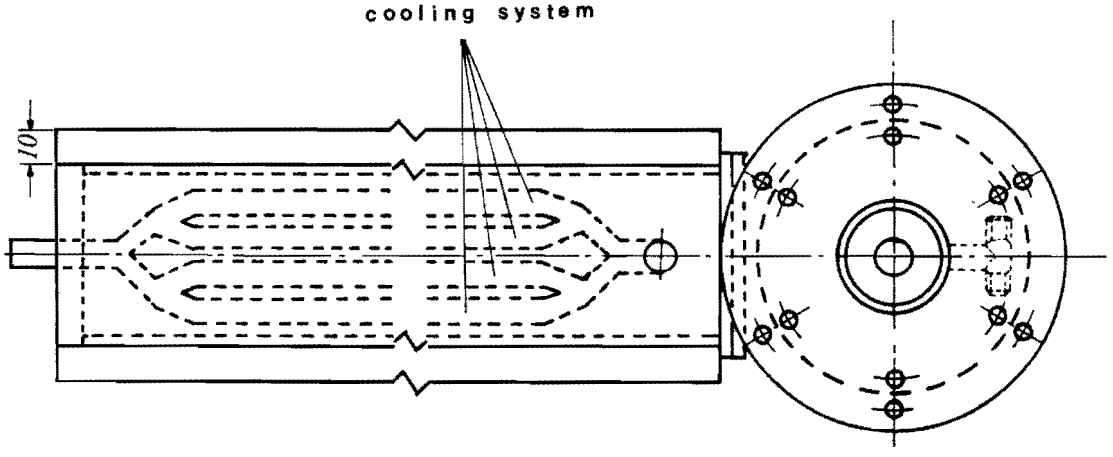

Figure 2.1.b Cooling system within the receiver.

2.3.2 Bellows

The main function of the bellows, is to provide a moving boundary (piston) between the receiver and the enviroment. Ideally the bellows should be of an inpermeable material, so as to ensure that air does not penetrate into the receiver, resulting in deterioration of the pump's operation.

Table C.1 in appendix C gives the permeability of various types of rubber in air. Unfortunately, readily available bellows were made out of natural rubber, and although their permeability coefficient for air is quite high, they were chosen for this application.

The final configuration of the two bellows in series, became a necessary feature of the system, because of heat transfer considerations. At first the pump operated with one set of bellows contained within an airtight perspex cylinder. Water was drawn in and expelled from this cylinder simply by the contraction and expansion of the bellows. However in this manner the working fluid was exposed to unecessary cooling by the pumped water across the bellows' wall, with the result being long cycle times and greater heat input demand.

When testing began it was observed that during the cooling process, bellows no.2 collapsed in a radial manner, a fact both undesirable and inadmissible for the proper operation of the system. This problem was solved by

inserting thin brass rings in bellows no.2, as shown in figure 2.2.

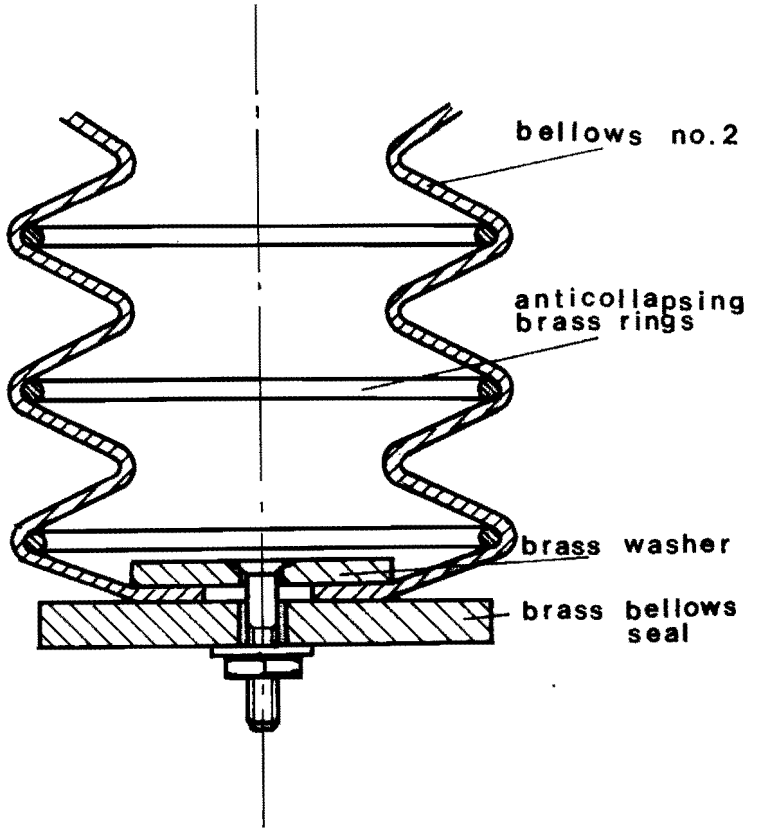

Figure 2.2 Bellows no.2 anti-collapsing device.

2.3.3 Non-return valves

The non-return valves serve to ensure the water flow through the suction line during the suction stroke, and alternatively through the delivery line during the delivery stroke. It is obviously desirable to have the pressure drop through the non-return valves as small as possible, a problem not necessarily solved with the types used in this investigation.

A non-return valve can also be employed as a water head simulator by adjusting the pressure drop across it, so that it equals the pumped water head requirements. To achieve this, an existing valve was modified as shown in figure 2.3 (dark cross section).

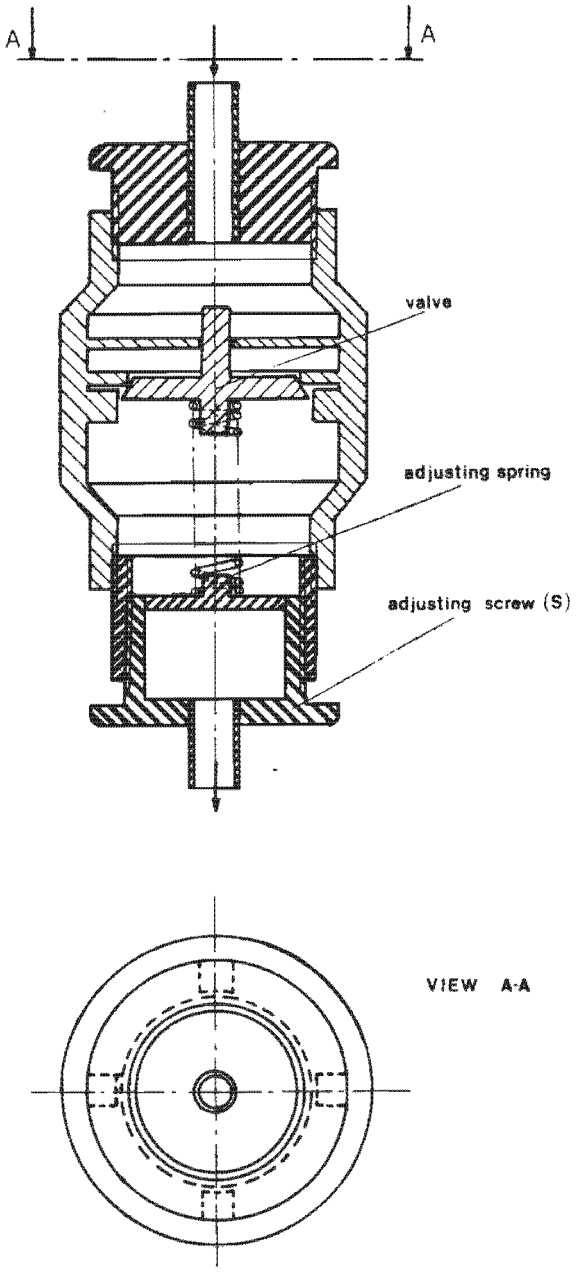

Figure 2.3 Head simulator non-return valve.

The valve operates only when the pressure difference across it equals the desired head. The simulated head is achieved by means of a spring, whose lengh can be adjusted through the adjusting screw (S), part of the valve's modification.

2.3.4. Over-balanced mechanism

The over-balanced mechanism was constructed using galvanized sheet metal and is shown in figure 2.4.
The pumped water is first accumulated in a smaller container (C1) that can be rotated round an horizontal shaft (S). The adjustable weight (W) is used to regulate the amount of water in the container (C2). When sufficient amount of water has collected in order to over-balance the mechanism, the water is directed to container (C2). From there, it flows through tap (T1) via the cooling system to its final destination. Tap (T2) directs the amount of the remaining water (not needed for cooling) to its final destination (the user).

Although the over-balanced mechanism has a moving part, it proved to be a very reliable, and easy method of regulating the cooling water flow rate.

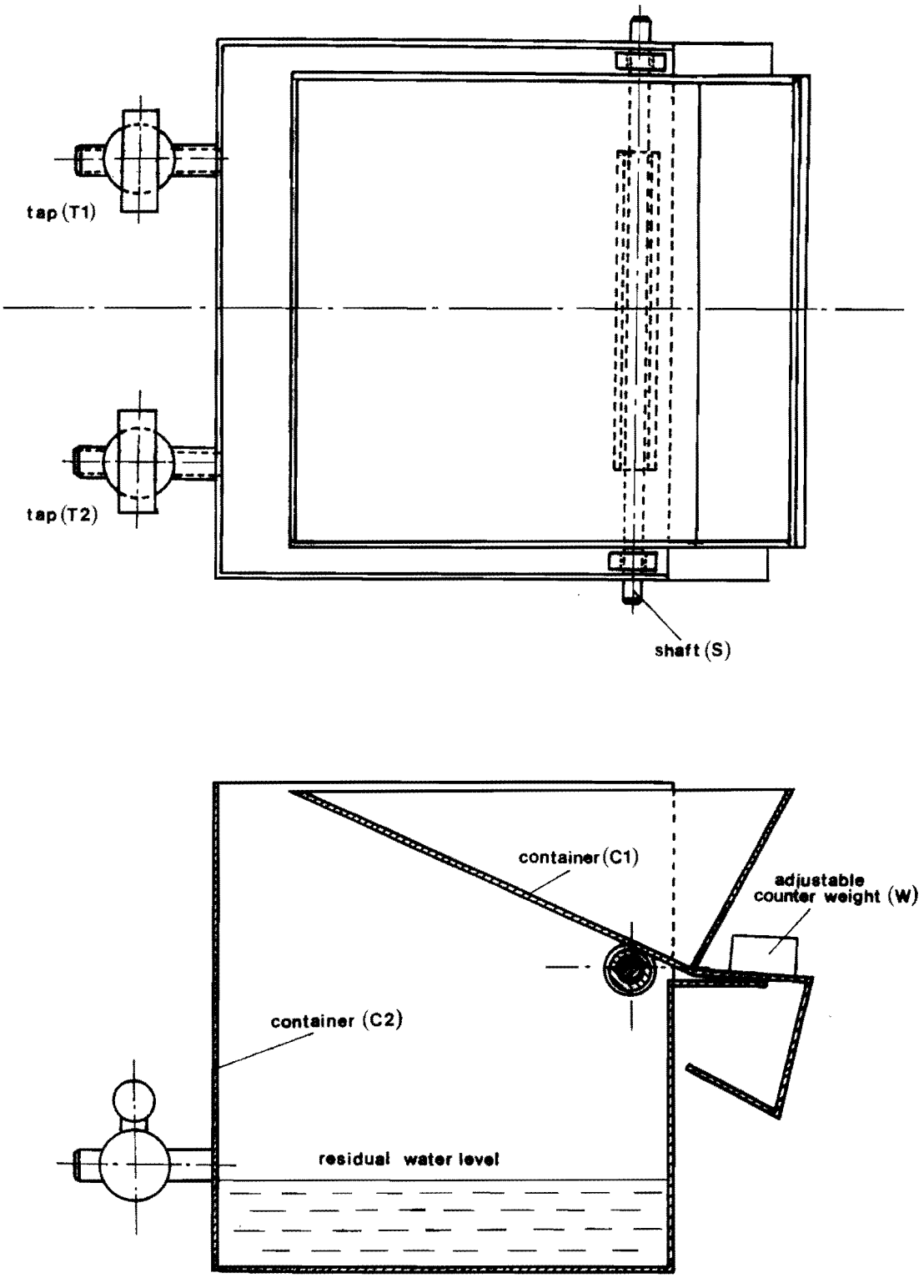

Figure 2.4 The over-balanced mechanism.

2.3.5. Parabolic reflector

The parabolic reflector consists of a wooden base, on which an easily bent polished mild steel plate is placed as shown in figure 2.5. The aperture area is $0.4m^2$. The parabola was designed to have a focal length of: f=0.19m. Analytical calculations for the geometric characteristics of the reflector are given in appendix D. The particular reflecting surface was chosen simply for its high reflectance (approximately 0.90, measured with a Lesley cube, in a manner similar to P.Bam (30)), extremely low cost, market availability, and expected long life.

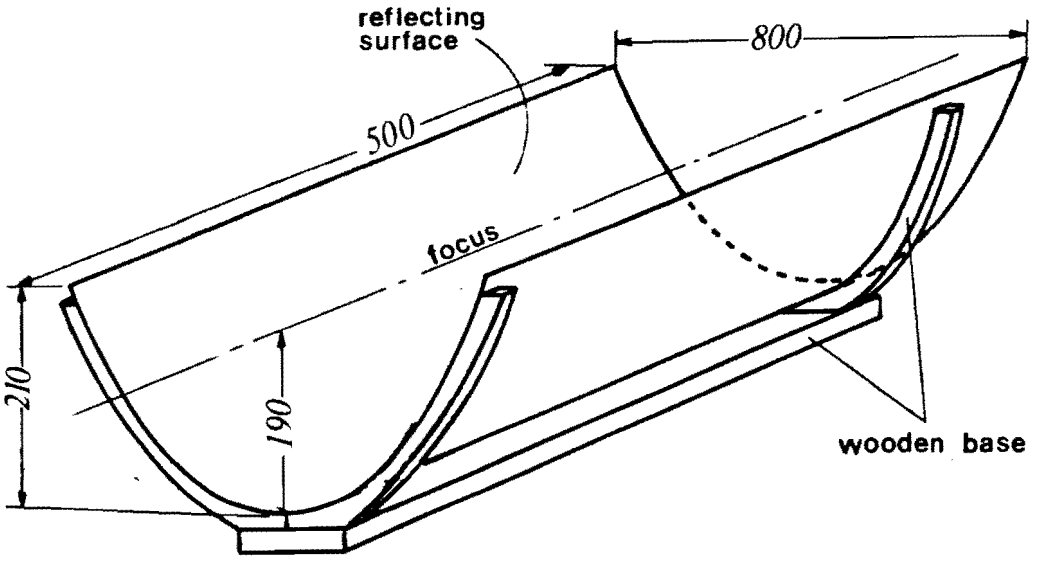

Figure 2.5 Parabolic reflector

2.3.6. Solar simulator.

Since sunlight is subject to large fluctuations, the sun is an unsuitable source of radiation for a multiplicity of tests requiring repeatability. Therefore it was necessary to use a solar simulator to provide the necessary radiation for the testing of the system.

The solar simulator employed for the tests, was previously constructed and used in another solar energy investigation by P.Bam (30). It consists of two C.S.I. lamps mounted on a trolley that can move along a semi-circular track. This provides altitude variation. Azimuthal variation is achieved by rotating the collector on an horizontal plane. Radiation intensity is controlled by varying the input voltage to the lights, while the input voltage is made independent of mains supply fluctuation by means of a voltage stabilising device.

The simulator is shown in photograph 2.2 of the general lay-out of the experimental apparatus.

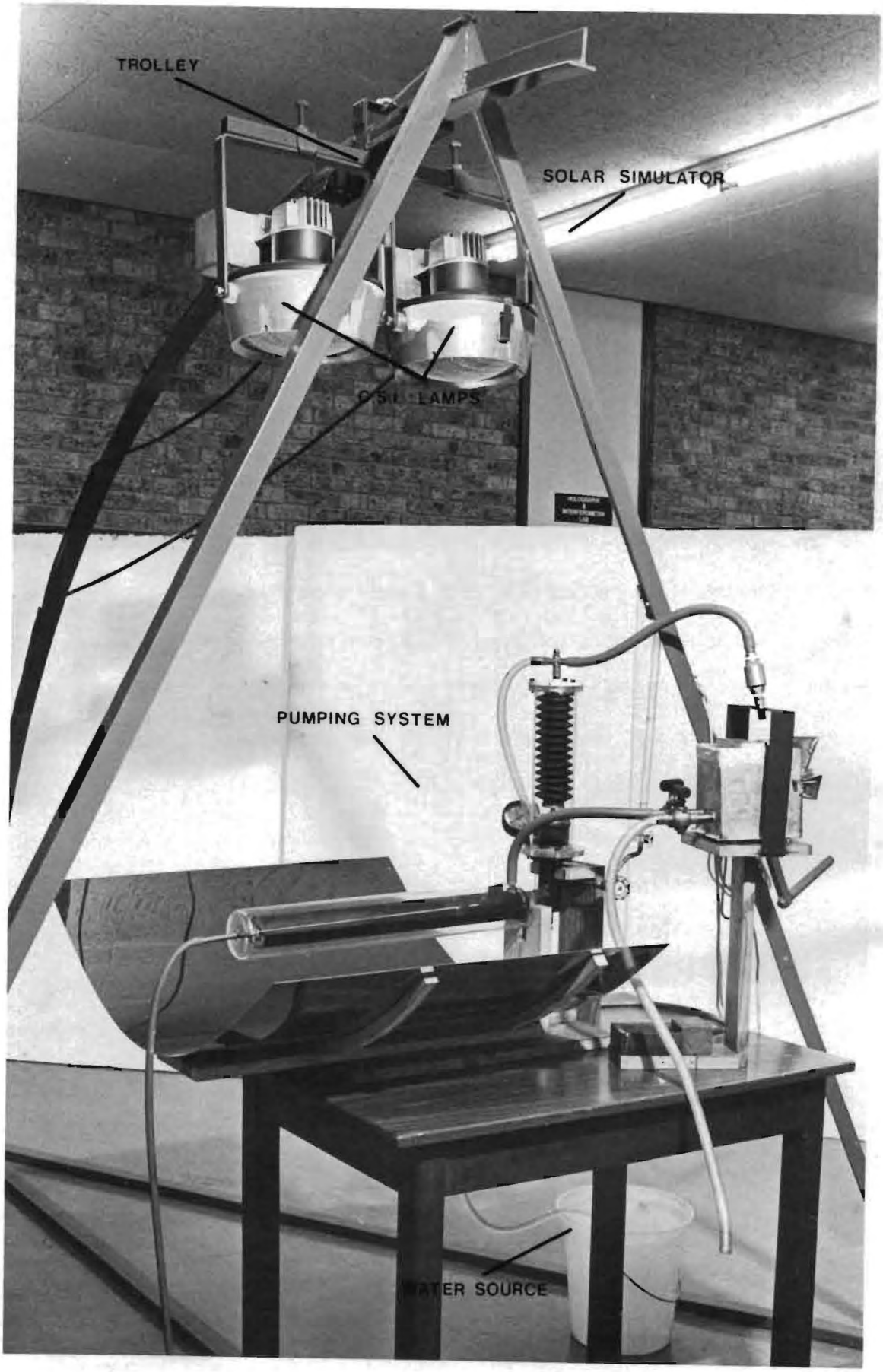

Photograph 2.2 General layout of apparatus

CHAPTER 3

THEORETICAL ANALYSIS

3.1/ DESCRIPTION OF THE THERMODYNAMIC CYCLE AND ANALYSIS

The pump's operation can be described by means of a thermodynamic cycle as follows:

Before the collector is exposed to the solar radiation, the temperature of the system and of the working fluid is equal to the ambient temperature. At this stage, bellows no.1 are collapsed and the volume of the receiver is V_1. When the receiver starts absorbing radiation, heat is transfered to the working fluid increasing its pressure, temperature and internal energy. However, the pressure in the receiver is still less than the necessary pressure P_2 to expel the water out of bellows no.2 into the over-balanced mechanism. Therefore we have a constant volume process, until the pressure equals P_2 (point 2 in figure 3.1).

When the pressure in the receiver becomes slightly greater than P_2, bellows no.1 start expanding, pushing the water out of bellows no.2. This expansion lasts until the desired volume of water (V_d) is discharged into the over-balanced mechanism. At this state, (point 3 in figure 3.1) the volume of the working fluid is:

$$V_3 = V_1 + V_d$$

During the expanding movement of bellows no.1, the pressure in the receiver remains constant, so the process 2-3 is an isobaric one.

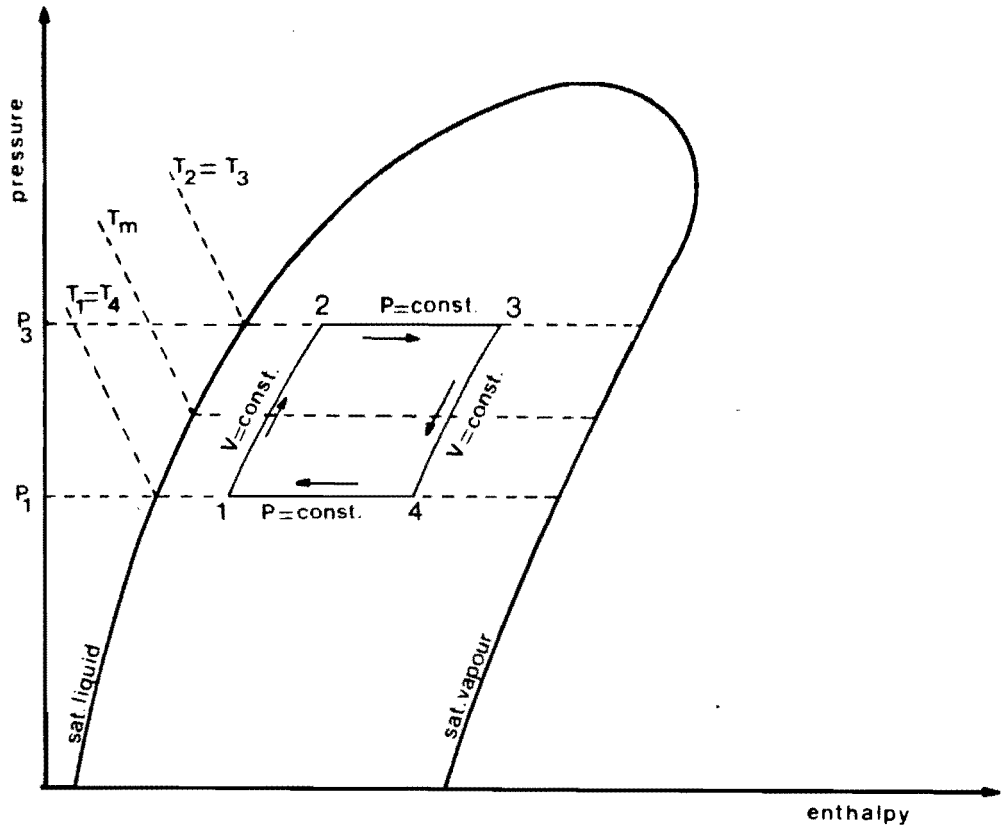

Figure 3.1 Thermodynamic cycle.

Having obtained the desired amount of water in the over-balanced mechanism, some of the water is now diverted through the cooling system, where heat is rejected from the working fluid, thus decreasing its temperature and pressure. As long as the pressure in the receiver is greater than P_4, (the necessary pressure to draw the water in the cylinder from the water source) bellows no.1 remain expanded (ie. constant volume process).

When the working fluid's pressure becomes slightly less than P_4 (point 4 in figure 3.1), contraction of bellows no.1 begins. Mechanical work is generated and water is drawn into bellows no.2. While bellows no.1 contract,the pressure in the receiver remains constant. The amount of the cooling water is regulated so that the cooling process is terminated, only when the necessary volume of water is drawn into bellows no.2 (point 1 in figure 3.1). The process 4-1 is an isobaric one.

Before proceeding to the calculations of the heat requirements, let us consider that the working fluid belongs to a thermodynamic system, whose boundaries are the receiver and bellows no.1. Since the system does not admit the transfer of mass across its boundaries, it is a closed thermodynamic system. The energy equation for this system -see J.Holman (31)- can be written as:

$$d'q + d'w = du \qquad 3.1$$

For the analysis, the following sign convention was adopted:

"Work and heat when added to the system are positive."

From the defining equations of enthalapy and work, the following expressions will be used:

$$dh = du + pdv + vdp$$

$$dw = pdv$$

Applying equation 3.1 to the cycle, as depicted in figure 3.1, the following equations per unit mass of working fluid are derived:

Process 1-2:

v=constant..... $q_{12} = h_2 - h_1 - v_1 \cdot (P_2 - P_1)$ 3.1.a

Process 2-3:

P=constant..... $q_{23} = h_3 - h_2$ 3.1.b

Process 3-4:

v=constant..... $q_{34} = - \left[h_3 - h_4 - v_3 \cdot (P_3 - P_1) \right]$ 3.1.c

Process 4-1:

P=constant..... $q_{41} = - (h_4 - h_1)$ 3.1.d

For the cycle ~~is~~:

Heat added:

$$q_{add} = q_{12} + q_{23} = h_3 - h_1 - v_1 \cdot (P_3 - P_1) \qquad 3.2$$

Heat rejected:

$$q_{rej} = q_{34} + q_{23} = - \left[h_3 - h_1 - v_3 \cdot (P_3 - P_1) \right] \qquad 3.3$$

Work output:

$$w = q_{add} + q_{rej} \qquad 3.4$$

$$= (v_3 - v_1) \cdot (P_3 - P_1)$$

Cycle thermal efficiency:

$$\eta_c = \frac{w}{q_{add}} \qquad 3.5$$

$$= \frac{(v_3 - v_1) \cdot (P_3 - P_1)}{h_3 - h_1 - v_1 \cdot (P_3 - P_1)}$$

3.2. HEAT TRANSFER ANALYSIS

In the previous chapter, we introduced the description of the experimental model of the solar pump, employed in this study. In this section we will proceed to develop the equations describing the heat transfer processes taking place while the system is pumping water.

From the description of the system's operation, it is evident that the heat transfer processes occur in different stages. For example, for a certain period of time, emphasis may be placed on the heating cycle, which results in the delivery of the water. Later, when this pumping action comes to an end, the emphasis may be shifted to the cooling process, which results in the suction of the water. Yet it is obvious, that during the cooling operation, the heating process continues.

The general equation for the heat balance of the system at a given instant is:
(input heat)=(heat losses)+(change of internal energy of the system) or:

$$Q_{in,s} = Q_{l,s} + \delta U_s \qquad 3.6$$

The input heat is the net heat transfer by radiation reflected by the reflector and arriving at the cover.
Heat losses are from the cover and bellows no.1 to the

enviroment as well as from the cooling system.

The internal energy of the system (U_s) consists of the internal energies of the cover (U_c), receiver (U_r), cooling system (U_p), bellows (U_b), and working fluid (U_f).

Before proceeding to a detailed heat transfer analysis of the system, the following assumption was made:

Conduction through the cover's wall, the receiver, the cooling system's pipes and the bellows is negligible, ie:

$$T_{co} = T_{ci} = T_c \qquad T_{ro} = T_{ri} = T_r$$

$$T_{po} = T_{pi} = T_p \qquad T_{bo} = T_{bi} = T_b$$

Energy balance for the cover.

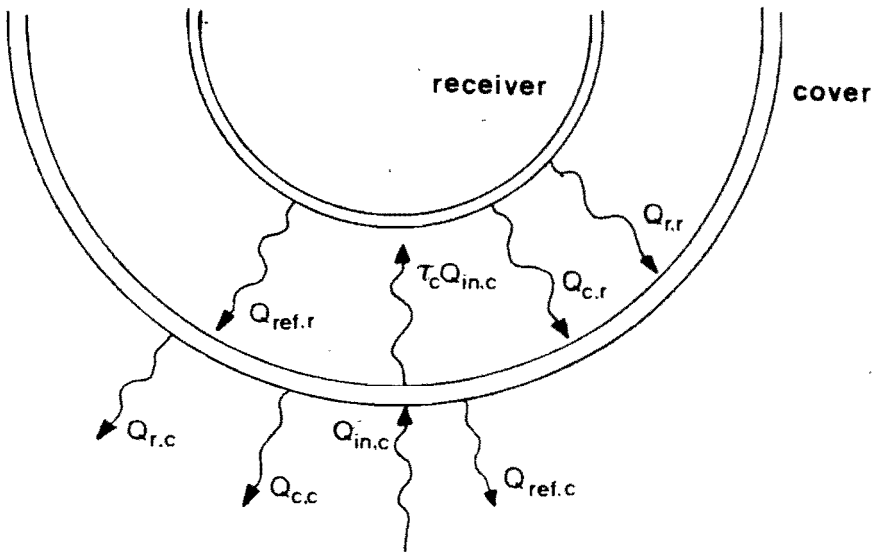

Figure 3.2 Energy balance for the cover

The input energy is the incident radiation plus the heat transfered from the receiver. (figure 3.2)
The radiation reflected by the reflector and arriving at the cover, at a given instant is given by:

$$Q_{in,c} = \gamma \cdot I_a \qquad 3.7$$

A small portion of it will be absorbed, some will be reflected, and the rest will be transmitted to the receiver. Heat transfered from the receiver to the cover, at a given instant, is due to radiation ($Q_{r,r}$), and convection ($Q_{c,r}$).

$$Q_{r,r} = h_{r,r} \cdot (T_r - T_c) \qquad 3.8$$

$$Q_{c,r} = h_{c,r} \cdot (T_r - T_c) \qquad 3.9$$

where:

$$h_{r,r} = \left(\frac{1}{\epsilon_r} + \frac{1}{\epsilon_c} - 1 \right)^{-1} \frac{T_r^4 - T_c^4}{T_r - T_c} \qquad 3.10$$

as recomended by A.Rabl (14), and

$$h_{c,r} = \frac{k}{r_c - r_r} \cdot 0.55 \cdot \left[Pr \cdot g \cdot \beta \cdot (r_c - r_r)^3 \cdot \frac{T_r - T_c}{V^2} \right]^{1/4} \qquad 3.11$$

for free convection in horizontal cylindrical enclosures, as recomended by Evans and Stefany (32). The properties of air are evaluated for the mean temperature:

$$T_{m,a} = \frac{T_r + T_c}{2}$$

The reflected radiation from the receiver to the cover is:

$$Q_{ref,r} = \rho_r \cdot \tau_c \cdot \gamma \cdot I_a \qquad 3.12$$

which is assumed to be absorbed completely by the cover (long-wave radiation blocked by glass).

Heat losses from the cover to the enviroment, are due to convection ($Q_{c,c}$) and radiation ($Q_{r,c}$). (figure 3.2)

$$Q_{c,c} = h_{c,c} \cdot (T_c - T_a) \qquad 3.13$$

$$Q_{r,c} = h_{r,c} \cdot (T_c - T_a) \qquad 3.14$$

where:

$$h_{r,c} = F_{c-a} \cdot \sigma \cdot \epsilon_c \cdot \frac{T_c^4 - T_a^4}{T_c - T_a} \qquad 3.15$$

$$h_{c,c} = 1.32 \cdot \left(\frac{T_c - T_a}{d_c} \right)^{1/4} \qquad 3.16$$

for free convection from horizontal cylinder to air and for laminar flow, as recomended by J.Holman (33).

For the cover, the change in internal energy is given by:

$$\delta U_c = (mc_p)_c \cdot \frac{\delta T_c}{\delta t} \qquad 3.17$$

The resulting energy balance for the cover is:

$$\gamma I_a + \gamma \rho_r \tau_c I_a + (T_r - T_c) \cdot (h_{r,r} + h_{c,r}) =$$

$$= (T_c - T_a) \cdot (h_{r,c} + h_{c,c}) + \tau_c \gamma I_a + \rho_c \cdot \gamma I_a + (mc_p)_c \cdot \frac{\delta T_c}{\delta t} \qquad 3.18$$

Energy balance for the receiver.

The input energy, to the receiver, is the energy transmitted through the cover, arriving at the receiver's surface under the assumption of nill multiple internal reflections or losses. (figure 3.3)

$$Q_{in,r} = \tau_c \cdot \gamma \cdot I_a \qquad 3.19$$

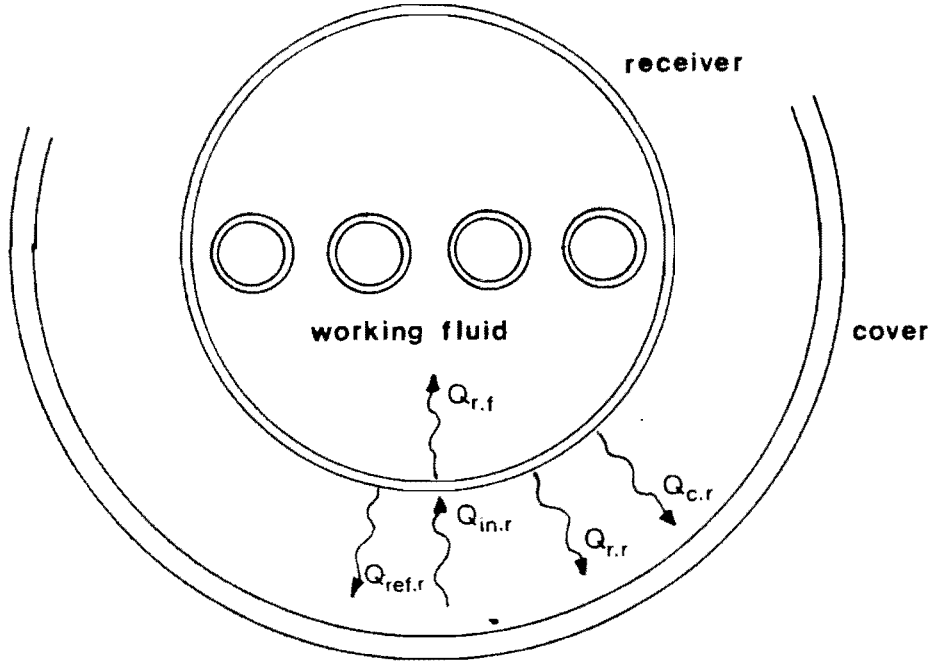

Figure 3.3 Energy balance for the receiver.

The heat losses from the receiver to the cover (as described previously) are given by equations 3.8, 3.9, and 3.12.

Heat transfer from the receiver to the working fluid is assumed to be only due to convection (boiling).

$$Q_{r,f} = h_{r,f} \cdot (T_r - T_f) \qquad 3.20$$

(the heat transfer coefficient in equation 3.20 could be evaluated from boiling heat transfer conciderations; however, it is unecessary, since it is not used in the final equation 3.40)

The change in internal energy is:

$$\delta U_r = (mc_p)_r \cdot \frac{\delta T_r}{\delta t} \qquad 3.21$$

resulting in the following equation for the energy balance:

$$\gamma \cdot \tau_c \cdot I_a = (T_r - T_c) \cdot (h_{r,r} + h_{c,r}) + h_{r,f} \cdot (T_r - T_f) + (mc_p)_r \cdot \frac{\delta T_r}{\delta t} \qquad 3.22$$

Energy balance for the working fluid.

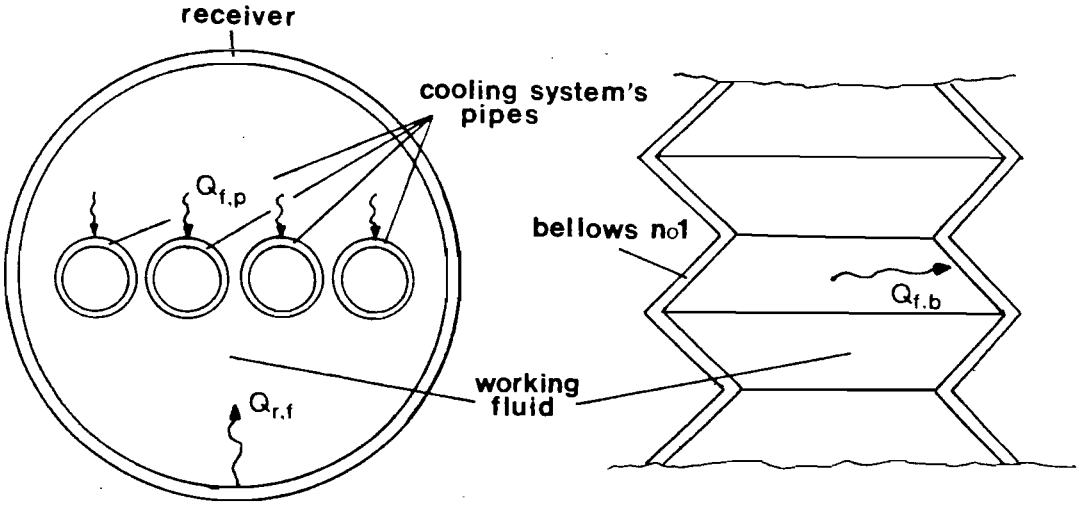

Figure 3.4 Energy balance for the working fluid.

The heat input to the working fluid is expressed by equation 3.20 (above).

The heat transfer to the cooling system and to bellows no.1, is both due to convection. (figure 3.4)

$$Q_{f,p} = h_{f,p} \cdot (T_f - T_p) \qquad 3.23$$

$$Q_{f,b} = h_{f,b} \cdot (T_f - T_b) \qquad 3.24$$

(similar comments for the heat transfer coefficients in equations 3.23 and 3.24 to those in equation 3.20 can be made)

For the working fluid, the change in internal energy is given by:

$$\delta U_f = (mc_p)_f \cdot \frac{\delta T_f}{\delta t} \qquad 3.25$$

and the working fluid's energy balance becomes:

$$h_{r,f} \cdot (T_r - T_f) = h_{f,p} \cdot (T_f - T_p) + h_{f,b} \cdot (T_f - T_b) + (mc_p)_f \cdot \frac{\delta T_f}{\delta t} \qquad 3.26$$

Energy balance for bellows no.1.

The input energy is by convection from the working fluid, and it is given by equation 2.24. The solar radiation impinging on bellows no.1 has been assumed negligible.

Heat losses from bellows no.1 to the enviroment, are due to convection ($Q_{c,b}$) and radiation ($Q_{r,b}$).

$$Q_{c,b} = h_{c,b} \cdot (T_b - T_a) \qquad 3.27$$

$$Q_{r,b} = h_{r,b} \cdot (T_b - T_a) \qquad 3.28$$

where, assuming the bellows to be a vertical cylinder, the radiation heat transfer coefficient is given by:

$$h_{r,b} = F_{b,a} \cdot \epsilon_b \cdot \sigma \cdot \frac{T_b^4 - T_a^4}{T_b - T_a} \qquad 3.29$$

and the convection heat transfer coefficient is given by Holman (33):

$$h_{c,b} = 1{,}32 \cdot \left[\frac{T_b - T_a}{L_b} \right]^{1/4} \qquad 3.30$$

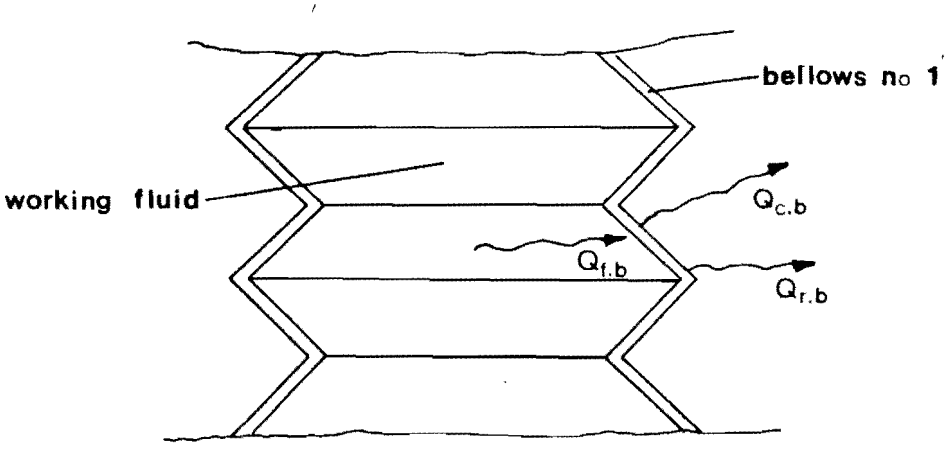

Figure 3.5 Energy balance for bellows no.1.

Since the length of bellows no.1 is not constant during the pumping process, the calculations were based on a

mean length defined as:

$$L_b = \frac{L_{open} + L_{close}}{2} \qquad 3.31$$

The change in internal energy is given by:

$$\delta U_b = (mc_p)_b \cdot \frac{\delta T_b}{\delta t} \qquad 3.32$$

and the energy balance equation is:

$$h_{f,b} \cdot (T_f - T_b) = (T_b - T_a) \cdot (h_{r,b} + h_{c,b}) + (mc_p)_b \cdot \frac{\delta T_b}{\delta t} \qquad 3.33$$

Energy balance for the cooling system.

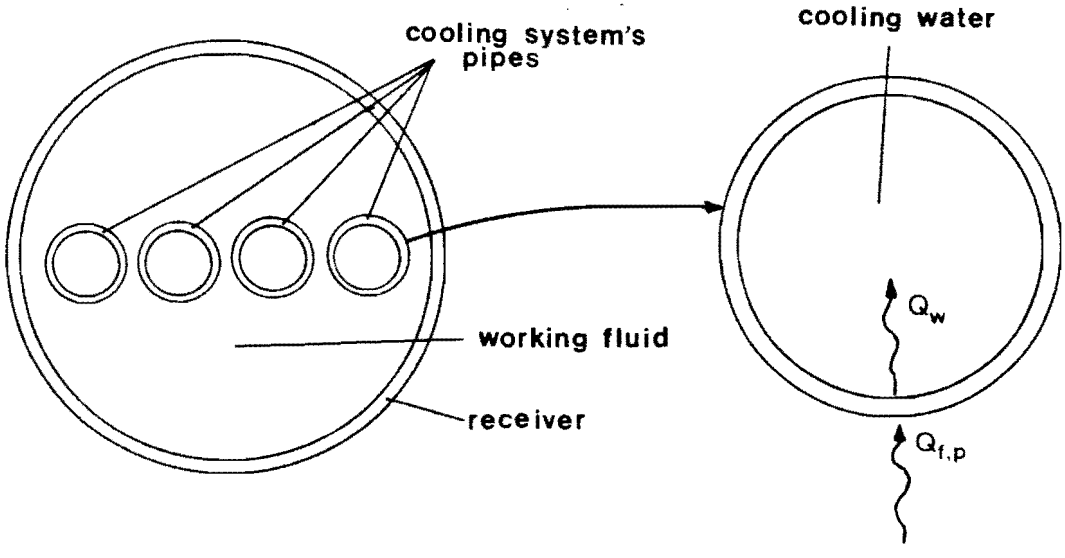

Figure 3.6 Energy balance for the cooling system.

The input heat is transfered from the working fluid by convection (condensation), and is given by equation 3.23.

Losses from the cooling system are, as seen in figure 3.6, only due to convection (Q_w). It is assumed that during the heating process, there is no heat loss through the air in the pipes of the cooling system (very low heat transfer coefficient of stagnant air inside the pipes). Therefore the heat losses from the cooling system are given by:

$$Q_w = h_w \cdot (T_p - T_w) \qquad 3.34$$

where:

$$h_w = \frac{k}{d_p} \cdot \frac{Re\ Pr\ d_p}{4\ L_p} \cdot \ln \left[1 - \frac{2.654}{p^{0.167} \cdot (Re \cdot Pr \cdot \frac{d_p}{L_p})^{0.5}} \right]^{-1} \qquad 3.35$$

for laminar flow inside short tubes as recomended by Kreith (34). The Reynolds number defined as:

$$Re = \frac{4 \cdot \dot{m}_{cw}}{n \cdot \mu \cdot d_p} \qquad 3.36$$

Properties of water are evaluated for the mean bulk temperature .

$$T_w = \frac{T_{w,in} + T_{w,out}}{2}$$

Finally, the cooling water outlet temperature is established from the energy balance equation:

$$n \cdot h_w \cdot n \cdot d_p \cdot L_p \cdot (T_p - T_w) = \dot{m}_{cw} \cdot (c_p)_w \cdot (T_{w,out} - T_{w,in}) \qquad 3.37$$

The change in internal energy for the cooling system is:

$$\delta U_p = (mc_p) \cdot \frac{\delta T_p}{\delta t} \qquad 3.38$$

and finally the energy balance equation is:

$$h_{f,p} \cdot (T_f - T_p) = h_w \cdot (T_p - T_w) + (mc_p)_p \cdot \frac{\delta T_p}{\delta t} \qquad 3.39$$

Based on the above analysis, an expression of the energy balance for the whole system can be obtained by combining equations 3.6, 3.7, 3.18, 3.22, 3.26, 3.33, and 3.39.

$$\gamma I_a = \rho_c \cdot \gamma \cdot I_a + (T_c - T_a) \cdot (h_{r,c} + h_{c,c}) + (T_b - T_a) \cdot (h_{c,b} + h_{r,b}) +$$
$$+ (mc_p)_c \cdot \frac{\delta T_c}{\delta t} + (mc_p)_r \cdot \frac{\delta T_r}{\delta t} + (mc_p)_f \cdot \frac{\delta T_f}{\delta t} + \qquad 3.40$$
$$+ (mc_p)_p \cdot \frac{\delta T_p}{\delta t} + (mc_p)_b \cdot \frac{\delta T_b}{\delta t} + h_w \cdot (T_p - T_w)^*$$

(* this term only applicable during the cooling process)

The above equation is further simplified according to the following assumptions:

1. The temperature of the working fluid is assumed very near that of the solid partitions (walls of reveiver, bellows and

pipes). During the boiling and condensation processes, the heat transfer coefficient is very high, of the order of 10^3 -10^4 $W/m^2\,^0C$, and since the net heat transfer between the working fluid and the system is of the order of 10^2 -10^3 $W/m^2\,^0C$, (estimated from appendix F), the temperature difference between the solid partitions and the working fluid is neglected ie:

$$T_r \simeq T_f \simeq T_p \simeq T_b$$

2. Because the system's temperature fluctuates between the temperatures coresponding to the pressures P_1 and P_3 (as indicated in figure 3.1), all heat transfer quantities will be evaluated at an average temperature, which in reference to figure 3.1 is defined as:

$$T_m = \frac{T_1 + T_3}{2} \qquad 3.41$$

According to the above assumptions, and using equation 3.18, equation 3.40 becames:

$$\eta_o \cdot I_a + Q_l + Q_w^* = (mc_p)\frac{\delta T_m}{\delta t} + (mc_p)_f \frac{\delta T_m}{\delta t} \qquad 3.42$$

where:

$$Q_l = (h_{r,r} + h_{c,r}) \cdot (T_r - T_c) + (h_{r,b} + h_{c,b}) \cdot (T_b - T_a) \qquad 3.43$$

$$(mc_p) = (mc_p)_r + (mc_p)_p + (mc_p)_b \qquad 3.44$$

Introducing the concept of the solar concentrator's optical efficiency, defined as:

$$\eta_o = \frac{Q_{abs,r}}{I_c} = \gamma \cdot \tau_c \cdot \alpha_r \qquad 3.45$$

equation 3.42 reduces to:

heating process:

$$\eta_o \cdot I_a + Q_l = (mc_p) \cdot \frac{T_3 - T_1}{t_{heat}} + Q_{add} \qquad 3.46.a$$

cooling process:

$$\eta_o \cdot I_a + Q_w + Q_l = (mc_p) \frac{T_1 - T_3}{t_{cool}} + Q_{rej} \qquad 3.46.b$$

where Q_{add} and Q_{rej} are given from equations 3.2 and 3.3 respectively.

3.3/ PROCEDURE TO PREDICT THE PUMP'S PERFORMANCE

The obvious question that we should be able to answer is HOW MUCH WATER does the pump deliver in a certain period of time. This is possible if the following data are known:

1. The volume of water pumped per cycle. (a characteristic of the pump's bellows displacement; a constant)
2. The area of the solar concentrator. (a physical parameter of the system; a constant)
3. The cooling water flow rate. (an experimentaly predetermined system's parameter; a constant)
4. The optical efficiency of the collector. (a predetermined parameter of the system)
5. Direct solar radiation impinging on the concentrator. (as calculated in appendix F, based on the time of the year in question)
6. The concentrator's position relative to the sun. (a parameter which may be set periodically by the user)
7. The total head requirements of the pumped water. (the user's requirement)

With the above data known, we proceed as follows:

Equations 3.46.a and 3.46.b can be rewritten:

$$t_{cool} = \frac{(mc_p)_s \cdot (T_3 - T_1) + |Q_{rej}|}{|Q_w + Q_{l,s}| - \eta_o \cdot I_a} \qquad 3.47.a$$

$$t_{heat} = \frac{(mc_p)_s \cdot (T_3 - T_1) + Q_{add}}{\eta_o \cdot I_a - |Q_{l,s}|} \qquad 3.47.b$$

where the variables T_1, T_3, Q_{add}, Q_{rej}, Q_l, Q_w can be calculated when the thermodynamic cycle is known (see previous sections 3.1, 3.2)

The cycle time is the sum of the times involved in the heating and cooling process.

$$t_c = t_{cool} + t_{heat} \qquad 3.48$$

The volume of water pumped per unit time is:

$$\dot{V}_d = \frac{V_d}{t_c} \qquad 3.49$$

and the pump's efficiency as defined:

$$\eta_p = \frac{\gamma_w \cdot H \cdot \dot{V}_d}{I_a} \qquad 3.50$$

The procedure is continued bearing in mind that:

i. The amount of water allowed to flow through the cooling system must be sufficient to condense the working fluid and thus collapse the bellows, specially during the time of

maximum or peak solar radiation.

ii. Because of practical considerations the cooling water adjustment could be effected as often as on a daily basis.

iii. Again because of practical and economical considerations the concentrator's position (tracking) could be effected as often as on a daily basis.

iv. Because of (i) above, it is obvious that during the off peak solar radiation periods, even on a daily basis, the cooling water will be in excess of that required for the ideal thermodynamic cycle depicted in figure 3.1. The excess water will result in "subcooling" the working fluid and consequently increase the gap between the minimum and the maximum cycle temperatures as shown in figure 3.7. The effect of this will be to alter the average temperature T_m as well as the heat requirements of the thermodynamic cycle. Consequently, the solution of the energy balance equations 3.47.a and 3.47.b which enable us to solve for the system's cycle time is affected.

For peak radiation conditions the pump works in an "ideal" thermodynamic cycle as depicted in figure 3.1. Points 1, 2, 3, 4 are depended only on the pump's characteristics as well as the pressure head (H). The thermodynamic cycle's heat requirements are calculated from equations 3.2 and 3.3. The time required for the cooling

process is found solving equation 3.47.a. Subsequently the volume of cooling water is established since the cooling water flow rate is an experimentally predetermined parameter of the system. Finally, the solution of equations 3.48, 3.49, and 3.50 gives the pump's performance for peak radiation conditions.

For off peak radiation conditions, the thermodynamic cycle is depicted in figure 3.7.

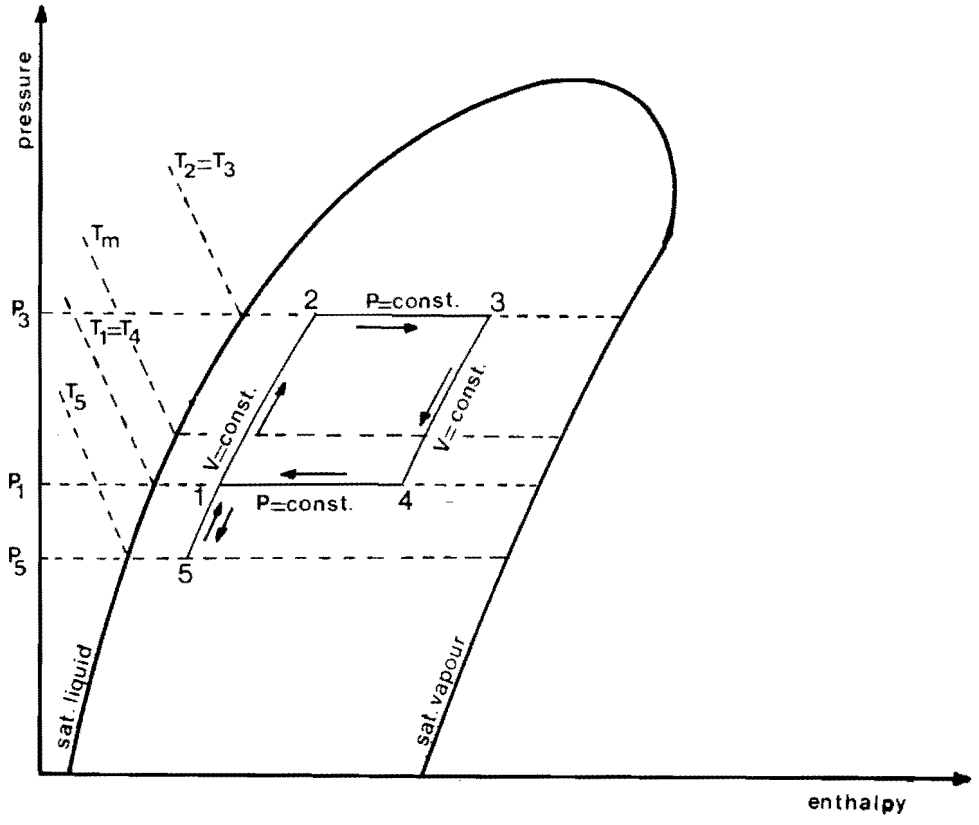

Figure 3.7 Thermodynamic cycle for off peak radiation conditions.

Points 1, 2, 3, 4 are the same as in the "ideal" cycle. However point 5 is the final state of the working fluid, as a result of "subcooling" due to relatively excessive cooling

for the given input solar radiation (obviously lower than peak). Since the time of the cooling process (t_{cool}) has already been established, equation 3.47.a can be solved by the following itterative technique. Assume a value for T_5, solve equation 3.47.a, and match the calculated value of the time of the cooling process (t_{cool}) with its already known value during peak conditions. Once T_5 has been established by the above technique, equation 3.47.b can be solved for the time of the cycle's heating process. Finally, by solving equations 3.49 and 3.50 the volume flow rate of the pumped water and the pump's efficiency can be calculated.

In order to clarify further how the above technique is applied, an numerical example in appendix F helps to explain the procedure in predicting the daily pump's capacity for a given day of the year.

3.4 PROCEDURE TO CALCULATE THE SYSTEM'S ADJUSTEMENTS AS REQUIRED BY A USER.

Two important features for the pump's operation are the concentrator's angular position (β), (tilt), and the amount of cooling water (V_{cw}). The former influences the radiation (I_a) impinging on the concentrator, while the later determines the heat rejected by the working fluid as well as the time of the cooling process (t_{cool}).

Both, the concentrator's tilt and the amount of the cooling water can be adjusted by the user in order to improve the pump's efficiency, and ensure trouble free operation. Tables are provided for the user, indicating how these adjustments should be done. These tables, based on the frequency of adjustments the user requires, are obtained in the following manner:

1. Frequency of system's adjustments.

For a given period of time, it is obviously desirable to maintain the concentrator's atitude with respect to the sun's rays at solar noon as perpendicular as possible, as shown in figure 3.8.

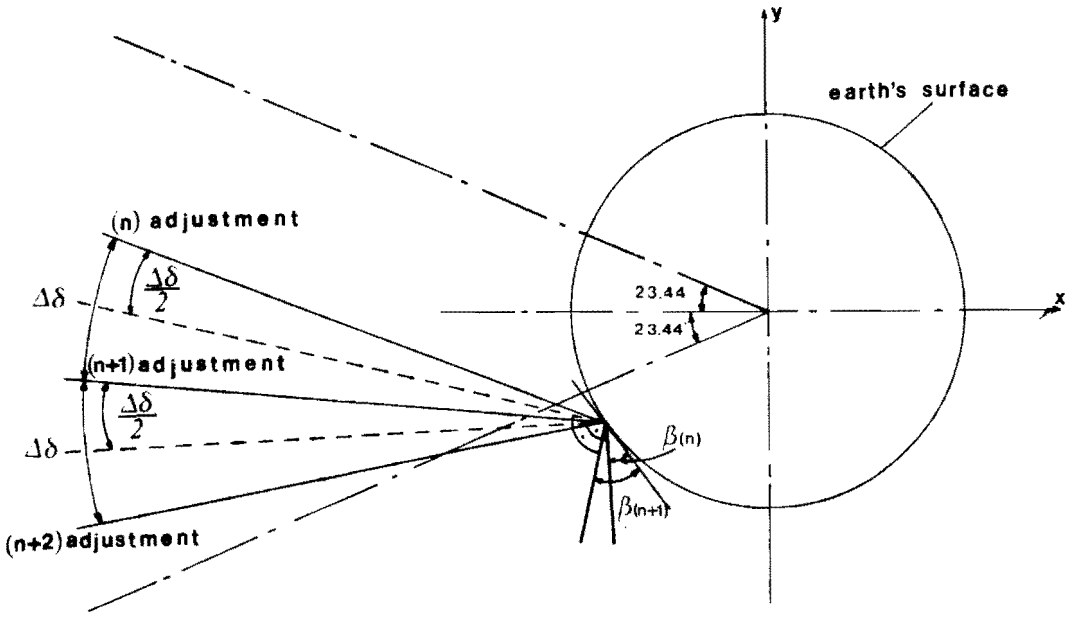

Figure 3.8 Concentrator's periodic adjustments.

During one year, the sun travels an angular distance of 4*23.44 degrees, where 23.44 degrees is the maximum absolute value of the solar declination. If n is the number of adjustments the user requires, then, in order to maintain the concentrator's position as perpedicular as possible to the sun's rays, the time between consecutive adjustments must be equal to the required time for the sun to travel an angular distance of

$$\Delta\delta = \left(\frac{4 \cdot 23.44}{n}\right) \qquad 3.51$$

For example, if the user requires twelve adjustments per year, the period between consecutive adjustments is the one,

during which the sun travels

$$\Delta\delta = \frac{4 \cdot 23.44}{12} = 7.81^0$$

Assume that the first adjustment is to be done at the winter solstice, ie the 21st of June, when the solar declination is

$$\delta_1 = 23.44^0$$

Then the second adjustment must be done on the day when the solar declination is

$$\delta_2 = 23.44 - 7.81 = 15.63^0$$

The number of this day, calculated from equation A.1, is 123 and the date, obtained from table A.1 is the 3rd of May.
The third adjustment must be done on the day when the solar declination is

$$\delta_3 = 15.63 - 7.81 = 7.82^0 \qquad \text{etc.}$$

2. Concentrator's tilt adjustment.

If D_a is the number of the day when an adjustment is required, and $\delta(D_a)$ is the solar declination for the same day, (see figure 3.9) the concentrator's tilt must be adjusted to be

$$\beta_a = \delta(D_a) + \frac{\Delta\delta}{2} - \varphi \qquad 3.52.a$$

from summer solstice to winter solstice, and

$$\beta_a = \delta(D_a) - \frac{\Delta\delta}{2} - \varphi \qquad 3.52.b$$

from winter solstice to summer solstice.

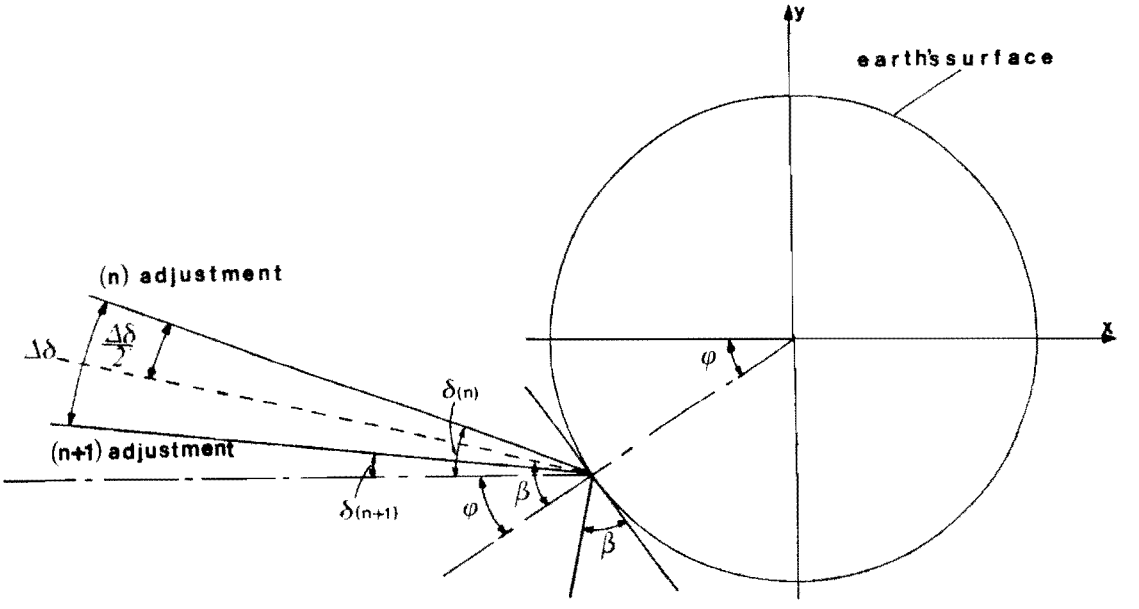

Figure 3.9 Typical concentrator's tilt adjustments.

To continue with the above example, at the first adjustment (the 21st of June) the concentrator's tilt must be adjusted to be

$$\beta_1 = [23.44 - \frac{7.81}{2} - (-26)] = 45.54^0$$

At the second adjustment the tilt must be

$$\beta_2 = [15.63 - \frac{7.81}{2} - (-26)] = 37.72^0$$

3. Cooling water volume adjustment.

In order to ensure that the amount of cooling water available for the heat rejection by the working fluid is

sufficient, specially during periods of maximum or peak insolation, the following procedure was adopted:

We assume that the maximum possible direct radiation on the earth's surface is constant, during the period between consecutive adjustments. (relatively short period of time and therefore similar radiation and atmospheric conditions) The maximum possible direct radiation, calculated from equation 1.2, reaches the reflector at the solar noon of the day when the solar declination, as shown in figure 3.9, is

$$\delta = \varphi + \beta \qquad 3.53$$

To continue with the same example, the maximum possible direct radiation for the period between the first and second adjustments is based on the day when the solar declination is

$$\delta = -26 + 45.54 = 19.54^{0}$$

This is the 138^{th} day of the year or the 18^{th} of May. At the solar noon of the above day the direct normal radiation, calculated from equation 1.2, is

$$I_{D,n} = 877.7 \ W/m^2$$

In order to illustrate further the above described procedure, a numerical example is given in appendix F.

CHAPTER 4

EXPERIMENTAL PROCEDURE AND RESULTS

4.1 PRELIMINARY EXPERIMENTS

With a rough idea of what the system should look like and how it would work, we proceeded in selecting the working fluid. The selection was done by consulting thermodynamic data of refrigerants and other fluids; such as boiling and condensing temperatures, specific volume changes etc.

For example, the boiling point of the working fluid should be preferably less than 100 ^{0}C in order to minimize the collector's demands in terms of heat losses, efficiency, necessity for selective surfaces etc. The condensing temperature should be around atmospheric temperature, or slightly higher, in order to ensure that the pumped water would have the ability to effect condensation of the working fluid. Further restrictions on the working fluid selection are considerations about corrosion to the metalic parts of the pump, possible molecular damage to the rubber bellows, and of course market availability as a whole.

A survey of fluids based on the considerations mentioned above yielded in our opinion three working fluids which

could be utilized in our system.

Freon 113 (Trichlorotrifluoroethane-$C_2Cl_3F_3$)

Methanol (Methyl alcohol-CH_3OH)

Cyclohexane (C_6H_{12})

In order to ascertain the optimum charge of working fluid within a given receiver, and appraise the pump's operation for each fluid, preliminary tests were performed in the manner described below:

A pump was constructed consisting of a receiver manufactured from brass tubing, rubber bellows attached to the receiver via a 90 degree brass tubing bend, an airtight cylinder placed over the bellows, and two non-return valves. The receiver was equiped with semi-cylindrical electrical heating elements placed along its entire lower half outer surface, thus simulating solar radiation input from a parabolic concentrator. The outer upper part of the receiver was covered with a cylindrical segment of brass tubing resulting into a passage where cooling water could pass in order to condense the working fluid. The 90 degree bend was equiped with thermocouples, one into the space of the working fluid, and the other on the outer surface of the brass tubing, a valve arrangement for the evacuation and charging of the cylinder, and a pressure gauge. The suction and delivery lines were equiped with commercially available low pressure drop non-return valves that were atached to the perspex cylinder. Figure 4.1 depicts a sketch of the preliminary testing apparatus.

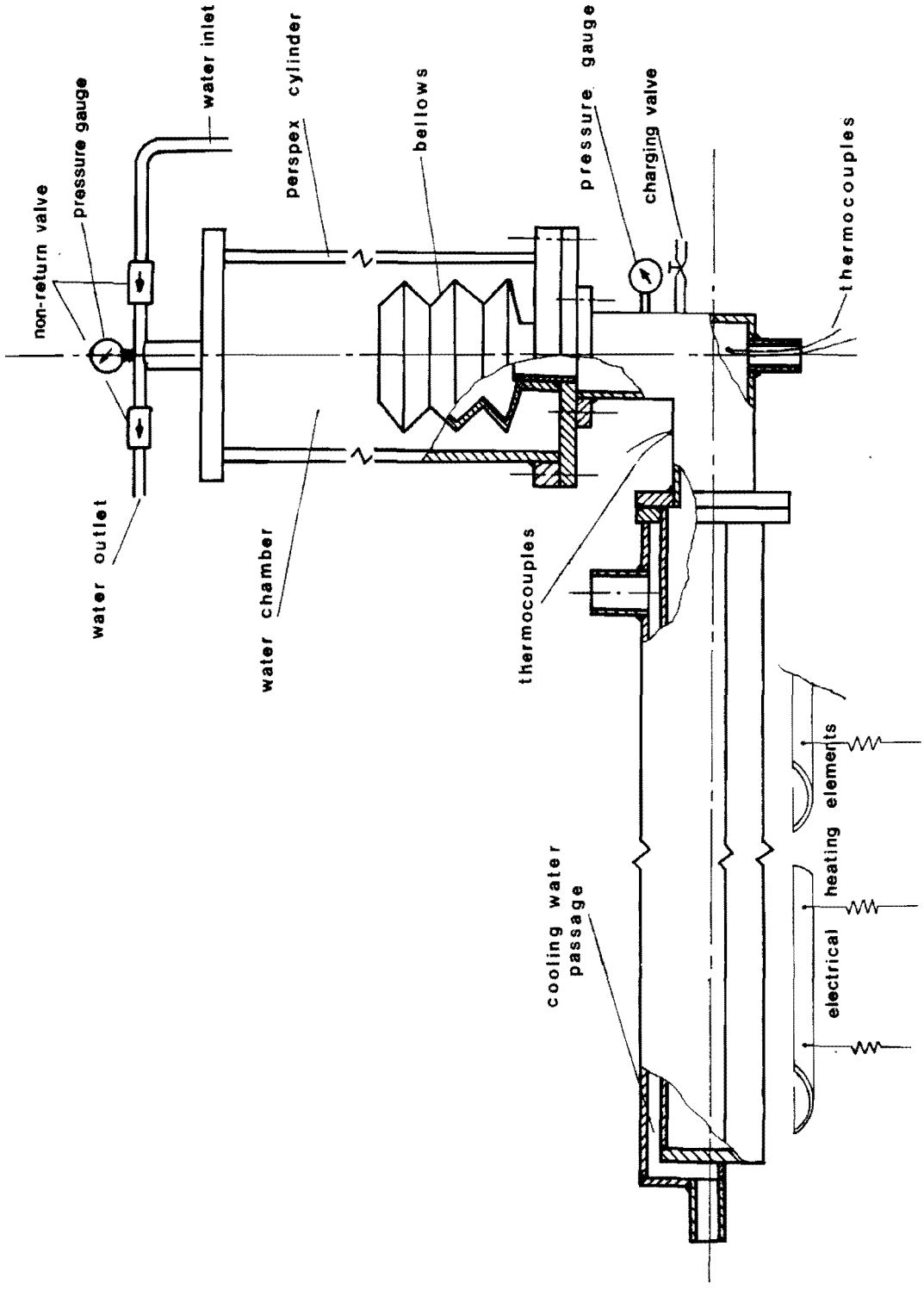

Figure 4.1 Sketch of preliminary testing apparatus

Assuming that parameters such as the amount of pumped water, the depth from which it was being pumped, as well as the rate at which heat could be absorbed by the receiver, influenced the optimum mass or charge of the working fluid, we proceeded to a numder of tests, the description of which, because of their volume and complexity is best given in a flow chart manner. (figure 4.2).

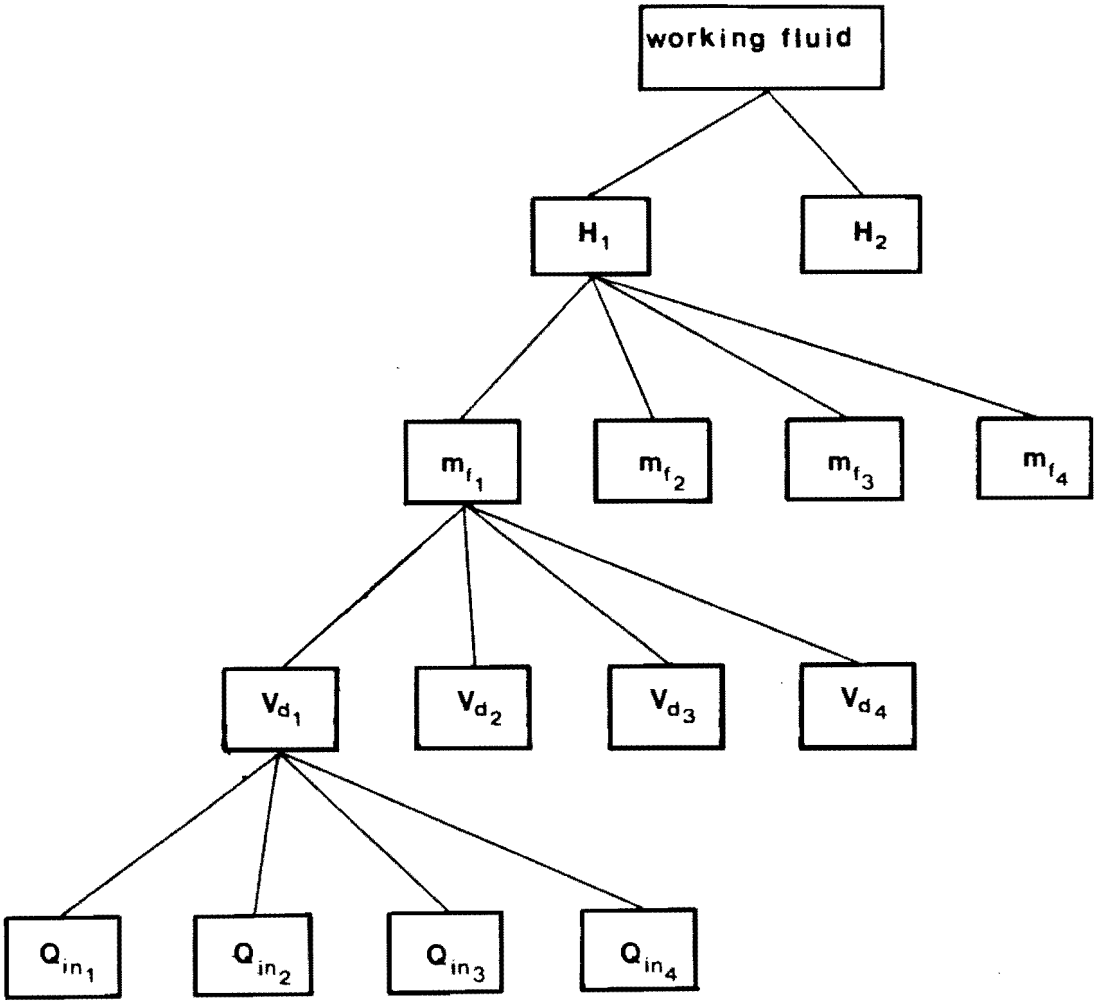

Figure 4.2 Flow chart of the sequence of the preliminary experiments.

For a given working fluid and a required head, different masses of fluid were charged in the receiver. For each charge, the volume displaced by the bellows was controlled with the minimum necessary constant temperature cooling water flow over the receiver. The amount of cooling water divided by the volume of water displaced by the bellows was defined as the "utilization ratio".

$$\lambda = \frac{V_{cw}}{V_d} \qquad 4.1$$

The minimum necessary cooling water was established for every parameter such as pressure head, heat input, charge etc. Cycle times were recorded as well as the pressures and temperatures of the working fluid, which incidently coincided with the fluid's thermodynamic data.

The results of all the above tests appear in the tables of appendix G, with the optimum conditions in heavy lined blocks, and serve to illustrate the following observations:

i. It appears that the optimum charge, or optimum mass of working fluid in the receiver for all three fluids was in the vicinity of 50 gr. The criteria used to establish this fact, were the combination of maximum water volume flow rate ($\dot{V}_d$) and the minimum utilization ratio (λ). This is easily established from the tables in appendix G as well as from typical graphs (figures 4.3 and 4.4).

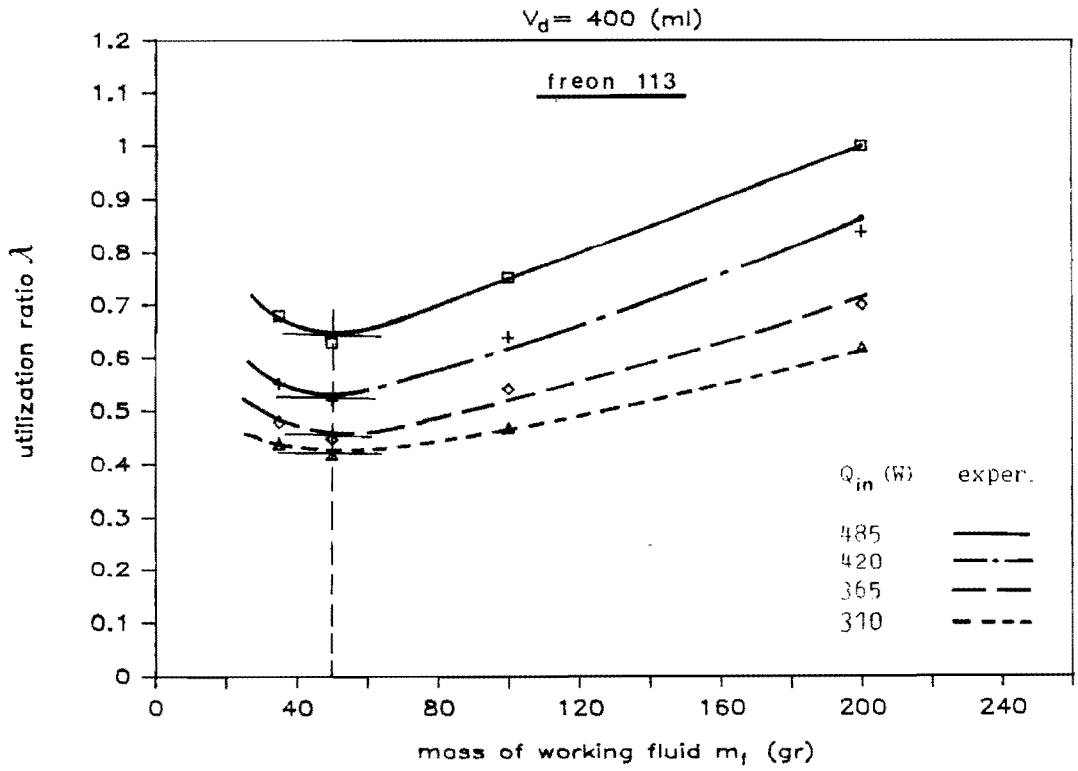

Figure 4.3 Utilization ratio versus mass of working fluid

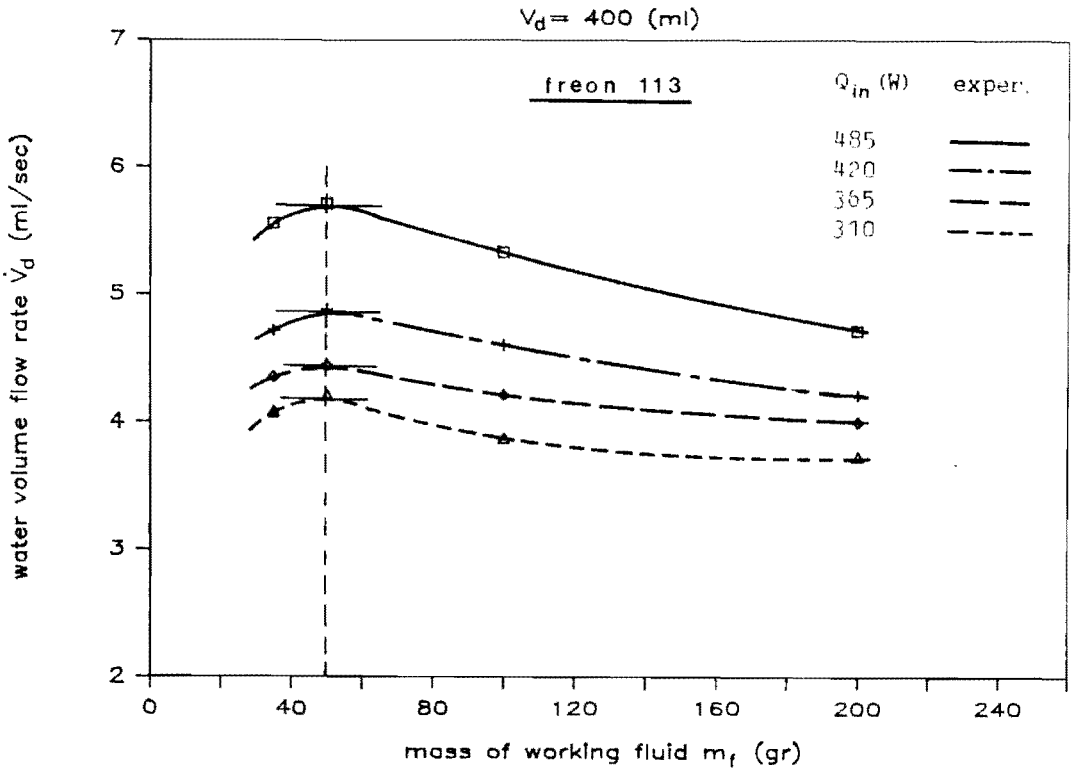

Figure 4.4 Water volume flow rate versus mass of working fluid

ii. The choice of the parameter $\dot{V}_d$, which is obtained when dividing the volume of water displaced by the cycle time observed, as one of the pump's optimum characteristics, is an obvious one.

iii. However the choice of the utilization ratio needs comment. Since some of the pumped water must be used in order to cool the receiver, it is obvious that when $\lambda=1$ the pump has reached its working limit. On the other hand if the pump is operating with a low utilization ratio it means that the excess available cooling water could be used to pump water from deeper reservoirs, since excess cooling water creates greater vacuum in the receiver (subcooling). Also from the point of view of the user there might be a reluctance or a necessity to avoid the use of the hot water, therefore low utilization ratio indicates larger quantities of cool usable water.

iv. When the minimum utilization ratio is plotted versus the pumped water volume flow rate, as well as versus the input heat requirements, (figures 4.5 and 4.6) it appears that the most desirable working fluid is the Cyclohexane.

v. However the above conclusion is ammended when the pumped water volume flow rate is plotted against input heat requirements (figure 4.7). Here it is seen that although considerable improvement in pumped water volume flow rate can be achieved by using cyclohexane as the working fluid, the heat input requirements become excessive.

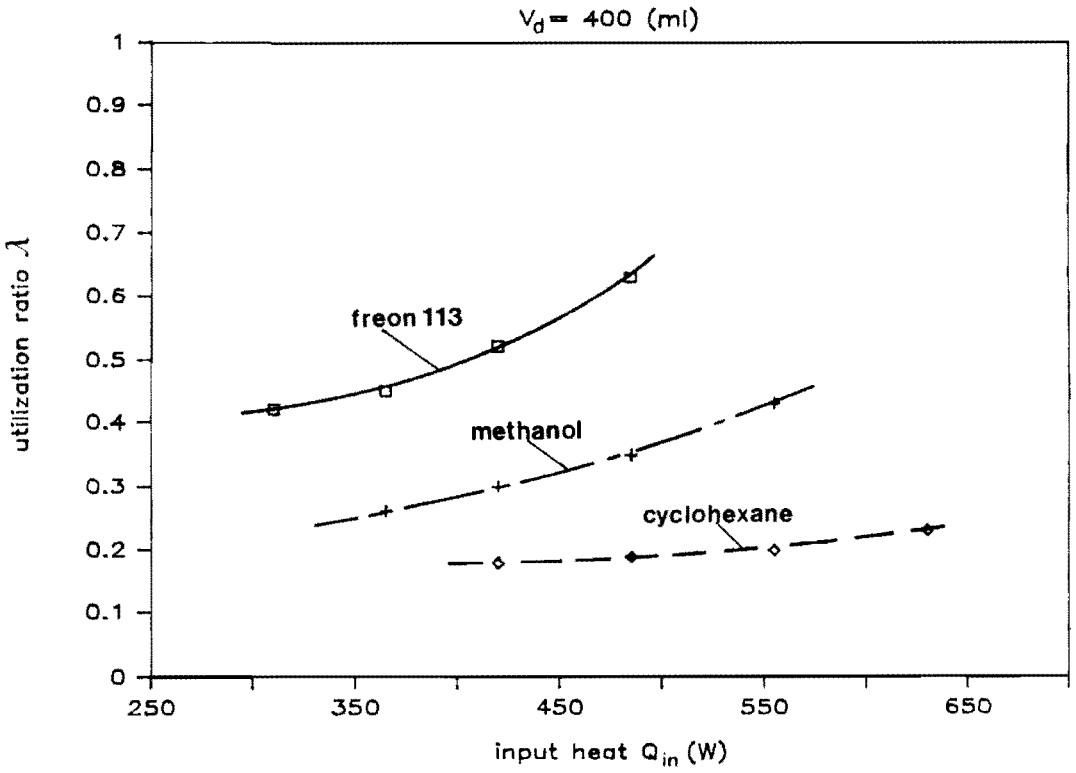

Figure 4.5 Utilization ratio versus input heat

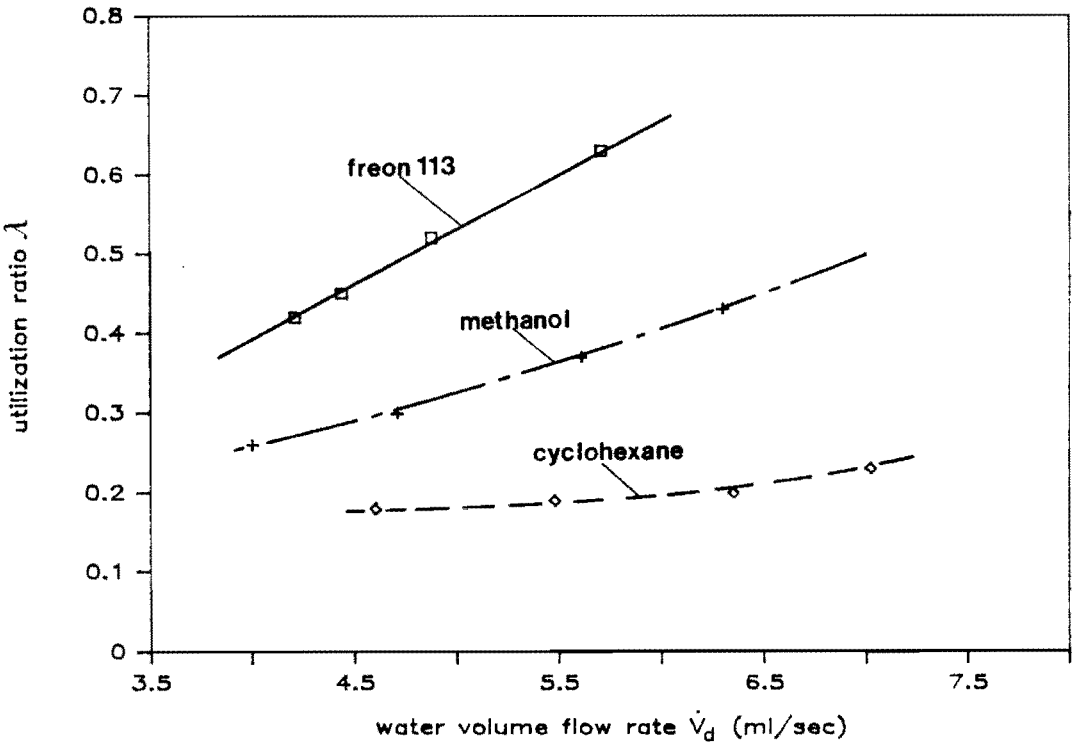

Figure 4.6 Utilization ratio versus water volume flow rate

This would necessitate larger and more sophisticated solar concentrators, a feature which we wish to avoid for economical reasons.

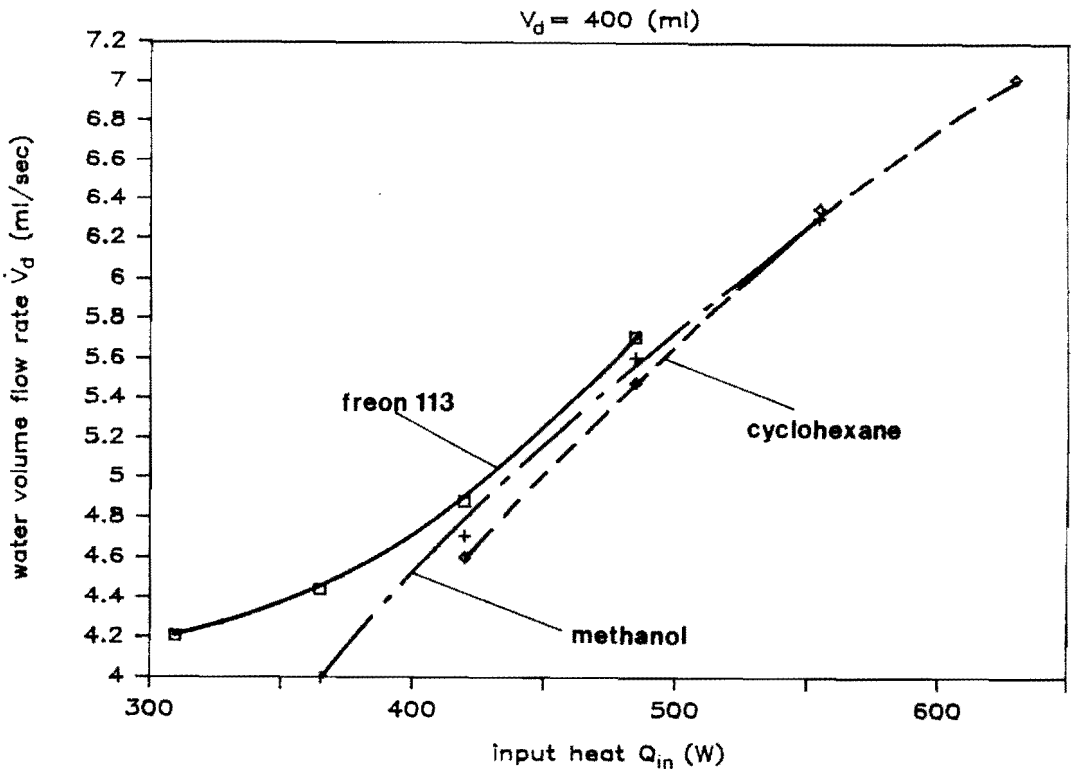

Figure 4.7 Water volume flow rate versus input heat.

vi. From figures 4.6 and 4.7 it is also seen that as the working fluid's boiling point approaches the ambient temperature, the input heat requirements are minimized; however the utilization ratio increases, thus rendering limitations to the depth from which water may be pumped.

4.2. COLLECTOR'S OPTICAL EFFICIENCY

As we have seen from the energy balance performed in chapter 3, a very important parameter of our system, which must be known, is the collector's optical efficiency as defined in equation 3.45. Bearing in mind that further experiments would have to be performed with the system as described in chapter 2, besides the previous section's preliminary tests, experiments were undertaken to establish the system's optical efficiency.

Unlike the previous tests where the heat input requirements were provided by electrical resistance heating, the system's receiver was now heated by the solar simulator's lights.

The optical efficiency has been defined as:

$$\eta_o = \frac{Q_{abs}}{I_a}$$

so if the energy absorbed by the receiver ($Q_{abs,r}$) could be measured for a given simulated radiation (I_a), the optical efficiency would be found. In addition to the "peak" efficiency measured at normal incidence, the angular responce of the concentrator must also be measured. In our

case, two angular variables must be taken into account, namely the angles θ_{xy} and θ_{yz} as shown in figure 4.8.

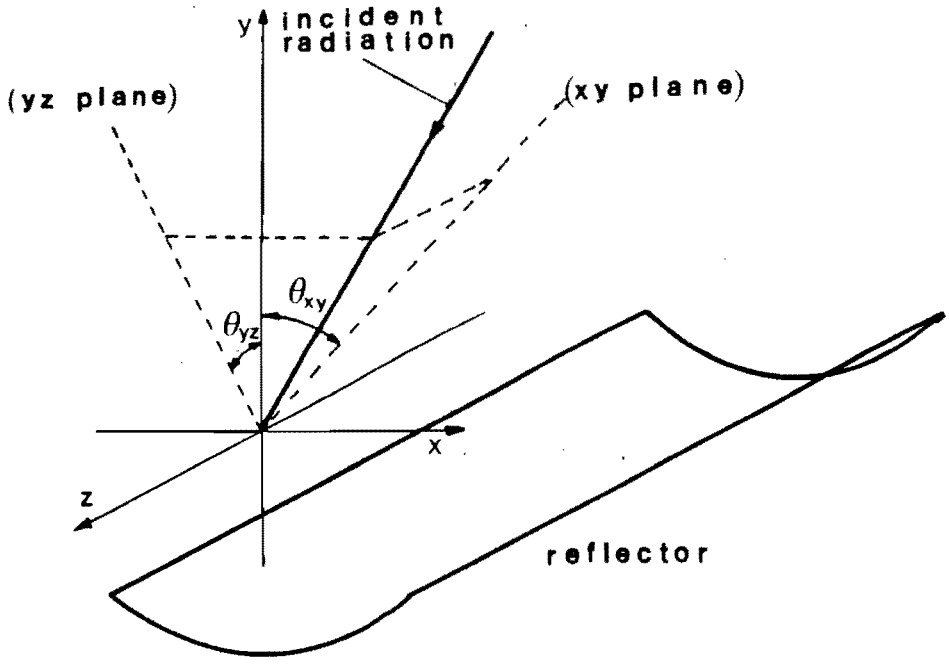

Figure 4.8 Angles θ_{xy} , θ_{yz}

The C.S.I. lamps, which were mounted on a trolley as described in more detail in section 2.3.6, provided the simulated direct insolation, which was measured using a solarimeter. Sample calculations for the direct simulated normal incidence radiation are found in appendix H.

For the purpose of establishing the energy absorbed by the receiver ($Q_{abs,r}$), the system's heat capacity was approximated as follows:

It was assumed that the bellows' heat capacity is negligible. The receiver, with a thermocouple attached on its surface, was covered with glass wool insulation so that the heat losses to the enviroment were minimized. Begining with the receiver evacuated and empty and its thermocouple indicating ambient temperature, 500 gr of 30°C hot water was introduced via the charging valve, and soon after, the equilibrium temperatures both in the water and on the receiver's surface were recorded. The energy balance between water and receiver yielded the receiver's heat capacity. (see appendix H)

Having established the receiver's heat capacity as described above, we proceeded to evaluate the optical efficiency as follows:
The receiver was partially filled with ambient temperature water, for the purpose of increasing its thermal inertia, and allowed to stand under the C.S.I. lights until its temperature rose slightly (2-3°C) above ambient level. The heat losses from the receiver to ambient were neglected, because of the small temperature differences involved. The receiver's temperature as well as the time required to reach this temperature, were recorded. The above procedure was repeated for various angles (θ_{xy}) and the data collected were used in equation H.3 in order to calculate the collector's optical efficiency. The results appear in figure 4.9 and detailed steps of sample calculations are found in appendix H.

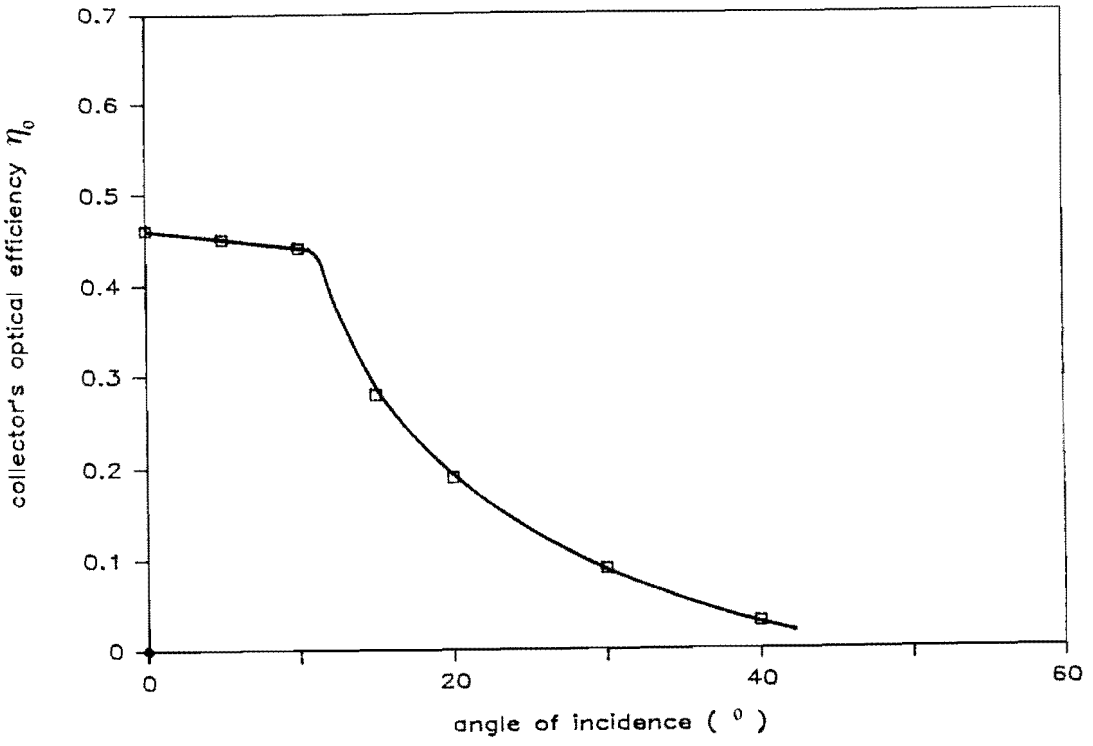

Figure 4.9 Collector's optical efficiency.

Unfortunately it was not possible to establish the collector's optical efficiency as a function of angle θ_{yz}, because the C.I.S. lights could not provide a uniform intensity field in the y-z plane, of sufficient large enough dimensions to encompass the system's collector.

4.3. FINAL EXPERIMENTS, RESULTS AND DISCUSSION.

4.3.1 In the previous sections the infuence of different variables, such as the mass of working fluid, volume of displaced water per cycle etc. on the pump's performance was investigated, and the system's optical characteristics were evaluated.

In this section we will proceed to investigate the actual pump's operation as a function of the parameters: utilization ratio (λ), pressure head (H), and sun's isnolation (I). The experiments were carried out using only two of the selected working fluids, namely Freon 113 and Methanol. The reason why the third fluid (Cyclohexane) was not used is that this fluid appeared to attack the rubber bellows after relatively short periods of contact.

The final tests were performed in the following manner: The system was charged with the optimum mass of working fluid. For a particular head, and volume of cooling water, the system's input radiation conditions were varied and cycle times as well as cooling water temperatures were recorded. The above process was repeated each time for different utilization ratios holding the pressure head constant, and subsequently again for various pressure heads. The results appear in appendix I and figures 4.10 to 4.27.

In order to check the validity of the analysis as developed in chapter 3, theoretical results are compared with the experimental ones in figures 4.10 to 4.17 for the case when Freon 113 is used as the working fluid. These results were obtained by applying the method explained in section 3.3.1. Unfortunately, lack of complete thermodynamic data precluded any direct comparison between experimental and theoretical results for Methanol.

Figures 4.10 to 4.13 depict the experimentally obtained results for volume flow rate vs. head, for Freon 113. In the same figures the theoretically predicted performance is shown so that direct comparison is possible. The agreement between theoretically predicted and experimentally obtained data appears to be very good on the whole, with the odd experimental data points showing errors between -7.3% and 4.7%.

In any given graph shown, it appears that for low heat inputs greater suction heads were experienced, however there is a trade off with the water volume flow rate, which appears to increase with higher heat inputs and decrease for the lower ones.

A similar trend appears to be also true when the results are compared for different utilization ratios. For example, whereas in figure 4.10 the span of suction heads is between 0.7m and 1.1m, in figure 4.13 it is shown to have increased for the same input conditions to between 1.3m and 1.8m,

however the volume flow rates have been decreased from between 2.8 ml/sec and 5.8 ml/sec to between 1.9 ml/sec and 4.4 ml/sec.

Figures 4.14 to 4.17 depict the theoretically predicted pump's efficiencies superimposed on the experimentally determined efficiency points, where very good agreement is noted. The results show that the efficiency curves are slightly heat input depended (lower efficiencies for lower heat inputs).

In figures 4.18 to 4.27 are shown the experimentally determined values for Methanol as the working fluid. Identical comments about the volume flow rates and suction heads can be made as previously were made for the case where the working fluid was Freon 113. As previously explained we find ourselves in the unfortunate position of not having detailed thermodynamic data for Methanol, hence no direct comparison with theoretical results is possible.

The results of figures 4.18 to 4.22 are identical in trend with the ones for Freon, however the results of figures 4.23 to 4.27, which pertain to the efficiencies, appear to have different trend to the ones shown for Freon 113 (figures 4.14 to 4.17), and we are at loss to explaine the reasons. It appears that the efficiency curves for Methanol are much more heat input dependent than the ones observed for Freon 113.

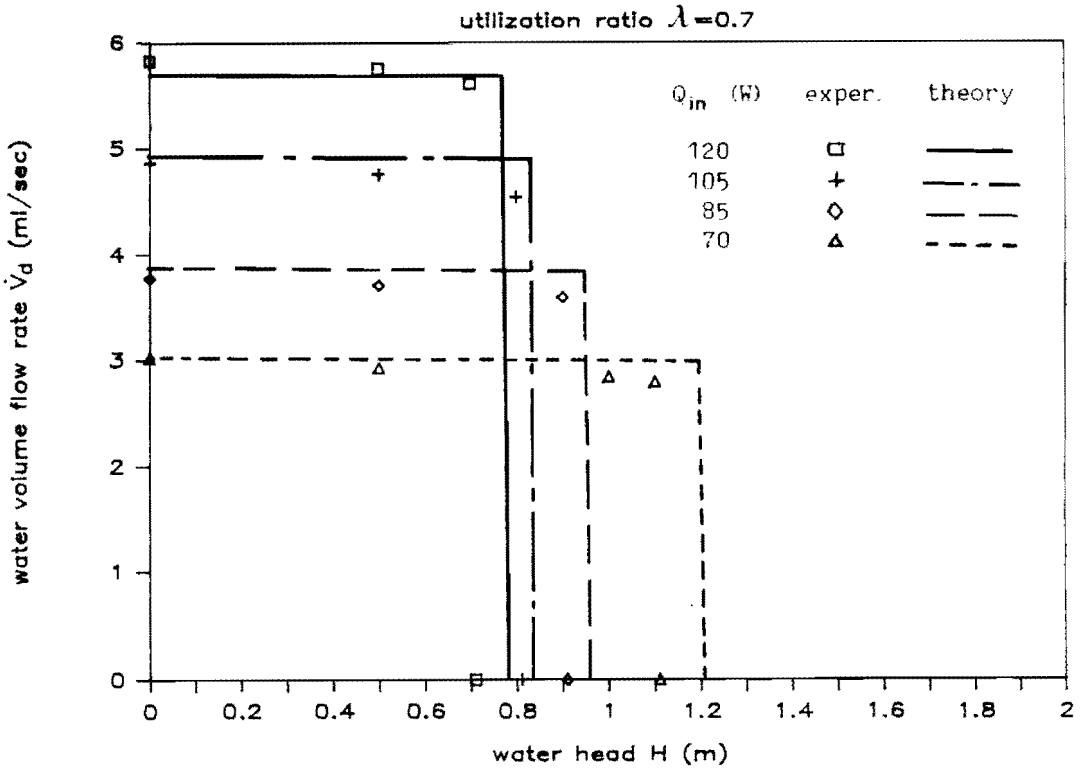

Figure 4.10 $\dot{V}_d$ -H diagram for Freon 113 (λ=0.7)

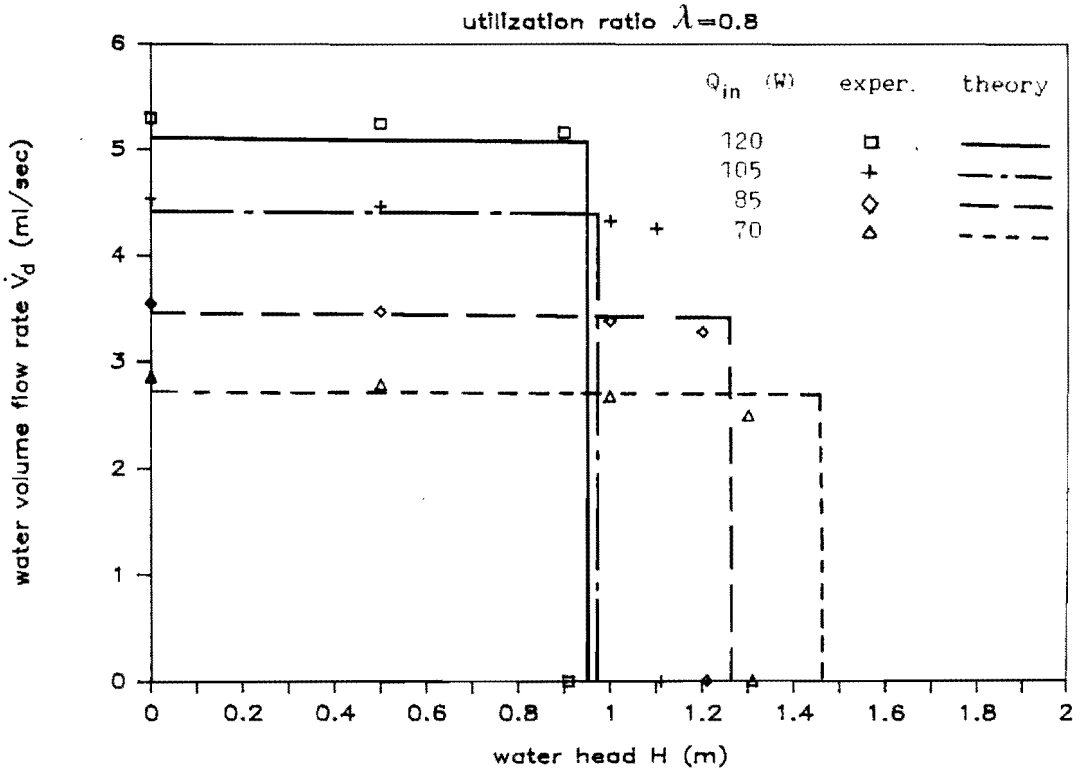

Figure 4.11 $\dot{V}_d$ -H diagram for Freon 113 (λ=0.8)

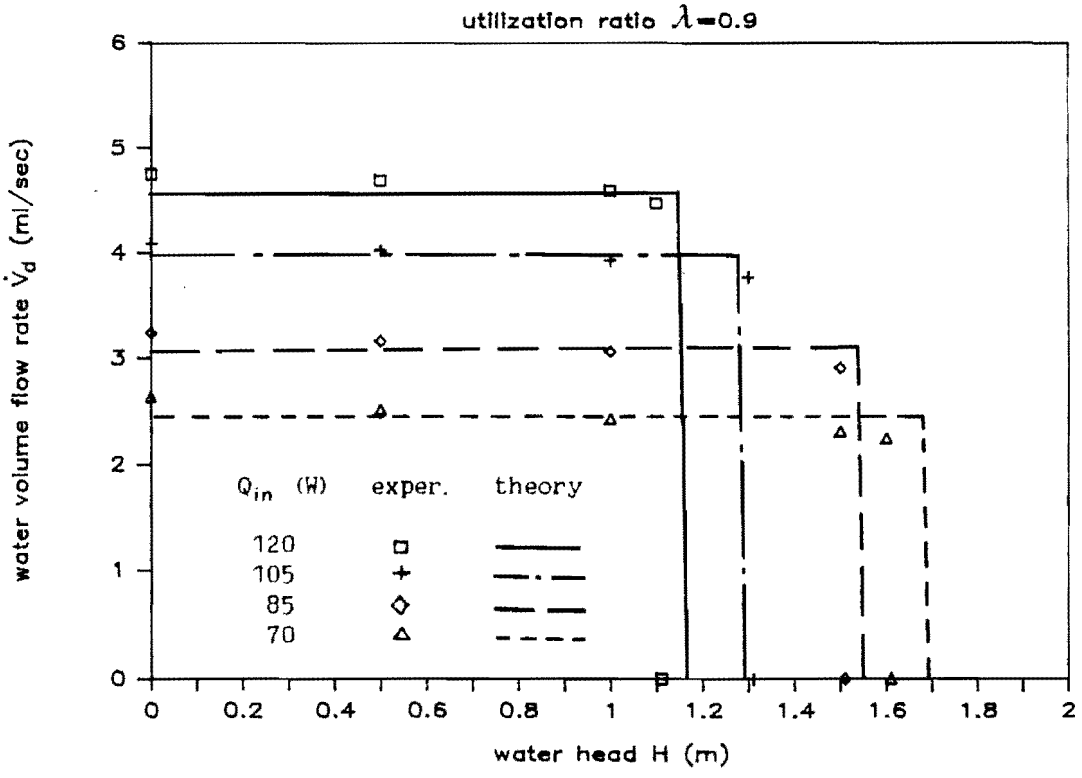

Figure 4.12 $\dot{V}_d$-H diagram for Freon 113 (λ=0.9)

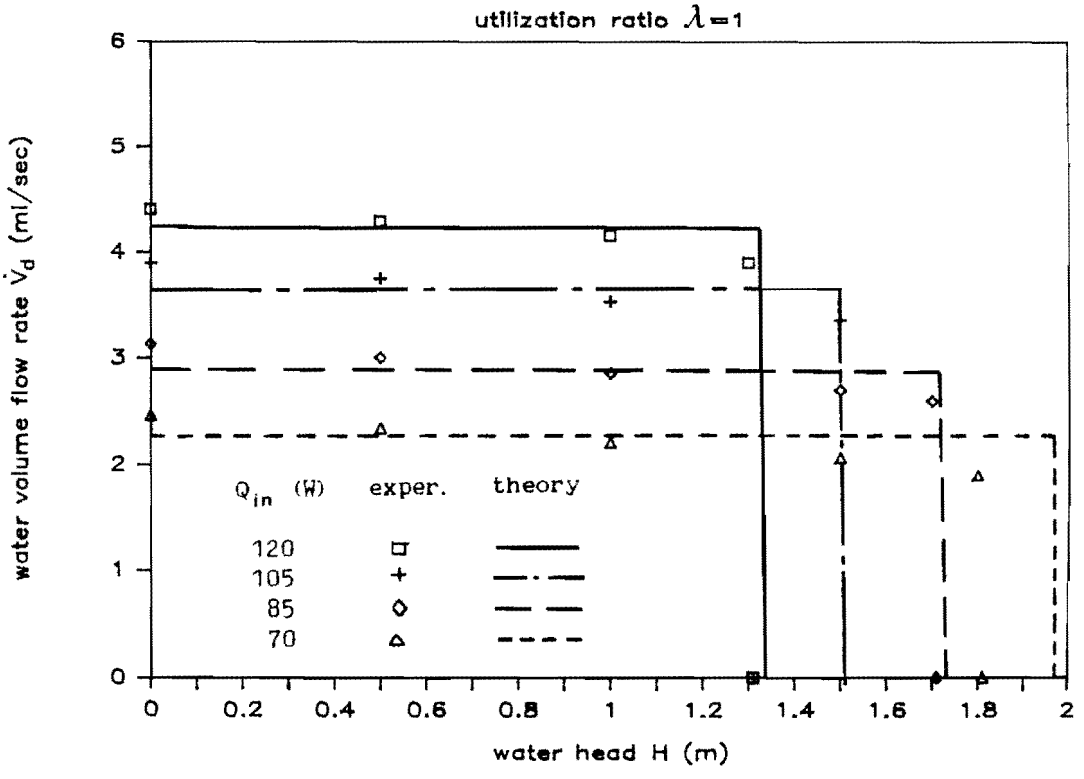

Figure 4.13 $\dot{V}_d$-H diagram for Freon 113 (λ=1.0)

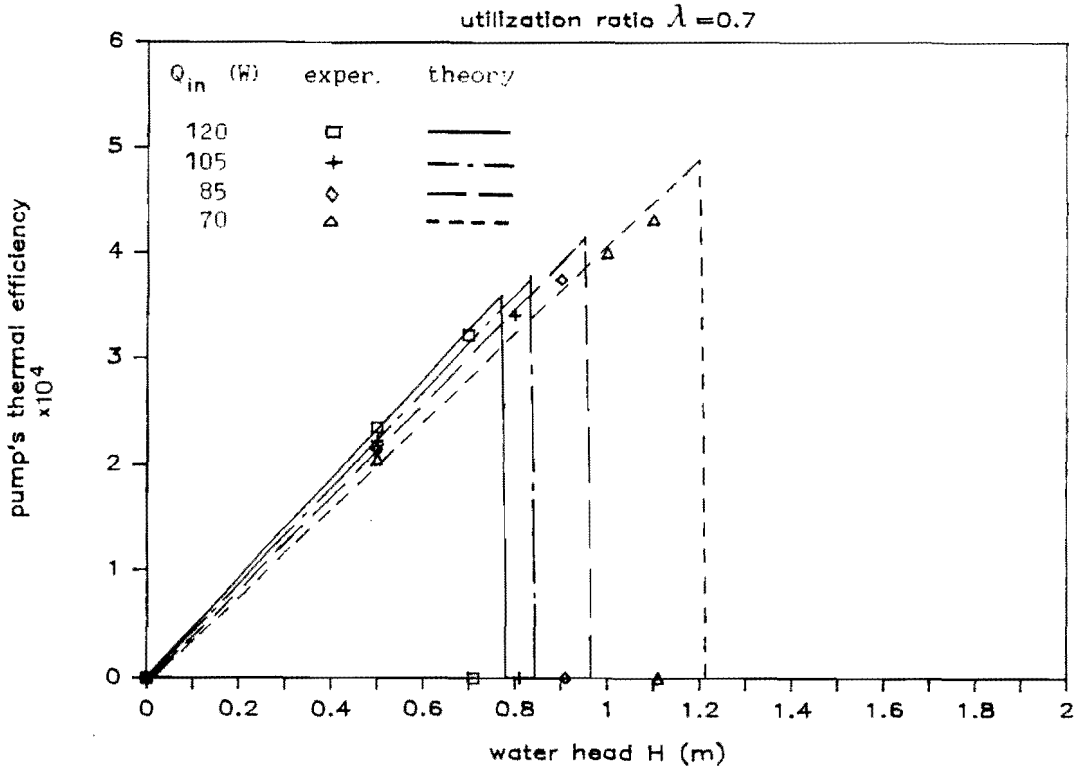

Figure 4.14 η_{th}-H diagram for Freon 113 (λ=0.7)

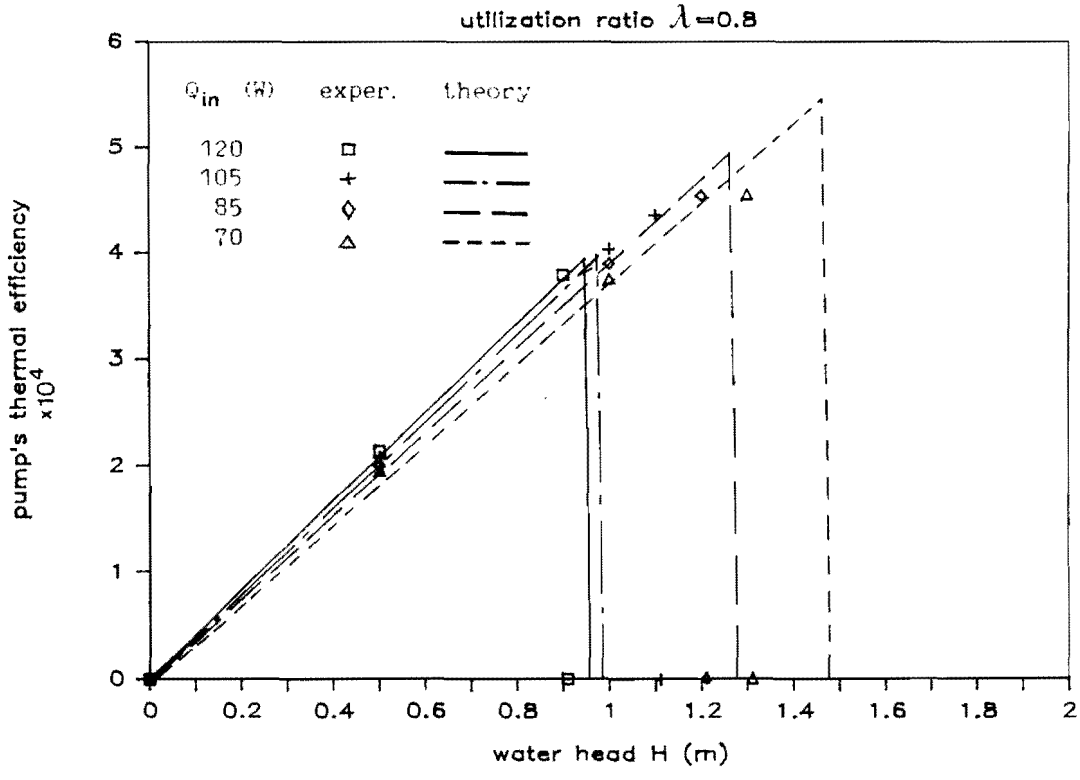

Figure 4.15 η_{th}-H diagram for Freon 113 (λ=0.8)

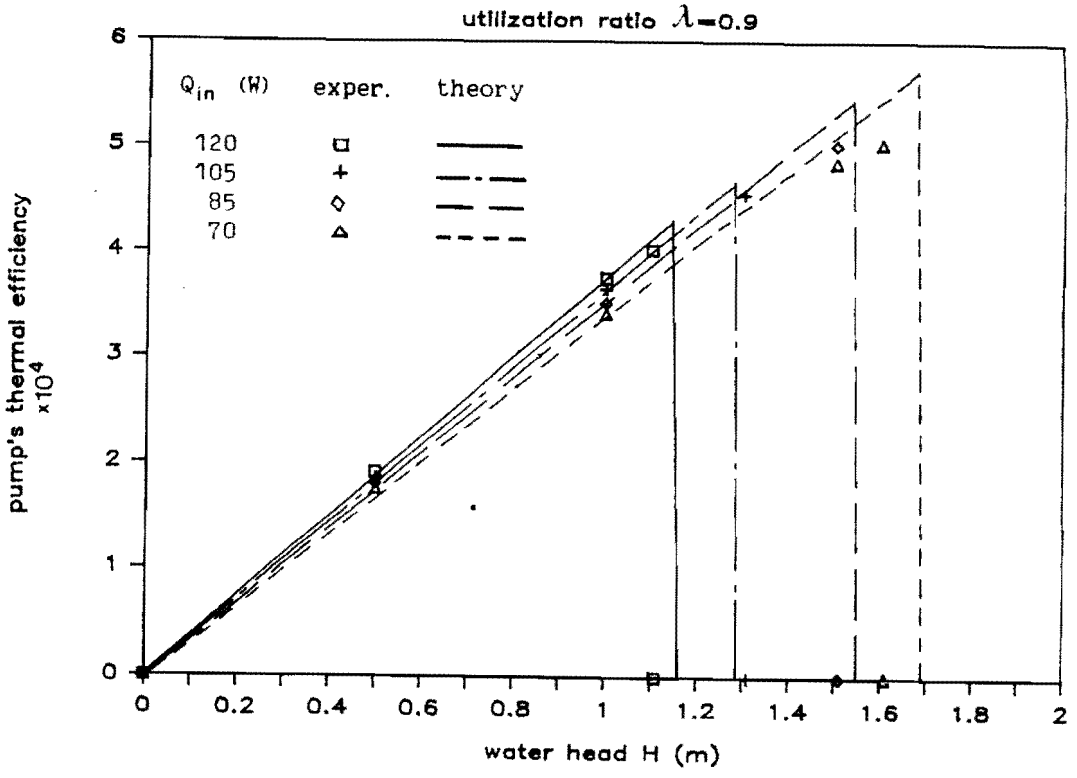

Figure 4.16 η_{th}-H diagram for Freon 113 (λ=0.9)

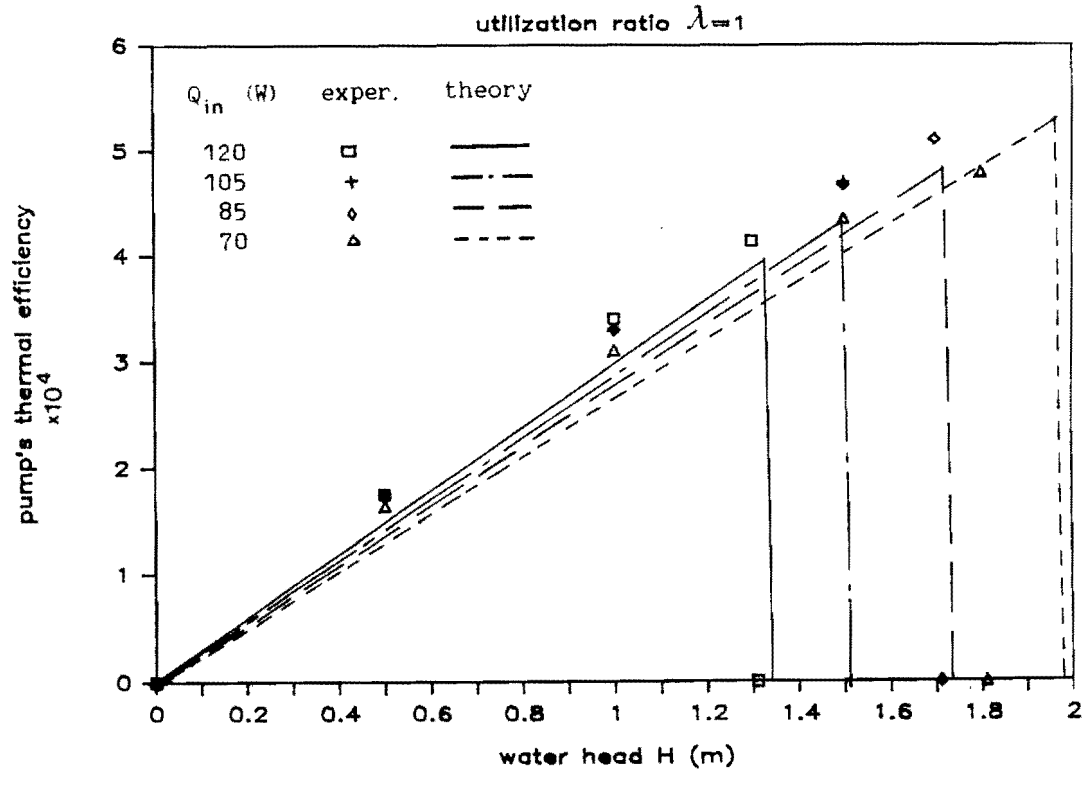

Figure 4.17 η_{th}-H diagram for Freon 113 (λ=1.0)

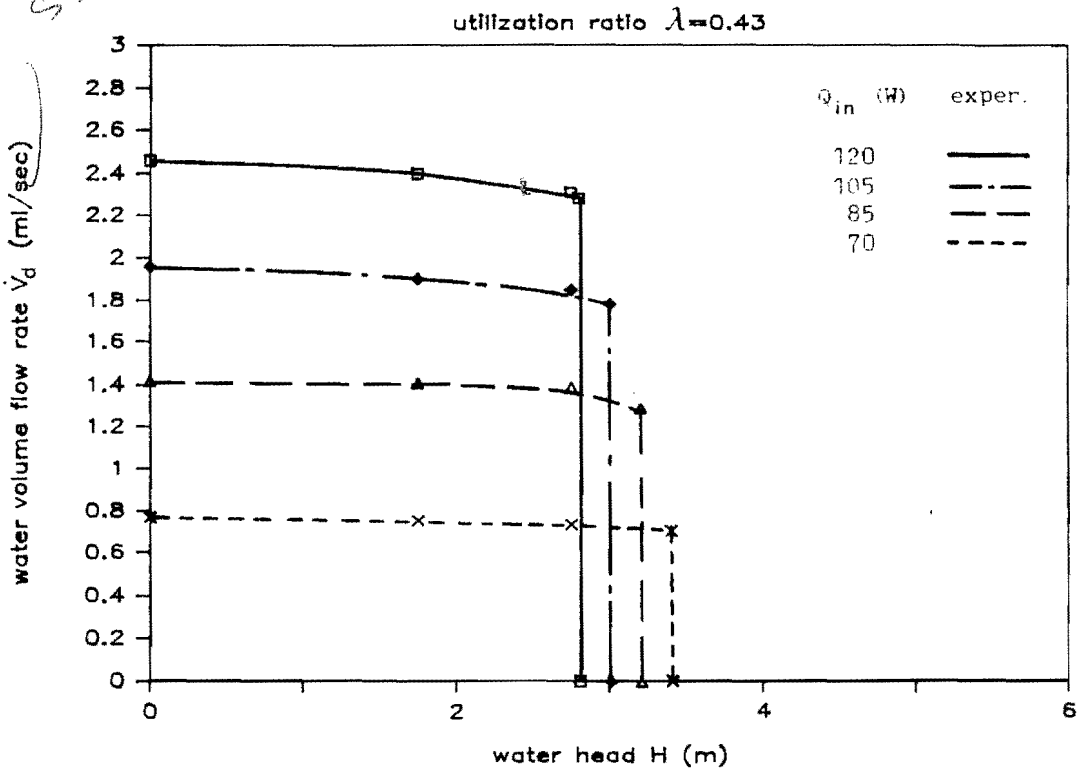

Figure 4.18 $\dot{V}_d$ -H diagram for Methanol (λ=0.43)

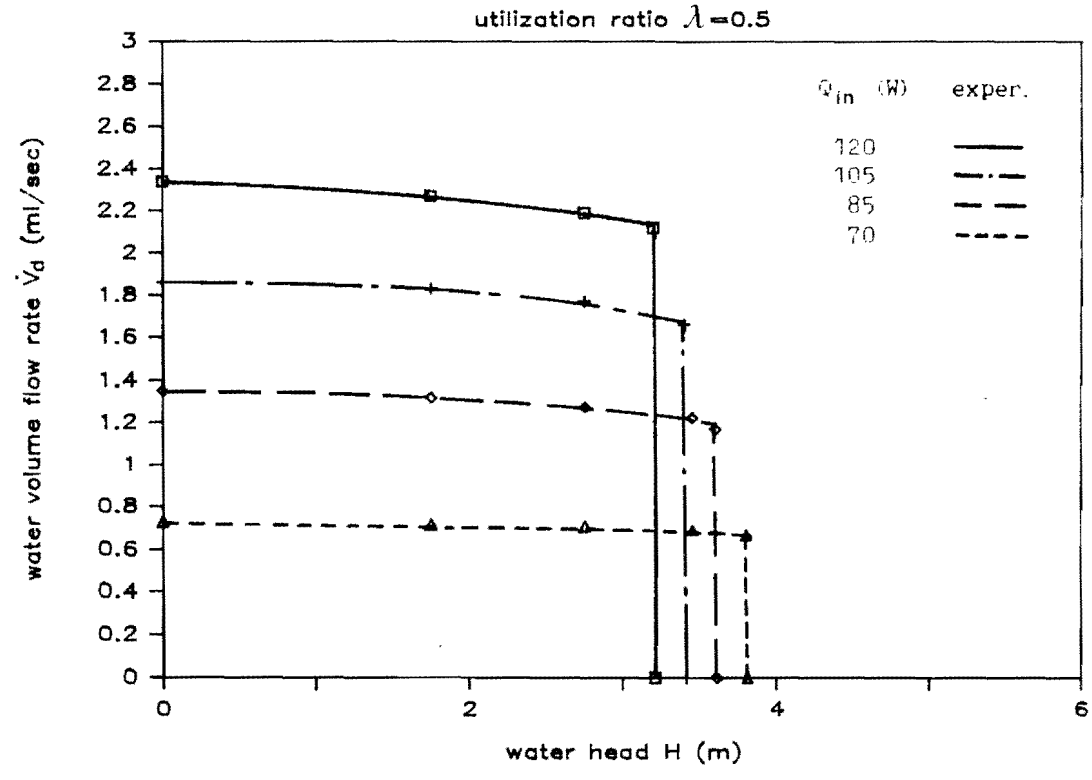

Figure 4.19 $\dot{V}_d$ -H diagram for Methanol (λ=0.50)

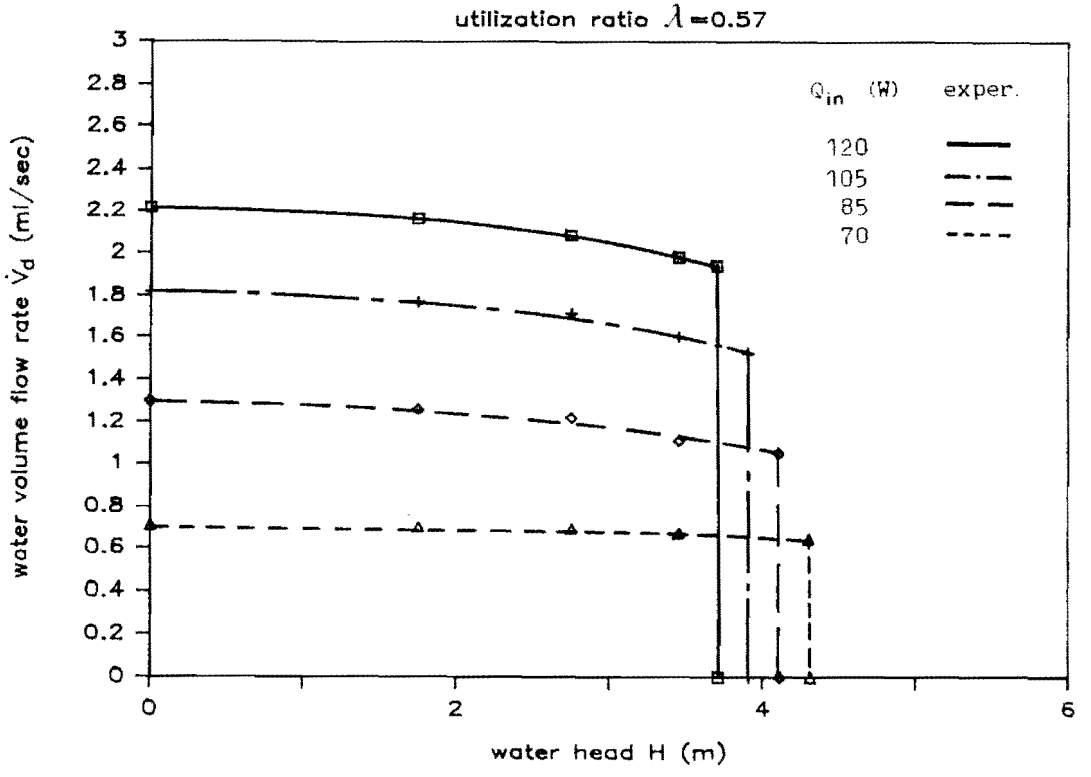

Figure 4.20 $\dot{V}_d$ -H diagram for Methanol (λ=0.57)

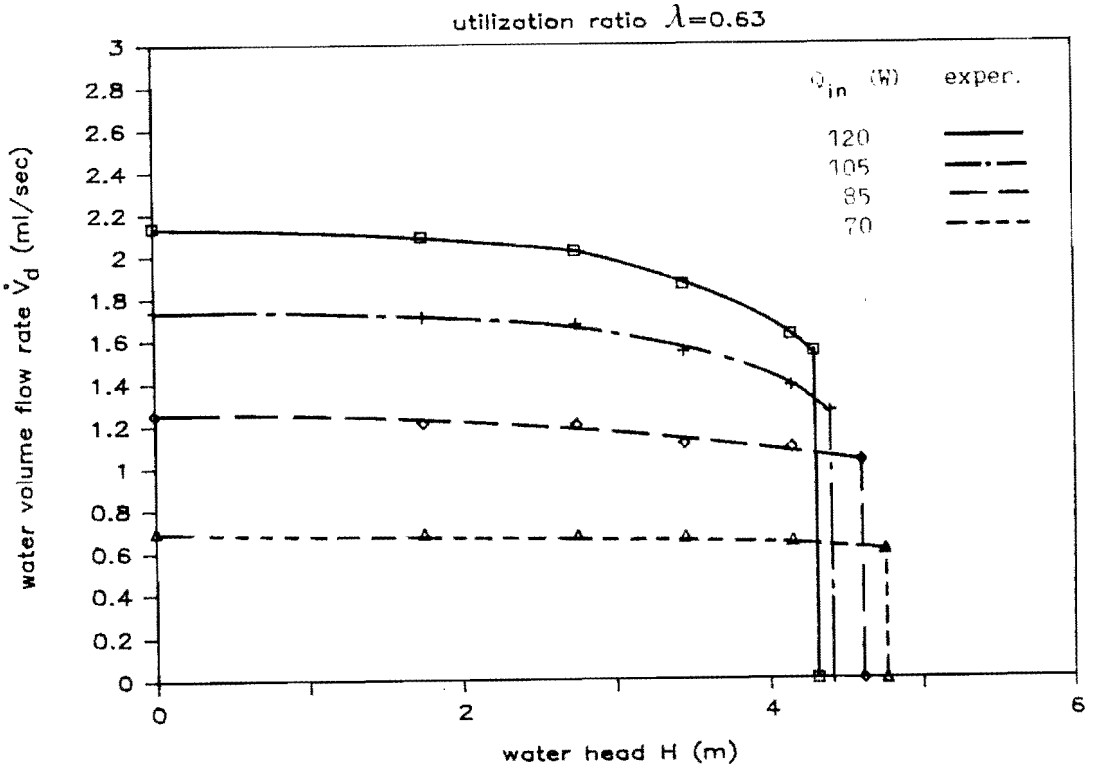

Figure 4.21 $\dot{V}_d$ -H diagram for Methanol (λ=0.63)

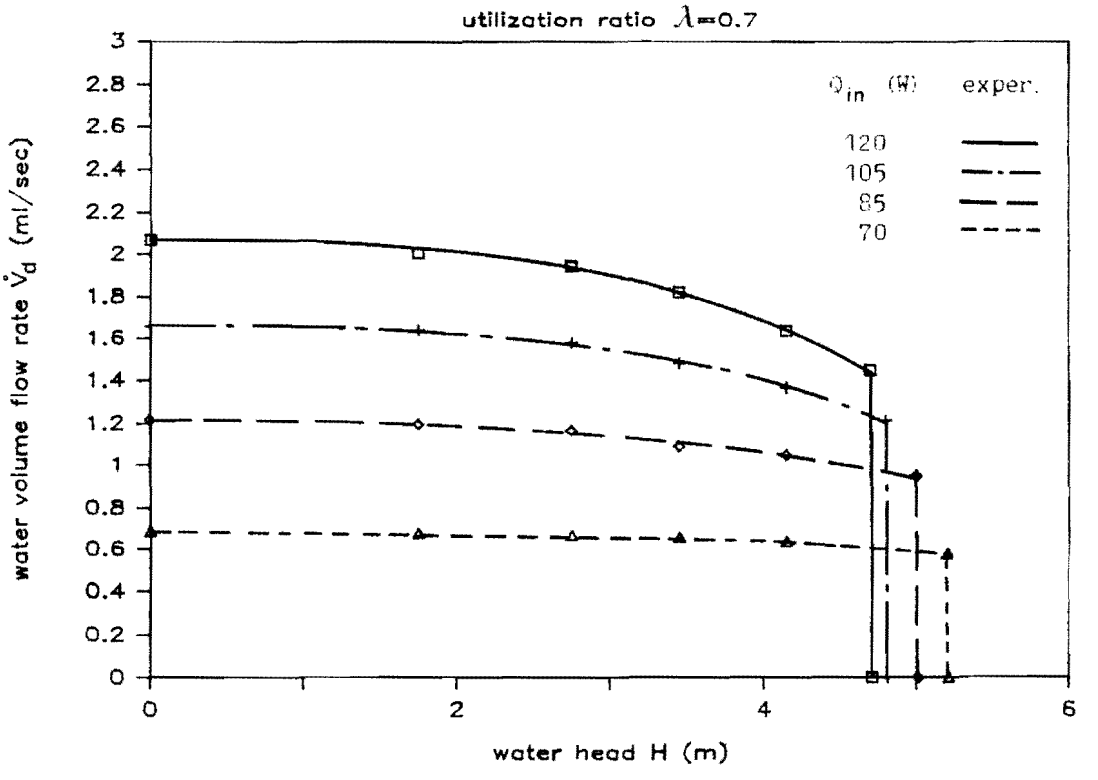

Figure 4.22 $\dot{V}_d$-H diagram for Methanol (λ=0.70)

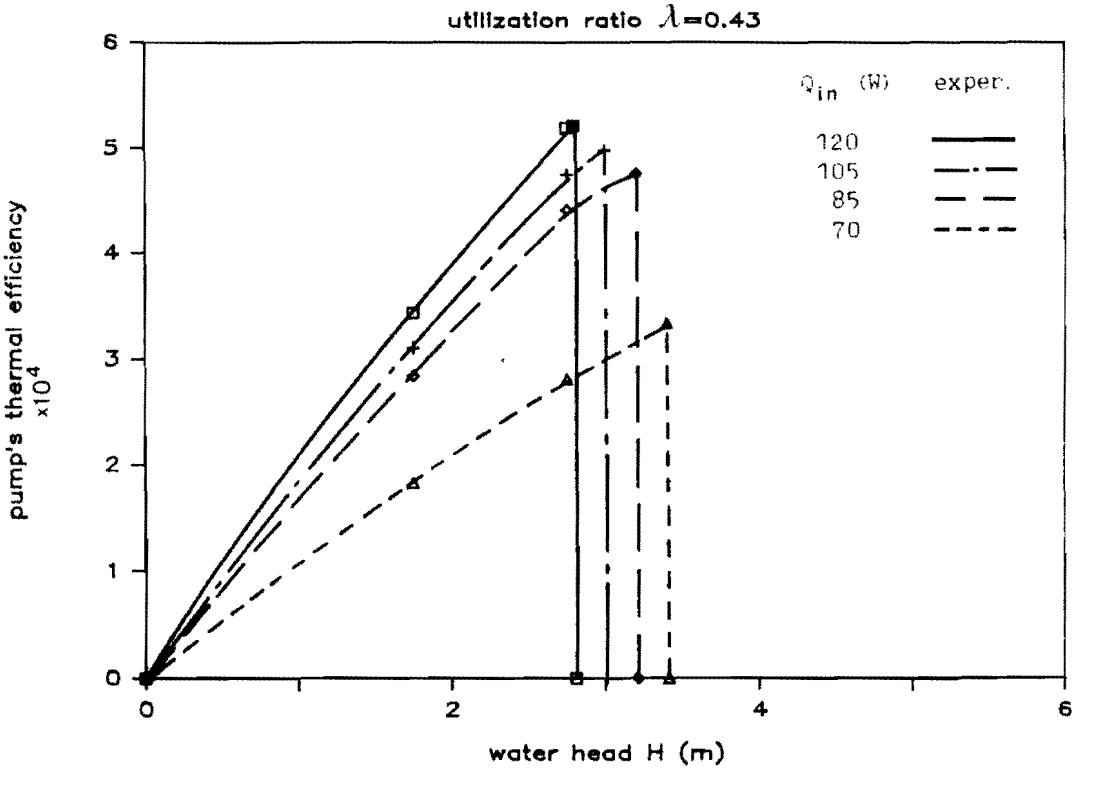

Figure 4.23 η_{th}-H diagram for Methanol (λ=0.43)

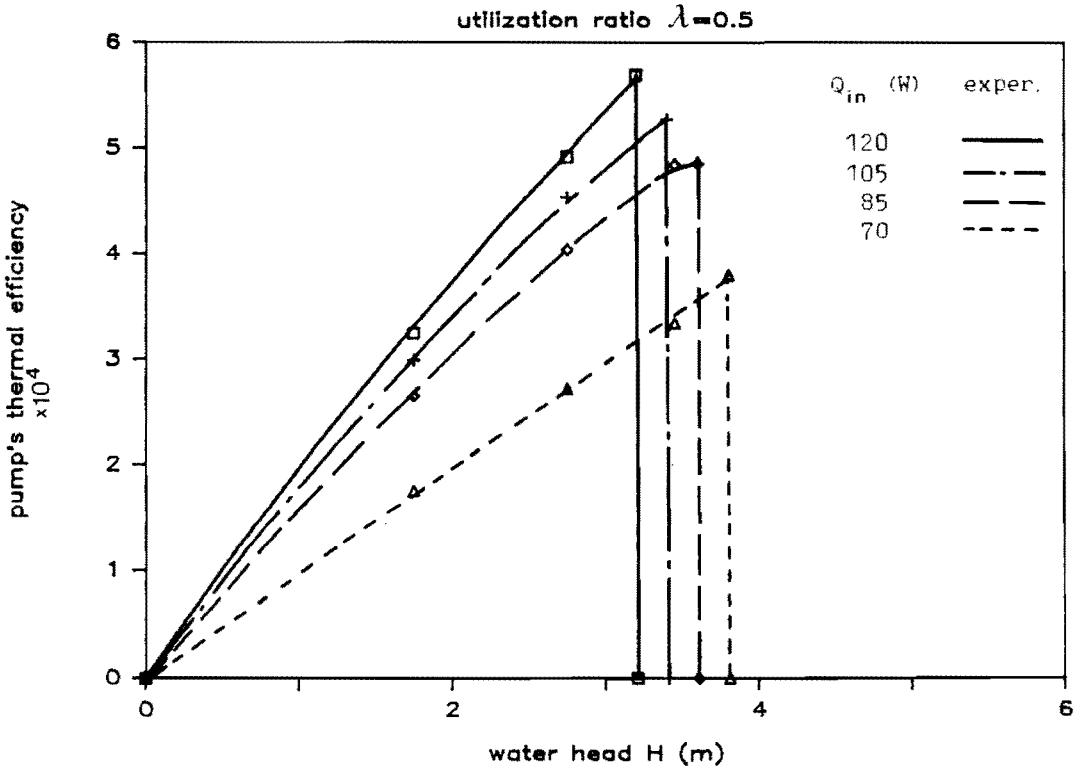

Figure 4.24 η_{th}-H diagram for Methanol (λ=0.50)

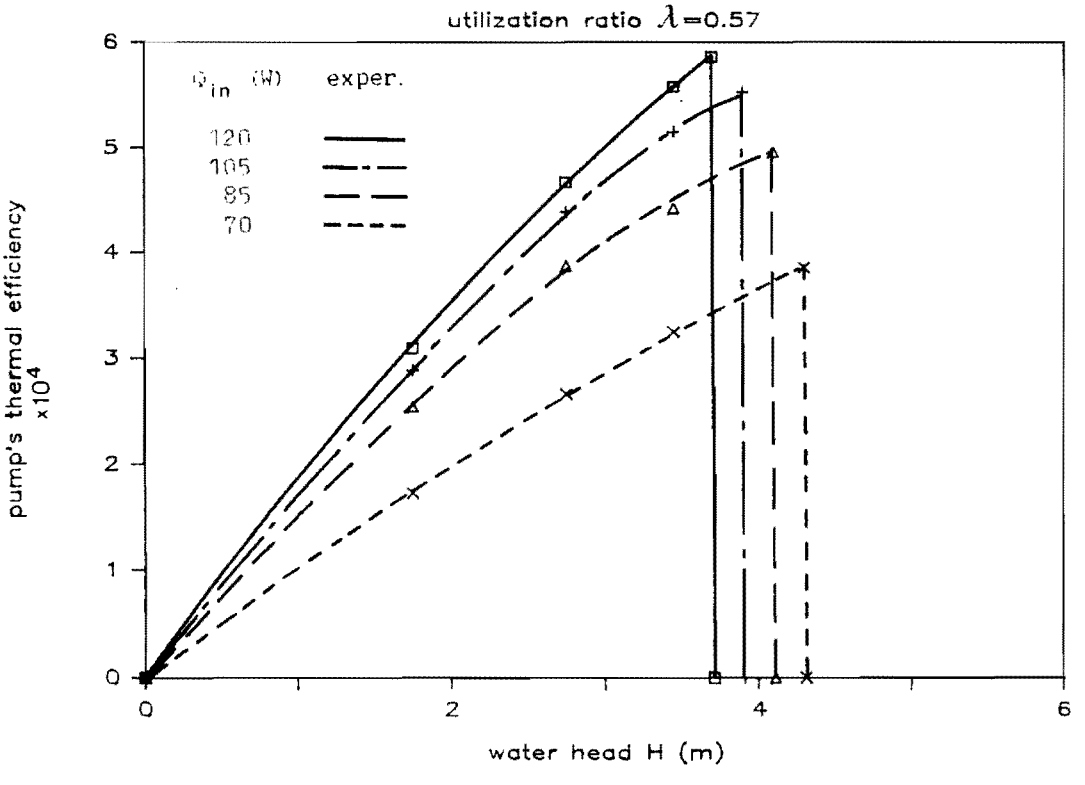

Figure 4.25 η_{th}-H diagram for Methanol (λ=0.57)

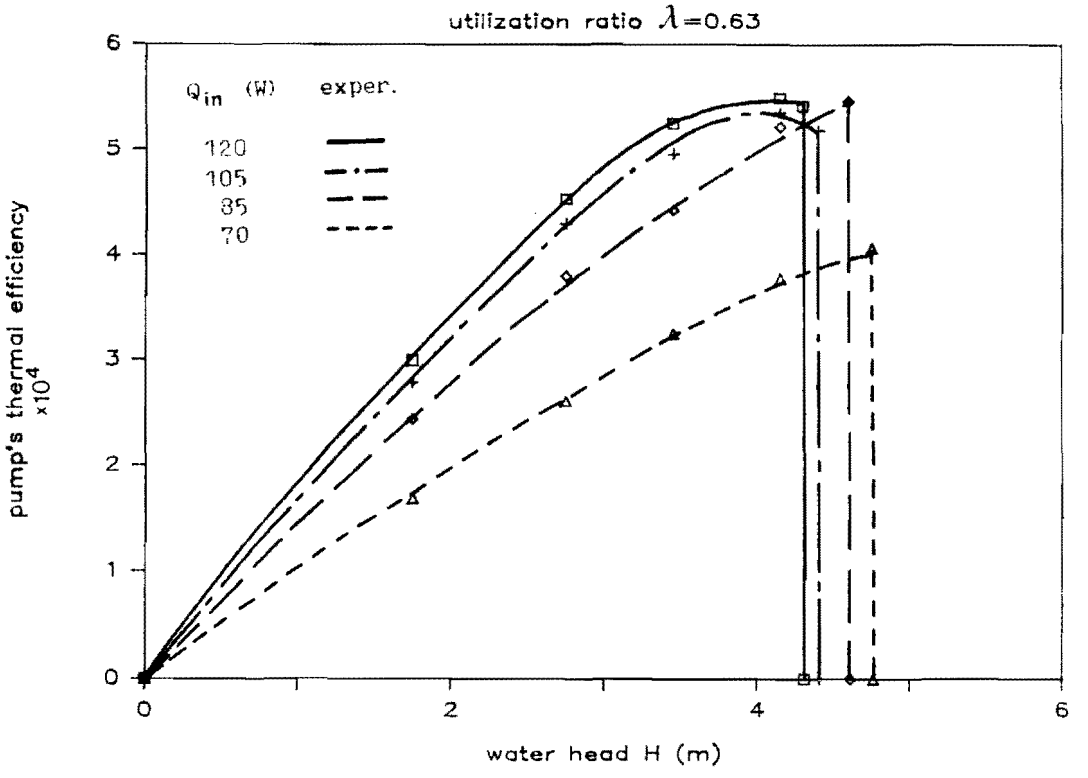

Figure 4.26 η_{th}-H diagram for Methanol (λ=0.63)

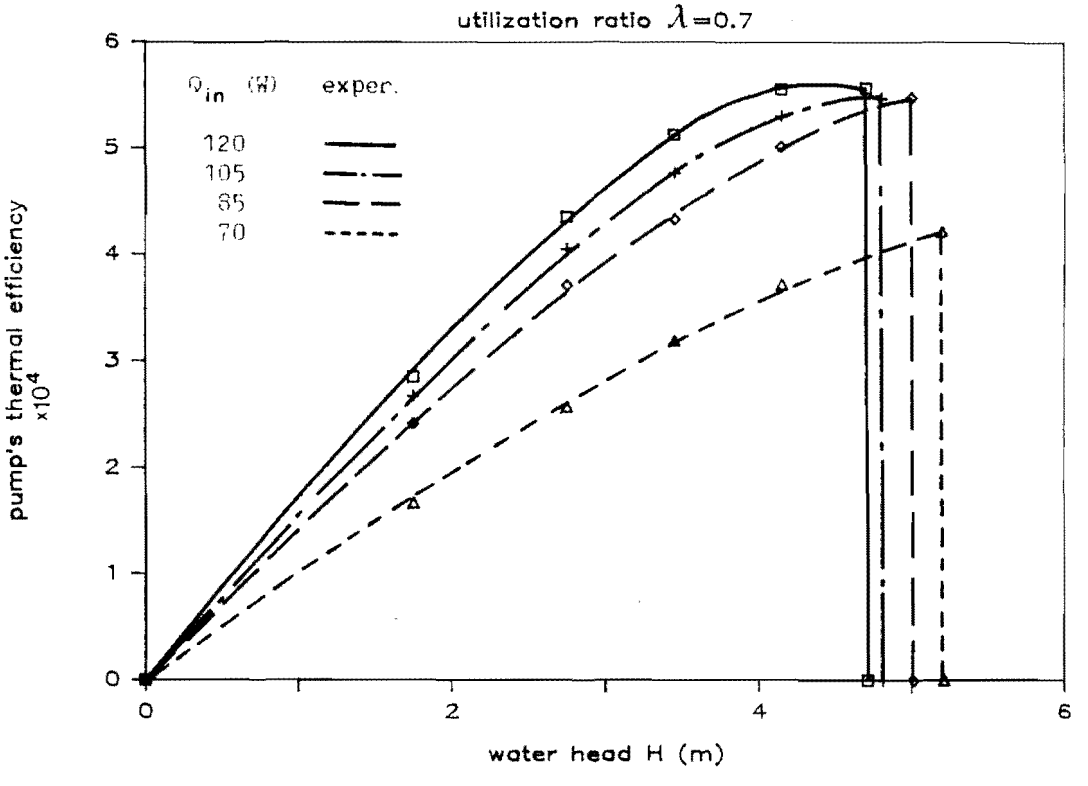

Figure 4.27 η_{th}-H diagram for Methanol (λ=0.70)

4.4.2. The results of the theoretical prediction of the pump's daily capacity for two given days, as for example the 15th of January and the 15th of June, are shown in figure 4.28. The calculations were based on the Pretoria's station radiation data. Sample calculations are found in appendix F.

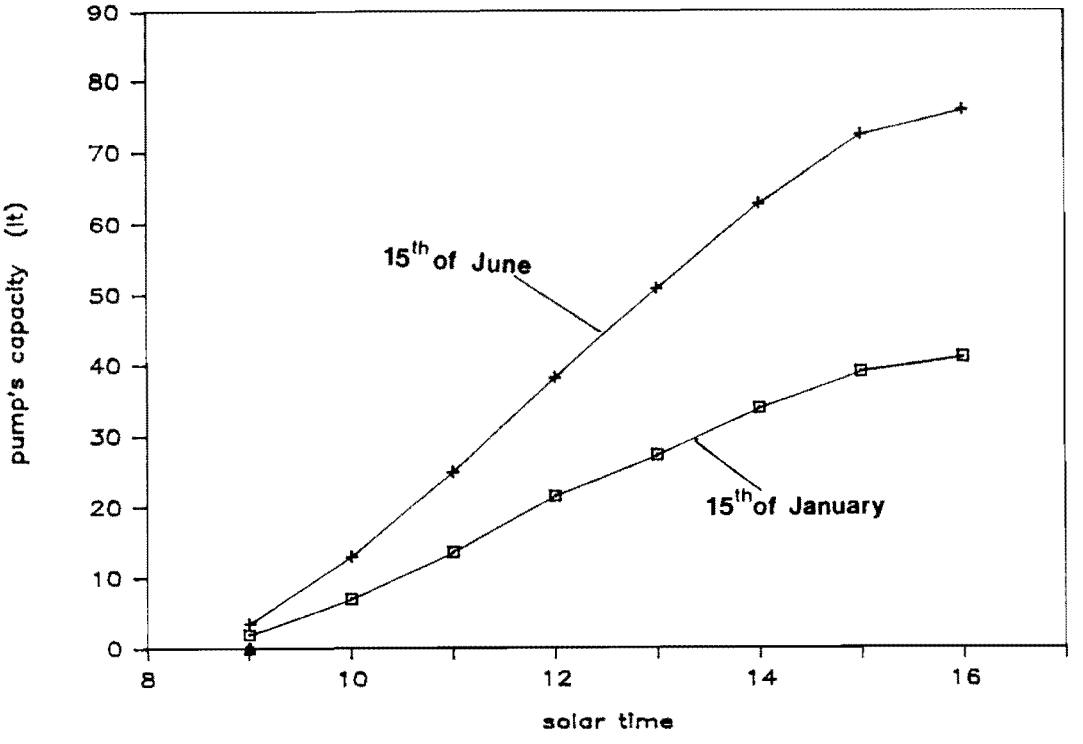

Figure 4.28 Daily pump's capacity

At first glance it would appear that the results are inconsistent with what is expected. The pump performs better and therefore collects more water during the winter months than it does during the summer. That in itself appears contradictory to what is expected, since the summer radiation is more intense, as well as daytime periods being

longer. For example, from table F.1 the mean daily direct solar radiation for January is 15476 MJ/m^2 and for June is 27% lesser (11256 MJ/m^2). As far as daytime periods, table F.2 indicates 13.47 hours of daylight for January and 10.61 hours for June. However these are corrected by the cloudiness factor seen in table F.2, and the roles of longer average sunshine are reversed; June now has 9.23 hours of sunshine and January 8.35 hours. Therefore, from that aspect, the pump will be exposed on average to longer sunshine periods during the winter months!

Another parameter which plays an important role in the pump's performance is the amount of cooling water, required to ensure safe operation, specially at peak radiation conditions. Table F.3 shows that the peak radiation during January requires 300 ml of cooling water. However for off peak conditions the amount of cooling water is in excess, and subcooling takes place, which has the adverse effect of increasing the total cycle time. This effect, although it occurs during June as well, is not as pronounced as in January. Therefore the combination of longer sunshine periods, although of lesser intensity, and shorter cycle times resulting from using less cooling water, explains why the pump performs better in June.

4.4.3. Finally, an example of a table indicating how the user should make the system's necessary adjustments is given below. The calculations were based on the following imaginary user's requirements:

Water pressure head: H=1.2m

Location: Pretoria (26^0 South)

Number of adjustments in a year: 12

Sample calculations are found in appendix F.

no of adj.	date	collector angular position $\beta(^0)$	cooling water flow rate adjustment V_{cw}(ml)
1	21/7	A ⟶ 45.54	i ⟶ 250
2	9/8	B ⟶ 37.71	ii ⟶ 260
3	1/9	C ⟶ 29.90	iii ⟶ 270
4	21/9	D ⟶ 22.10	iv ⟶ 280
5	10/10	E ⟶ 14.28	v ⟶ 290
6	2/11	F ⟶ 6.46	vi ⟶ 300
7	21/12	G ⟶ 6.46	vii ⟶ 300
8	8/2	H ⟶ 14.28	viii ⟶ 300
9	3/2	I ⟶ 22.10	ix ⟶ 290
10	22/3	J ⟶ 29.90	x ⟶ 280
11	11/4	K ⟶ 37.72	xi ⟶ 270
12	3/5	L ⟶ 45.54	xii ⟶ 260

Table 4.1 Table for the user

The table is self explanatory. At precisely the specified date, the user will physically change the collector's tilt

angle by rotating it to a pre-calculated angular position, labeled A, B, C etc. In addition, the tap controling the amount of cooling water will also be adjusted to a predetermined position labeled i, ii, iii etc. It is obvious that such tables could be produced at will.

CHAPTER 5

RECOMMENDATIONS

Future research and development work should investigate the following, being either physical or theoretical parameters of our proposed pumping system.

1. Bellows.

One of the most important features of the pump are the bellows. They infuence greatly both the life and the performance of the system.

The life of the system depends for one on its ability to retain the original charge of working fluid without it escaping to the atmosphere, or being diluted with air. Metallic bellows, besides being more durable, have zero permeability for air and most of the working fluids.

The performance of the system can be influenced by the size of the bellows employed. Calculations have shown that the use of larger bellows, which obviously means larger volume of pumped water, does not necessitate proportional increase in the heating and cooling requirements and therefore proportional increase in the cycle times. Figures 5.1 and 5.2 illustate the above mentioned. Whereas our pump

was equiped with bellows that when almost fully extended produced a volume of 300ml, figure 5.1 shows the theoretical approximate cycle times ranging from 50sec to 75sec, depending on the incident solar radiation. If these bellows were replaced by ones producing say sixfold the amount of pumped water, ie. 1800ml, figure 5.1 indicates cycle times between 80sec and 165sec, depending on the identical span of input solar radiation values.

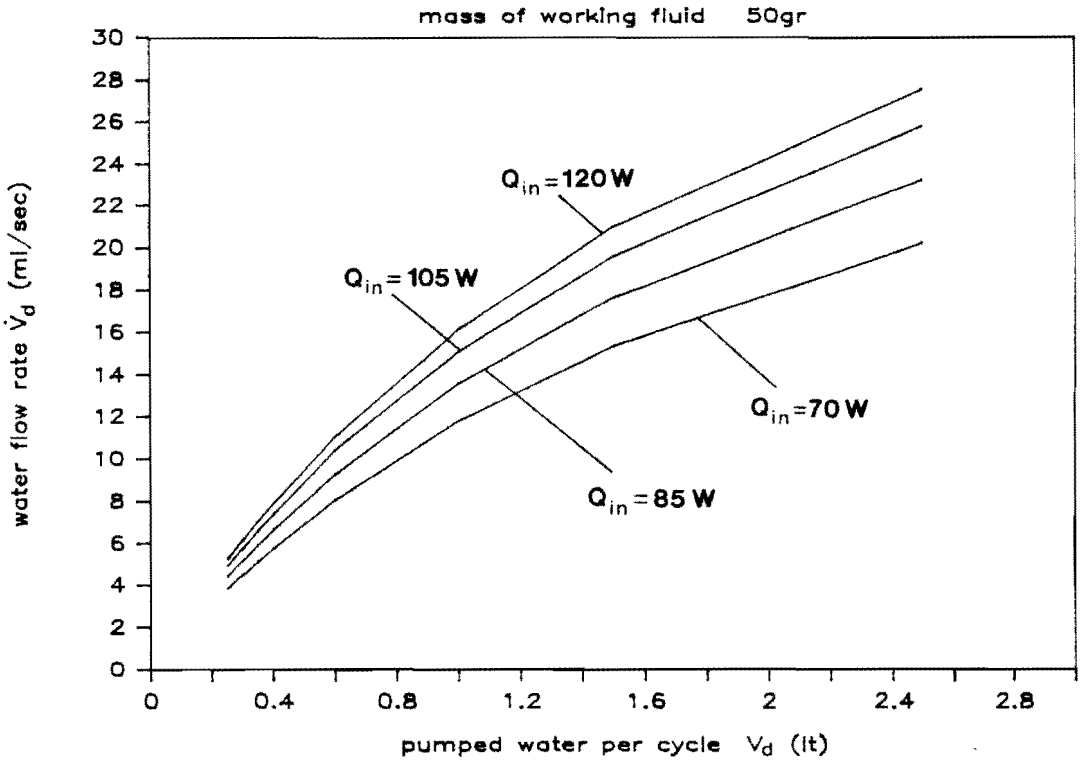

Figure 5.1 Water flow rate versus discharged water per cycle.

The explanation for this lies in the solution of equations 3.47.a and 3.47.b for t_{cool} and t_{heat}. The majority of terms in these equations are mostly independent of the size of the

bellows, with the main effect being in the amounts of Q_{add} and Q_{rej}. These depend mainly on point 3 in figure 3.1 which is the final state for the heating process and the initial state for the cooling process.

The added advantage of large bellows is that the utilization ratio decreases significantly as evidenced in figure 5.2. The advantages of the system operating at low utilization ratios have already been listed previously in section 4.1.

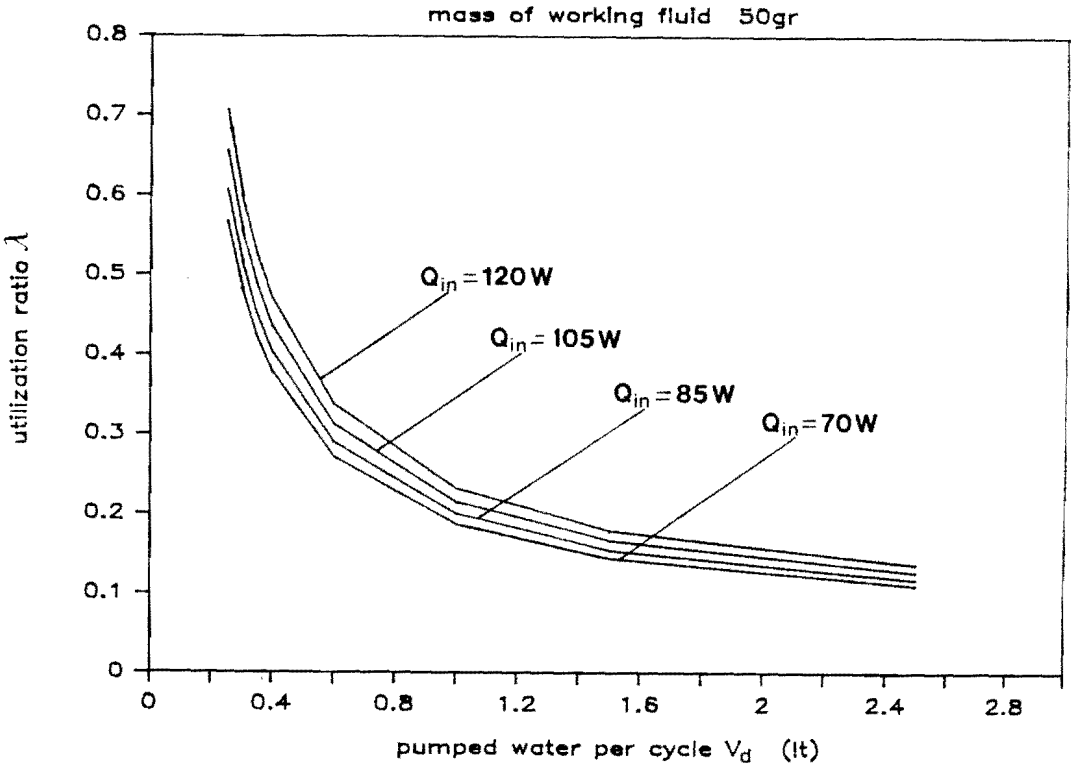

Figure 5.2 Utilization ratio versus discharged water per cycle.

2. Suction below the surface.

The system as proposed, can operate pumping water from depths which depend on the level of sub-atmospheric pressures that can be obtained in bellows no.1, as a result of the cooling of the working fluid. It is obvious that even for ideal conditions the maximum depth from which water may be pumped with the proposed system is approximately 10m of water head. This implies that a specific working fluid must be found, which when cooled to approximately atmospheric temperatures its pressure falls to almost absolute vacuum. This is born out from figures 4.10 to 4.27 and our discussion of the results using Freon 113 and Methanol.

If such a fluid is not available, a slightly different mechanical arrangement between bellows no.1 and no.2 may be used as shown in figure 5.3.

Utilizing the mechanical advantage of levers, one can obtain in bellows no.2 conciderable lesser pressures than the pressure that exists in bellows no.1. However, the mechanical advantage lever arrangement will result in diminished volume flow rate.

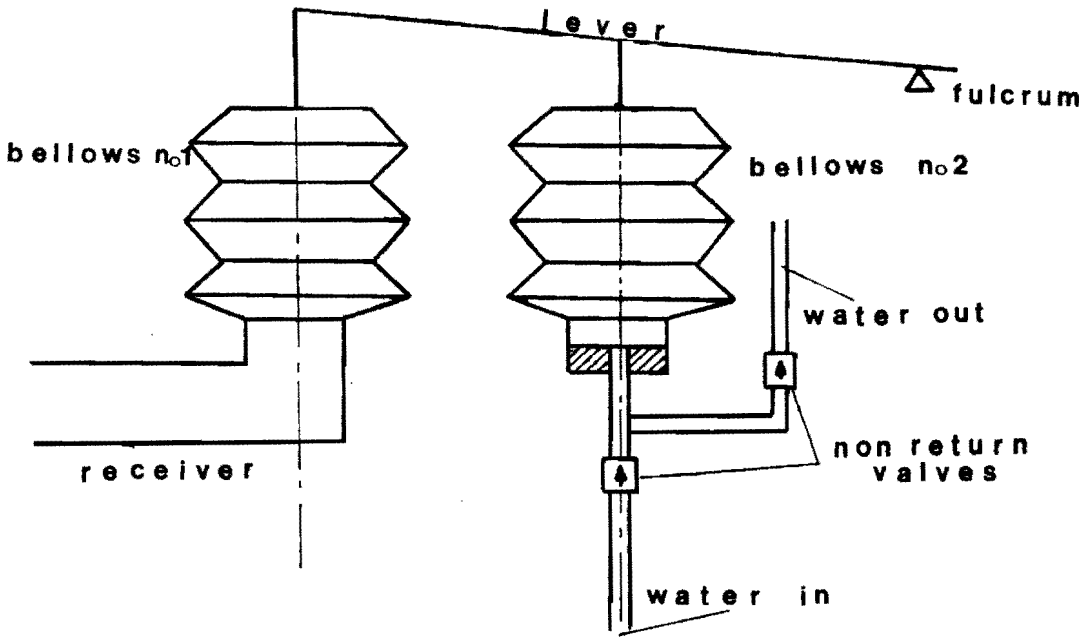

Figure 5.3 Lever arrangement for water heads less than 10m

From depths greater than approximately 10m, the system must be modified conciderably, along the lines of perhaps the existing practice of a conventional pumping system, such as the windmill type. A similar lever arrangement as the one described above could be used in this case, with bellows no.2 operating within the bore hole pipe, at the depth of the water bed. (see figure 5.4)

3. Cooling system

The cooling system affects very much the pump's performance, since it determines the amount of heat rejected

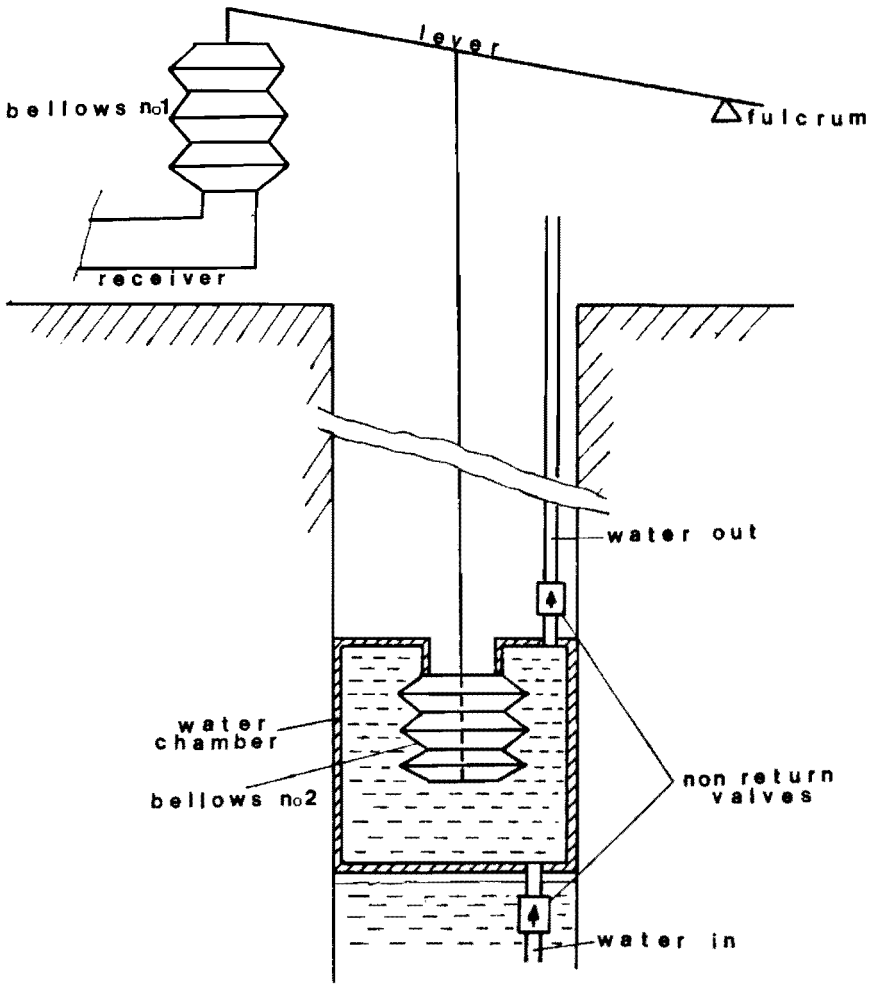

Figure 5.4 Lever arrangement for water heads greater than 10m.

from the system. In turn, this limits the amount of incidence radiation that one is allowed to collect in order to increase the working fluid's internal energy. The author attempted a number of cooling systems with the final one as presented in chapter 2. However it cannot be claimed that this is the best or ultimate design. One feels that further improvements can certainly be implemented in the cooling system.

4. Over-balanced mechanism.

As explained in chapter 2, the over-balance mechanism is a moving part of the system. Although its operation proved to be very reliable, for big scale applications the use of a siphon, that eliminates the moving parts, is recomended.

5. Solar concentrator.

An important characteristic of the concentrator is its acceptance angle, because the tracking requirements are minimized if larger acceptance angles are used. The acceptance angle is related to the concentration ratio as mentioned in section 1.2. As the concentration falls shorter than the ideal concentration, the acceptance angle decreases, and consequently the tracking requirements increase.

The compound parabolic concentrator (C.P.C) is the only concentrator that can reach the maximum concentration limit. However it requires a large reflectance area and therefore much higher costs. A solution to that problem is the use of a truncuated C.P.C. (see ref. 38) for future applications.

6. Non-return valves

It is obvious that the trouble free operation of the non-return valves is necessary for the pump's safe operation. For big scale applications flap rubber valves could possibly be used, together with suitable filters which would ensure minimum scale deposits on the sealing surfaces.

REFERENCES

1.THEKAEKARA,M.P., and DRUMMOND,A.J., "Standard Values for the Solar Constant and Its Spectral Components"
Nat. Phys. Sci., 229, 6 (1971)

2. BUSH,G.E., and RICHARDS,L.M., "Solar Geometry and Time" in Dickinson,W.C. and Cheremisinoff,P.N. Editors, "Solar Energy Handbook", Marcel Dekker, New York, Basel (1979)

3. THRELKERD,J.L., and JORDAN,R.S., "Direct Solar Radiation Available on Clear Days"
ASHAE Trans., vol.64, pp.45-59 (1958)

4. LUNDE,P.J., "Solar Thermal Engineering-Space Heating and Hot Water Systems"
John Wiley and Sons, New York (1980)

5. YELLOTT,J.I., "Available Sources of Insolation Data"
NAS Conf. Proc., "Solar Radiation Conciderations in Building, Planning and Design" (1976)

6. HAMLEN,S.S., and HAMLEN,W.A., "A Distributed Lag Model to Predict Incoming Solar Radiation"
Solar Energy 19, No 2, 217 (1977)

7. HOTTEL,H.C., "A Simple Method for Estimating the Transmittance of Direct Solar Radiation Through Clear Atmospheres"
Solar Energy 18, No 2, 129 (1976)

8. SAYIGH,A.A.M., "Solar Energy Availability Prediction from Climatological Data"
in Sayigh,A.A.M., Editor, "Solar Energy Engineering", Academic Press (1977)

9. BYERS,H.R., "General Meteorology"
McGraw-Hill Book Company, New York, p.33 (1944)

10. BOER,R., "Terrestrial Solar Radiation Availability"
in Dickinson,W.C. and Cheremisinoff,P.N. Editors, "Solar Energy Handbook", Marcel Dekker, New York, Basel (1979)

11. LIU,B.Y.H., and JORDAN,R.C., "The Interrelatinship and Characteristic Distribution of Direct, Diffuse and Total Radiation"
Solar Energy 4, No 3, 1 (1960)

12. HOFMANN,P.,FISCHER,R., and TALBERTS,S., "Irrigation Pumping"
in Dickinson,W.C. and Cheremisinoff,P.N. Editors, "Solar Energy Handbook", Marcel Dekker, New York, Basel (1979)

13. HOTTEL,H.C., and WHILLIER,A., "Evaluation of Flat-plate Solar Collector Performance"
Trans. Conf. on the Use of Solar Energy, 2, Part 1, University of Arizona Press (1958)

14. RABL,A., "Concentrating Collectors"
in Dickinson,W.C. and Cheremisinoff,P.N. Editors, "Solar Energy Handbook", Marcel Dekker, New York, Basel (1979)

15. WILSON,R., and HINTERBERGER,H., Rev. Sci. Instr. 37, 1094 (1966)

16. BARONOV,V.K., and MELNIKOV,G.K., Soviet Journal of Optics Technology 33, 408 (1966)

17. GUPTA,K.C., et al, "A Simple Solar Tracking System"
in De Winter,F., and Cox,M., Editors, "Sun, Mankind's Future Source of Energy", Proceedings of the International Energy Society Congress, New Delhi, India, Pergamon Press (1978)

18. FARBER,E.A., et al, "The Design and Evaluation of a Hydraulic Solar Powered Tracking Device"
in De Winter,F., and Cox,M., Editors, "Sun, Mankind's Future Source of Energy", Proceedings of the International Energy Society Congress, New Delhi, India, Pergamon Press (1978)

19. McVEIGH,J.C., "An Introduction to the Applications of Solar Energy"
Pergamon Press (1977)

20. BERNAND,R., "A Low Maintenance Solar Pump"
Appropriate Technology, v.18, pp 14-15

21. RAO,D.P., and RAO,K.S., "Solar Water Pump for Lift Irrigation"
Solar Energy , v.18, pp 405-411 (1976)

22. SOIN,R., et al, "Develoment and Performance of Solar Water Pumps"
in De Winter,F., and Cox,M., Editors, "Sun, Mankind's Future Source of Energy", Proceedings of the International Energy Society Congress, New Delhi, India, Pergamon Press (1978)

23. MUTHUVEERAPPAN,D., et al, "Irrigation Lift Pumping Utilizing Solar Energy and Biomass"
in De Winter,F., and Cox,M., Editors, "Sun, Mankind's Future Source of Energy", Proceedings of the International Energy Society Congress, New Delhi, India, Pergamon Press (1978)

24. REICHMUTH,H., and BARNNES,J., "Description and Analysis of a 7.5W Liquid Piston Solar Thermal Pumping Engine"
in De Winter,F., and Cox,M., Editors, "Sun, Mankind's Future Source of Energy", Proceedings of the International Energy Society Congress, New Delhi, India, Pergamon Press (1978)

25. AGRAWAL,H., and PAL,S., "A New Design of a Solar Pumping System"
in De Winter,F., and Cox,M., Editors, "Sun, Mankind's Future Source of Energy", Proceedings of the International Energy Society Congress, New Delhi, India, Pergamon Press (1978)

26. BHATTACHARYYA,T., et al, "Low Temperature, Bellows Actuated Solar Pump"
in De Winter,F., and Cox,M., Editors, "Sun, Mankind's Future Source of Energy", Proceedings of the International Energy Society Congress, New Delhi, India, Pergamon Press (1978)

27. SACHEDEVA, R., et al, "A Reciprocating Device Using Solar Energy"in De Winter,F., and Cox,M., Editors, "Sun, Mankind's Future Source of Energy", Proceedings of the International Energy Society Congress, New Delhi, India, Pergamon Press (1978)

28. BAHADORI,M.N., "Solar Water Pumping"
in Dixon,A.E., and Leslie,J.D., "Solar Energy Conversion", Pergamon Press (1979)

29. ADAMS,P.W., "Design of a Solar Powered Minto Wheel"
Mech. Eng., Design Project No1, Nov.1982 UCT

30. BAM,P., "The Performance of an Integral Greenhouse Solar Air-heater"
Master's Thesis, UCT (1984)

31. HOLMAN,J.P., "Thermodynamics"
McGraw-Hill (1969)

32. EVANS,L.B., and STEFANY,N.E., "An Experimental Study of Transient Heat Transfer to Liquids in Cylindrical Enclosures"
AIChE Pap.4, Heat Transfer Conf. Los Angeles (1965)

33. HOLMAN,J.P., "Heat Transfer"
Fourth edition, McGraw-Hill Book Company (1976)

34. KREITH,F., "Principles of Heat Tranfer"
Third edition, Scranton, Pa., International Textbook Co. (1973)

35. MICHAELS,A.S., and BIXLER,H.J.
J. Polymer Sci. 50, 413 (1961)

36. VAN AMERONGEN,G.J.
J. Polymer Sci. 5, 307 (1950)

37. VAN AMERONGEN, G.J.
Rubb. Chem. Technol. 37, 1065 (1964)

38. RABL,A., "Optical and Thermal Properties of Compound Parabolic Concentrators"
Solar Energy 18, pp. 495-511 (1976)

39. RABL,A., "Comparison of Solar Concentrators"
Solar Energy 18, pp.93-111 (1976)

40. CHINERY,D.N.W., "Solar Water Heating in South Africa"
CSIR Research Report 248 (1971)

APPENDIX A

ELEMENTS OF SOLAR GEOMETRY

A.1. The solar declination (δ), (ie. the solar noon elevation from the equatorial plane) can be approximated by the sine function:

$$\delta = 23.44 \sin \frac{360\ (D-81)}{365} \qquad \text{A.1}$$

where the number of the day D is given from table A.1.

A.2. The hour angle (ω) is given by:

$$\omega = 15\ (12 + H_s) \qquad \text{morning}$$
$$\omega = 15\ (H_s - 12) \qquad \text{afternoon} \qquad \text{A.2}$$

where H_s is the solar time.

The sunset hour angle (ω_s) is:

$$\cos \omega_s = - \tan \varphi \ \tan \delta \qquad \text{A.3}$$

where:

φ : from -90^0 (south pole) to $+90^0$ (north pole)

δ : from -23.44^0 (south hemisphere) to $+23.44^0$ (north hemispere)

Day of Mo.	Month												Day of Mo.
	Jan.	Feb.	Mar.	Apr.	May	Jun.	Jul.	Aug.	Sep.	Oct.	Nov.	Dec.	
1	1	32	60	91	121	152	182	213	244	274	305	335	1
2	2	33	61	92	122	153	183	214	245	275	306	336	2
3	3	34	62	93	123	154	184	215	246	276	307	337	3
4	4	35	63	94	124	155	185	216	247	277	308	338	4
5	5	36	64	95	125	156	186	217	248	278	309	339	5
6	6	37	65	96	126	157	187	218	249	279	310	340	6
7	7	38	66	97	127	158	188	219	250	280	311	341	7
8	8	39	67	98	128	159	189	220	251	281	312	342	8
9	9	40	68	99	129	160	190	221	252	282	313	343	9
10	10	41	69	100	130	161	191	222	253	283	314	344	10
11	11	42	70	101	131	162	192	223	254	284	315	345	11
12	12	43	71	102	132	163	193	224	255	285	316	346	12
13	13	44	72	103	133	164	194	225	256	286	317	347	13
14	14	45	73	104	134	165	195	226	257	287	318	248	14
15	15	46	74	105	135	166	196	227	258	288	319	349	15
16	16	47	75	106	136	167	197	228	259	289	320	350	16
17	17	48	76	107	137	168	198	229	260	290	321	351	17
18	18	49	77	108	138	169	199	230	261	291	322	352	18
19	19	50	78	109	139	170	200	231	262	292	323	353	19
20	20	51	79	110	140	171	201	232	263	293	324	354	20
21	21	52	80	111	141	172	202	233	264	294	325	355	21
22	22	53	81	112	142	173	203	234	265	295	326	356	22
23	23	54	82	113	143	174	204	235	266	296	327	357	23
24	24	55	83	114	144	175	205	236	267	297	328	358	24
25	25	56	84	115	145	176	206	237	268	298	329	359	25
26	26	57	85	116	146	177	207	238	269	299	330	360	26
27	27	58	86	117	147	178	208	239	270	300	331	361	27
28	28	59	87	118	148	179	209	240	271	301	332	362	28
29	29	a	88	119	149	180	210	241	272	302	333	363	29
30	30		89	120	150	181	211	242	273	303	334	364	30
31	31		90		151		212	243		304		365	31

[a]For dates after February 28 in leap years, add 1 to all numbers.

Table A.1 Day of the year D (2)

A.3. The zenith angle (θ_z), as shown in figure A.1 is

$$\cos\theta_z = \sin\delta\cdot\sin\varphi + \cos\delta\cdot\cos\varphi\cdot\cos\omega \qquad \text{A.4}$$

A.4. The general incidence angle between the normal to a surface and the incidence beam solar radiation, (as shown in figure A.1) is given by:

$$\cos\theta = \sin\delta \sin\varphi \cos\beta + \sin\delta \cos\varphi \sin\beta \cos\gamma +$$
$$+ \cos\delta \cos\varphi \cos\beta \cos\omega - \cos\delta \sin\varphi \sin\beta \cos\gamma \cos\omega - \quad \text{A.5}$$
$$- \cos\delta \sin\varphi \sin\beta \sin\omega$$

where:

ω : from 0^0 (noon) clockwise to 360^0

β : from 0^0 (horizontal) to 90^0 (vertical)

γ : from 0^0 (north) clockwise to 360^0

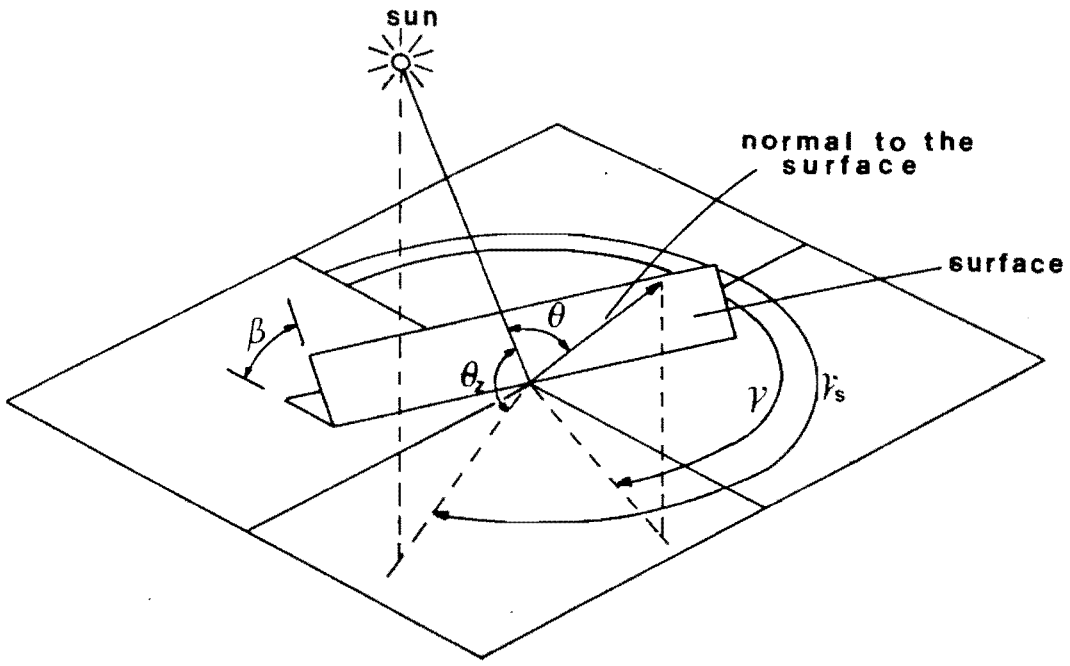

Figure A.1 Incidence angle θ

For the special case of surfaces that face north:

$$\cos\theta_{north} = \sin\delta \cdot \sin(\beta+\varphi) + \cos\delta \cdot \cos\omega \cdot \cos(\beta+\varphi) \quad \text{A.6}$$

A.5. The solar elevation (θ_{xy}), (vertical solar swing), as shown in figure A.2 is given by:

$$\tan(\theta_{xy}+\beta-\varphi) = \frac{\tan\delta}{\tan\omega} \qquad \text{A.7}$$

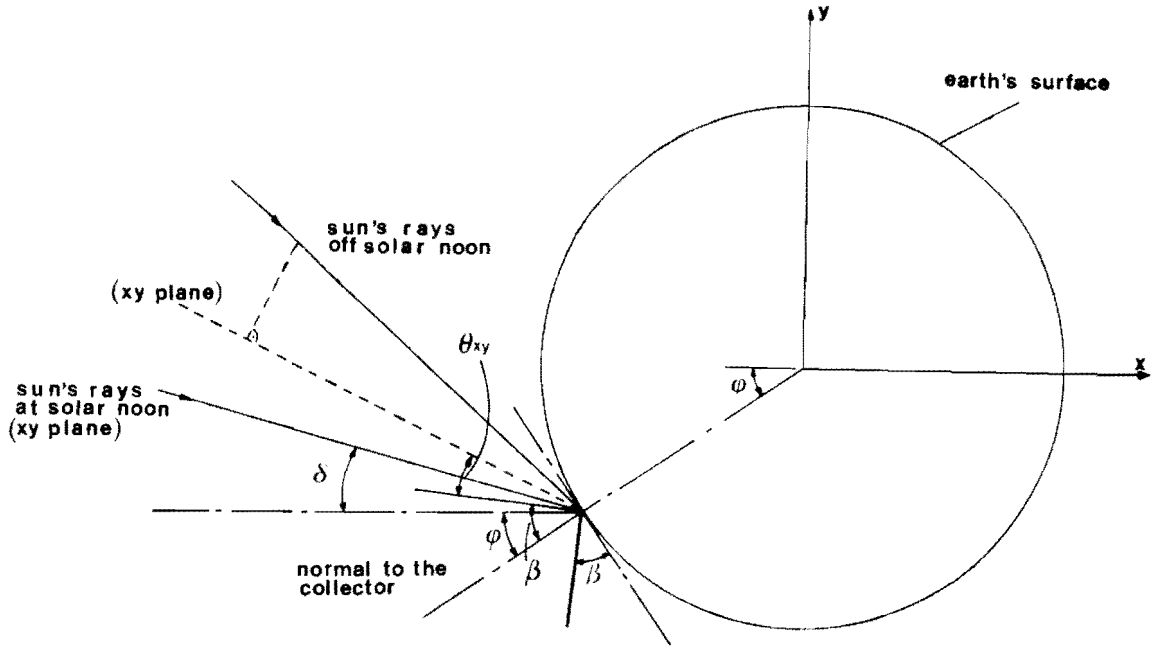

Figure A.2 Vertical solar elevation.

APPENDIX B

AVAILABLE SOLAR RADIATION FROM MEAN TOTAL HORIZONTAL DATA.

Since solar radiation data are not presented for intervals shorter than one hour, the nearest approach to the true average intensity at any instant, obtainable from the solar radiation data commonly available, is the hourly average intensity. The ratio of the hourly total radiation to the daily total radiation as a function of the sunset hour angle is shown in figure B.1.

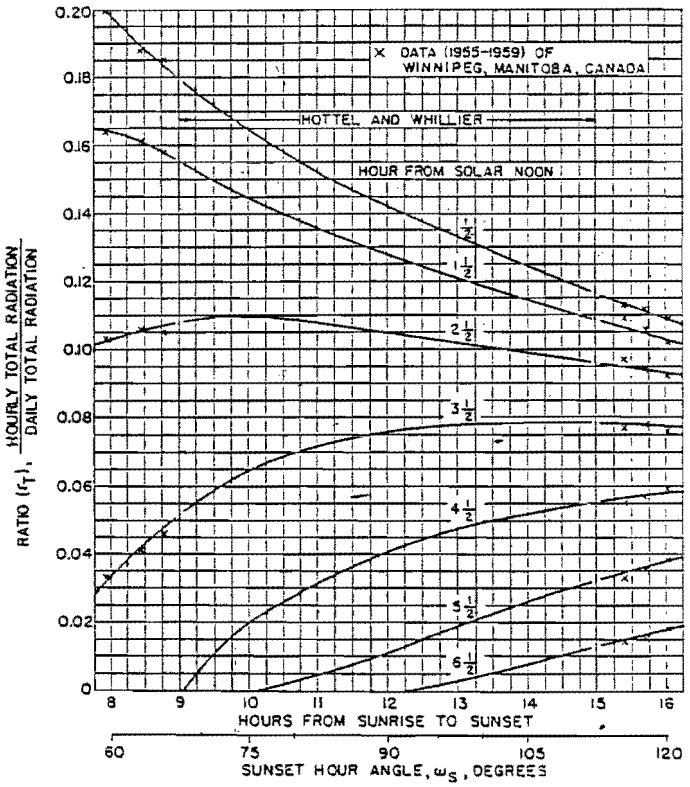

Figure B.1 Ratio of the hourly total radiation to daily total radiation

Figure B.2 depicts the ratio of the hourly diffuse radiation to the daily diffuse radiation as a function of the sunset hour angle.

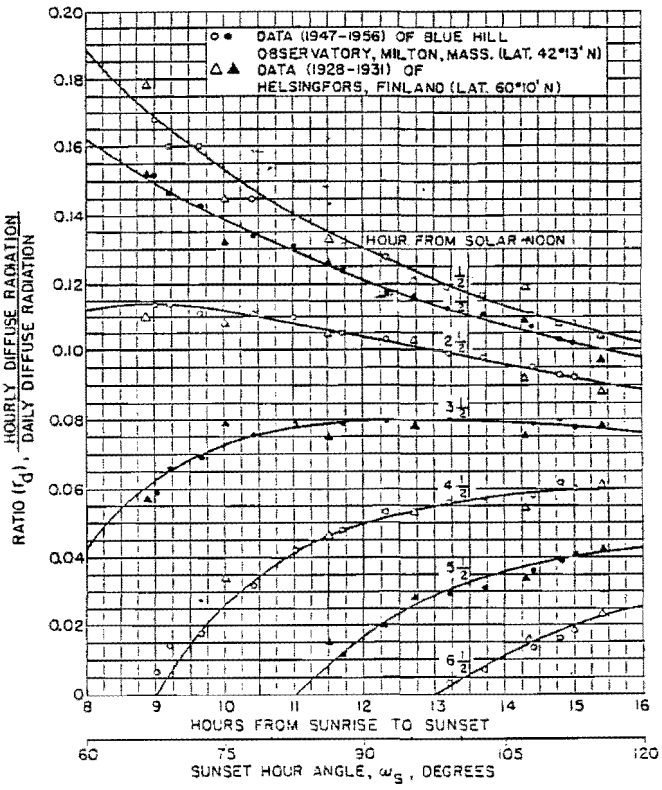

Figure B.2 Ratio of the hourly diffuse radiation to the daily diffuse radiation

APPENDIX C

PERMEABILITY COEFFICIENT

When small molecules permeate through a polymer membrane, the rate of permeation can be expressed by parameters which may be characteristic of the polymer. The general concept of the ease with which a permeant passes through a barrier is often reffered as "permeability". The coefficient which has the dimensions

$$P = \frac{(\text{amount of permeant})\cdot(\text{film thickess})}{(\text{area})\cdot(\text{time})\cdot(\text{pressure-drop across the film})}$$

$$= \frac{cm^3 \cdot cm}{cm^2 \cdot s \cdot cmHg}$$

may best be defined as the permeability coefficient.

Polymer	Permeant	Temper. ^0C	P x 10^{10}
Neopreme	H_2	25	13.6
	O_2	25	4.0
	N_2	25	1.2
	CO_2	25	25.8
Natural rudder	O_2	25	23.8
	N_2	25	9.43
	CO_2	25	153
Methyl rubber	H_2	25	17.0
	O_2	25	2.1
	N_2	25	0.47
	CO_2	25	7.47

Table C.1 Permeability coefficients. (35,36,37)

APPENDIX D

GEOMETRIC CHARACTERISTICS OF THE CONCENTRATOR

A cross section of the parabolic concentrator employed for the present study is shown in figure D.1.

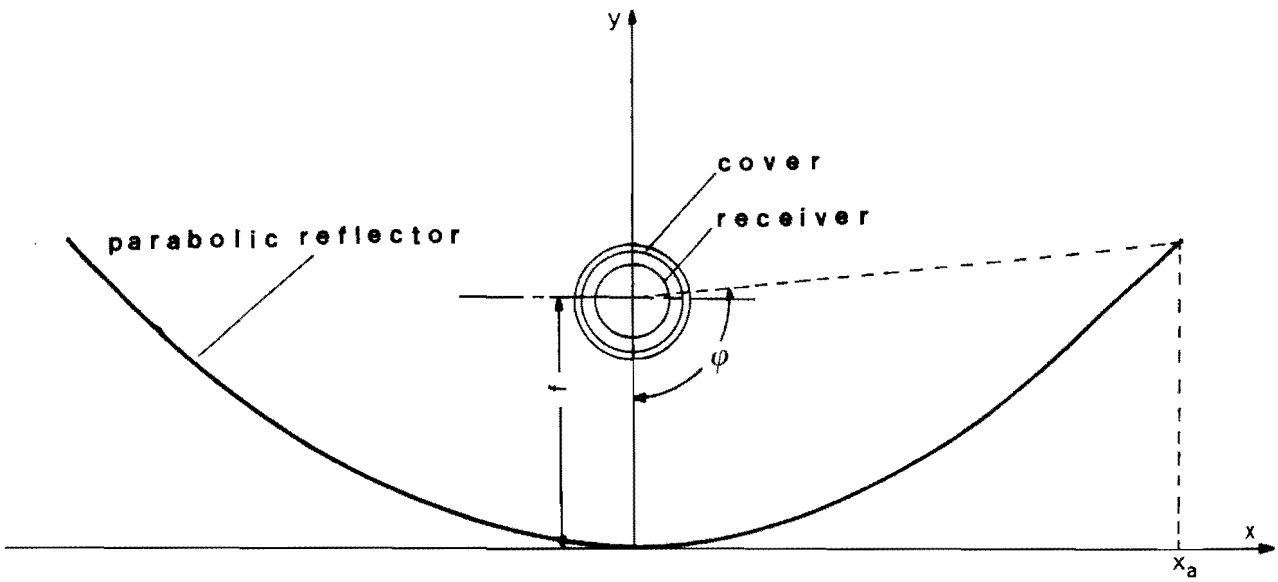

Figure D.1 Solar concentrator

Its main geometric characteristic are:

Aperture area:

$$A = 0.4 m^2$$

Focus length:

$$f = 0.19 m$$

Rim angle:

$$\varphi = \text{arc tan} \frac{4fx}{4f^2 - x_a^2}$$

$$= \text{arc tan} \frac{4 \cdot 19 \cdot 40}{4 \cdot 19^2 - 40^2}$$

$$= 94^0$$

Concentration ratio:

$$C = \frac{2x_a}{2\pi r_r + 4}$$

$$= \frac{2\ 40}{2\ 3.14\ 5+4\ 1}$$

$$= 2.26$$

APPENDIX E

THERMODYNAMIC CYCLE FOR OFF PEAK RADIATION CONDITIONS

The thermodynamic analysis developed in section 3.1 can also be applied to the thermodynamic cycle shown in figure E.1.

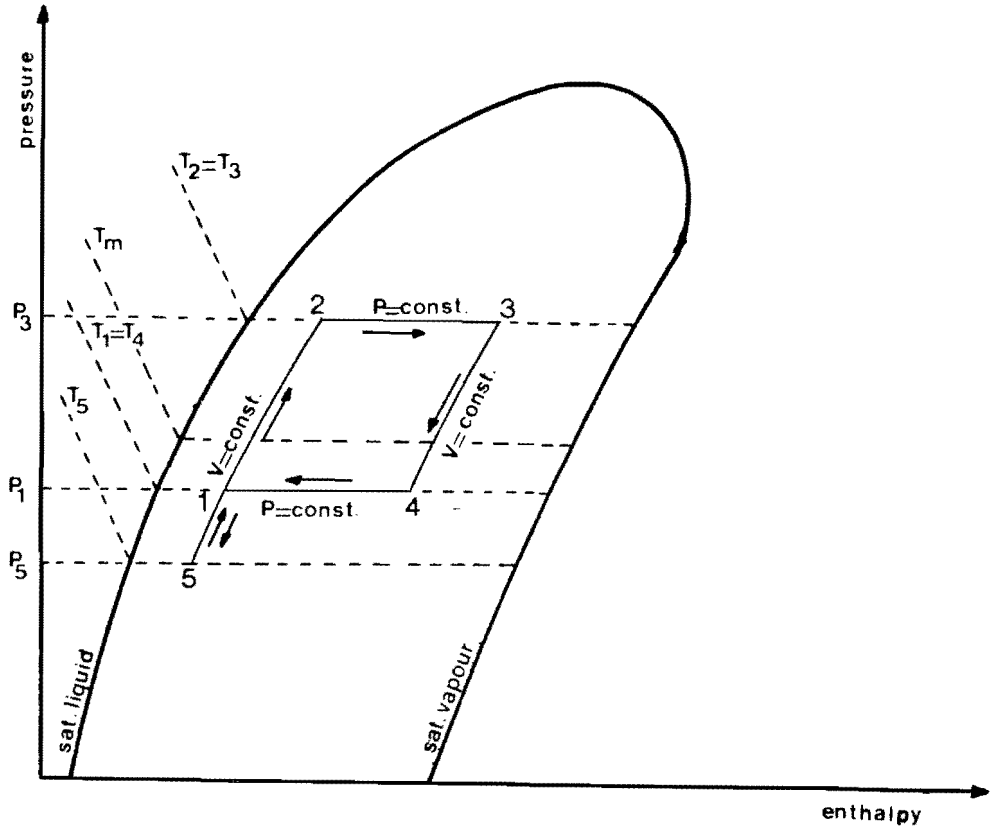

Figure E.1 Thermodynamic cycle for off peak radiation conditions.

Process 5-2:

v=constant.... $q_{52} = h_2 - h_5 - v_1 \cdot (P_2 - P_5)$ E.1.a

Process 2-3:

P=constant.... $q_{23} = h_3 - h_2$ E.1.b

Process 3-4:

v=constant.... $q_{34} = -[h_3 - h_4 - v_3 (P_3 - P_4)]$ E.1.c

Process 4-1:

P=constant.... $q_{41} = -(h_4 - h_1)$ E.1.d

Process 1-5:

v=constant.... $q_{51} = -[h_1 - h_5 - v_1 (P_1 - P_5)]$ E.1.e

Heat added:

$$q_{add} = q_{52} + q_{23}$$
$$= h_3 - h_5 - v_1 (P_3 - P_5) \qquad \text{E.2}$$

Heat rejected:

$$q_{rej} = q_{34} + q_{41} + q_{15}$$
$$= -[h_3 - h_5 - v_3 \cdot (P_3 - P_1) - v_1 \cdot (P_1 - P_5)] \qquad \text{E.3}$$

Net work:

$$w = q_{add} + q_{rej}$$
$$= (v_3 - v_1) \cdot (P_3 - P_1) \qquad \text{E.4}$$

Cycle themal efficiency:

$$\eta_c = \frac{(v_3 - v_1)\cdot(P_3 - P_1)}{h_3 - h_5 - v_1\cdot(P_3 - P_5)} \qquad \text{E.5}$$

APPENDIX F

PREDICTION OF THE PUMP'S PERFORMANCE

-AN EXAMPLE-

Using the theory developed in chapter 3, the following example illustrates the method applied to predict the model's performance as well as to establish the system's adjustment requirements. In the following example the pump's daily capacity, for two given days of the year, is calculated.

F.1. DATA

The following data must be known:

1. The location latitude: =26^{0} S, 1500m above sea level.

2. Radiation data: tables F.1 and F.2 by Chinery (40) give the required radiation data for different areas in South Africa. In this example we will make use of Pretoria's station radiation data.

3.Time: The pump's daily performance will be predicted for the 15th of January and the 15th of June.

4. Water head: H=1.2m

		Alexander Bay		Bloemfontein		Cape Town (Wingfield and D.F. Malan Airports)		Durban (Louis Botha Airport)		Keetmanshoop		Kimberley		Maun		Pietersburg		Port Elizabeth		Pretoria		Upington		Windhoek	
			S		S		S		S		S		S		S		S		S		S		S		S
Jan.	1	31,397	1,101	26,884	1,737	30,375	0,666	21,237	2,600	30,195	0,904	26,721	1,381	23,104	2,901	26,599	2,235	24,778	–	24,037	2,675	27,629	2,189	26,101	2,022
	2	6,899	0,042	7,305	0,804	6,225	0,435	8,619	0,603	5,438	0,615			8,904	0,787			9,356	–	8,501	1,335			8,008	0,720
Feb.	1	28,140	1,540	24,489	2,796	25,955	1,264	19,826	1,344	27,428	1,344	24,946	1,980	21,216	1,997	24,008	1,005	25,398	–	21,773	1,700	25,184	2,227	23,828	1,775
	2	6,242	–	6,807	0,816	6,095	0,833	7,962	0,628	5,626	0,130			8,984	–			6,786	–	7,895	0,699			7,498	0,812
Mar.	1	23,589	1,047	20,676	2,194	21,856	0,730	17,946	0,896	23,380	1,092	20,789	1,735	20,056	2,633	22,091	0,829	19,278	0,310	20,186	1,118	21,233	2,152	21,500	1,846
	2	4,563	–	5,903	0,477	5,103	0,364	6,196	0,477	4,517	0,448			5,990	0,155			5,706	0,151	6,807	0,783			6,459	0,791
April	1	19,516	1,356	18,164	0,879	15,271	0,203	15,029	0,833	21,061	0,548	17,741	0,942	18,704	2,528	19,541	1,143	14,041	0,339	17,469	1,377	18,168	1,490	20,504	0,825
	2	4,546	0,063	4,057	0,427	4,714	0,435	4,626	0,306	3,102	0,373			4,165	0,682			4,496	0,264	4,768	0,682			4,224	0,469
May	1	15,380	1,917	14,384	0,712	10,905	1,942	12,132	0,540	17,164	0,465	14,208	0,548	17,306	2,474	17,264	1,067	11,294	0,414	15,033	0,829	15,196	1,758	18,620	0,758
	2	4,182	0,360	3,454	0,385	4,015	0,435	3,487	0,460	2,847	0,193			2,608	0,180			3,098	0,205	3,315	0,331			2,951	0,448
June	1	13,287	1,239	13,040	1,063	9,373	0,557	11,303	0,506	15,506	0,573	12,781	0,716	16,004	2,361	15,707	1,093	9,779	0,661	14,124	0,561	14,212	1,540	16,996	0,833
	2	2,914	0,113	2,838	0,490	3,299	0,297	2,884	0,511	2,323	0,297			2,759	0,218			2,780	0,264	2,868	0,331			2,562	0,301
July	1	13,283	1,926	14,020	0,720	9,946	0,917	11,755	0,816	16,389	0,356	13,831	1,310	16,975	0,523	16,577	2,918	10,671	0,243	14,727	0,917	14,170	1,423	18,302	0,523
	2	3,173	0,205	2,968	0,393	3,646	0,490	3,131	0,402	2,478	0,100			3,391	0,561			2,935	0,188	3,119	0,410			2,595	0,234
August	1	16,695	2,118	17,750	1,172	12,772	0,833	13,714	0,896	19,512	0,410	18,089	1,390	20,019	2,055	18,859	3,219	13,517	0,699	18,198	0,502	17,331	1,298	21,052	0,594
	2	4,266	0,025	3,449	0,410	4,576	0,490	4,228	0,481	3,001	0,084			3,487	0,511			3,906	0,427	3,634	0,293			3,315	0,381
Sept.	1	21,814	1,394	21,735	1,273	18,047	0,896	16,142	1,461	23,761	0,791	22,191	2,361	22,614	1,402	21,358	3,575	17,277	0,917	20,400	1,679	20,814	0,728	23,933	1,197
	2	5,270	0,389	4,676	0,527	6,057	0,356	5,957	0,531	4,149	0,163			5,187	0,615			6,221	0,682	4,848	0,444			4,902	0,691
Oct.	1	27,022	2,499	24,418	1,582	22,999	0,980	17,147	1,402	27,391	1,197	26,294	2,491	23,012	2,357	24,456	2,068	20,948	1,000	22,246	1,256	24,247	1,415	25,959	1,474
	2	6,384	0,460	6,212	0,707	7,029	0,678	7,405	0,682	5,078	0,599			7,225	0,603			7,338	0,427	6,773	0,335			6,388	0,712
Nov.	1	30,338	1,808	27,353	2,160	27,591	1,612	19,236	1,955	30,693	0,724	28,965	2,855	23,652	2,491	26,587	2,076	25,854	1,846	23,841	1,469	27,210	1,474	27,575	1,679
	2	6,367	0,686	6,857	0,791	7,460	0,975	8,753	0,762	4,735	0,402			7,598	1,013			8,829	0,607	7,523	0,800			6,455	0,653
Dec.	1	30,932	3,600	27,801	1,432	29,969	1,076	20,885	0,774	31,229	0,933	29,157	3,290	22,639	1,758	26,101	3,604	25,770	0,875	23,267	1,566	27,638	1,105	28,056	2,323
	2	6,970	0,326	7,431	0,628	7,104	0,770	9,624	0,858	5,128	0,636			9,021	1,281			9,213	0,737	8,498	0,703			6,937	0,858
Total for year	1	8 243,837		7 618,371		7 138,762		5 965,706		8 621,699		7 770,566		7 459,712		7 840,354		6 633,625		7 153,154		7 688,067		8 284,774	
2/1%	2	1 877,633		1 881,799		1 985,169		2 212,989		1 469,902				2 102,259				2 147,893		2 083,165				1 890,523	
		22,8		24,7		27,8		37,0		17,0				28,1				32,3		29,1				22,8	
Approx. latitude		29°S		29°S		34°S		30°S		27°S		29°S		20°S		24°S		34°S		26°S		28°S		23°S	
No. of years		7		7		9		9		4		6		7		7		3		9		4		9	

Table F.1 Mean daily total (1), diffuse (2), and standard deviation (S) of solar radiation on a horizontal surface in MJ/m , for 12 stations in Southern Africa. (40)

Table F.2 Mean duration of sunshine for 12 station in Southern Africa (40)

(a) Mean daily hours of sunshine
(b) Mean daily hours of sunshine expressed as a percentage of the possible hours of sunshine
(c) Average no. of days with $\leq$10 per cent of the possible sunshine, expressed as a percentage of the no. of days in the month
(d) Average no. of days with 11-49 per cent of the possible sunshine, expressed as a percentage of the no. of days in the month
(e) Average no. of days with $\geq$50 per cent of the possible sunshine, expressed as a percentage of the no. of days in the month

	Alexander Bay		Bloemfontein		Cape Town (Wingfield)		Durban (Airport)		Keetmanshoop		Kimberley (Airport)		Mtoun		Pietersburg (Airport)		Port Elizabeth (Airport)		Pretoria		Upington		Windhoek	
	a	b	a	b	a	b	a	b	a	b	a	b	a	b	a	b	a	b	a	b	a	b	a	b
Jan.	10,24	75	9,79	71	10,94	77	6,49	47	11,44	84	9,69	70	7,98	61	7,99	59	8,55	60	8,35	62	11,52	84	9,26	70
Feb.	9,72	74	9,24	70	10,47	79	6,74	51	10,34	80	9,48	72	7,27	57	7,55	58	8,23	62	8,08	62	10,51	81	8,98	70
Mar.	9,09	73	8,52	70	9,10	74	6,17	50	9,92	81	8,87	72	8,03	67	7,55	62	7,51	61	7,68	63	9,53	78	9,05	74
Apr.	8,94	78	8,80	77	6,92	62	6,83	60	10,15	89	8,96	78	9,25	79	8,06	70	7,57	67	8,69	75	9,67	86	9,00	78
May	8,12	75	8,77	82	5,92	56	7,40	69	9,94	92	8,64	80	9,93	89	8,61	79	6,91	67	9,27	85	9,18	86	10,04	91
June	8,50	82	8,74	85	5,96	60	6,94	68	9,65	93	8,82	85	10,11	93	8,91	84	6,85	69	9,23	87	8,97	87	10,25	95
July	7,51	71	9,02	86	5,72	56	6,87	66	9,84	92	9,05	86	10,34	93	8,63	80	7,15	71	9,36	88	9,10	86	10,50	97
Aug.	8,29	74	9,60	87	6,42	59	6,91	63	10,51	94	9,71	88	10,77	94	8,84	79	7,61	70	9,91	88	10,00	90	11,01	97
Sep.	9,11	77	9,43	79	7,16	60	5,83	49	10,92	93	9,67	81	10,51	89	8,72	73	7,44	63	9,26	78	10,61	89	10,75	90
Oct.	9,55	75	9,66	76	6,87	69	5,24	41	11,32	89	9,70	76	9,15	72	8,73	69	7,67	60	8,90	70	10,92	85	10,30	82
Nov.	10,16	75	10,35	77	9,85	71	5,75	42	11,79	88	10,20	75	8,66	66	8,23	62	8,29	60	9,02	68	11,63	86	9,85	75
Dec.	10,28	74	10,57	76	11,10	77	5,97	43	11,95	87	10,54	76	7,25	54	8,13	60	8,93	62	9,05	66	11,65	84	9,21	69
Year	9,13	75	9,37	78	8,20	67	6,43	54	10,64	88	9,44	78	9,10	76	8,34	70	7,73	64	8,90	74	10,27	85	9,86	82

	c	d	e	c	d	e	c	d	e	c	d	e	c	d	e	c	d	e	c	d	e	c	d	e	c	d	e	c	d	e	c	d	e	c	d	e
Jan.	0,0	12,4	87,6	6,5	9,7	83,8	2,9	7,3	90,0	28,1	20,3	51,4	0,5	6,5	93,1	5,1	15,2	79,9	6,4	26,7	65,9	8,7	29,1	62,4	11,5	19,7	69,0	10,0	18,7	71,3	2,6	5,2	92,3	4,2	15,5	80,1
Feb.	2,3	11,2	86,5	7,8	12,4	79,8	1,6	10,0	88,4	23,0	17,3	59,7	0,5	13,6	85,9	3,3	13,6	83,2	8,5	29,3	62,2	10,0	31,8	58,2	13,4	18,9	69,8	12,0	16,5	72,0	0,6	12,4	87,2	0,0	18,3	81,7
Mar.	1,1	13,4	85,5	13,2	5,8	81,1	3,2	10,7	86,1	25,8	17,4	57,0	2,8	7,8	89,4	5,7	12,2	82,2	5,1	20,3	74,7	7,5	29,8	62,6	17,6	11,1	71,3	12,0	18,7	69,4	3,8	12,4	83,9	1,3	19,4	79,4
Apr.	1,1	9,4	89,4	4,6	10,3	85,0	8,0	25,0	68,9	18,0	15,0	67,1	1,4	3,8	94,8	2,6	12,1	85,2	4,8	8,6	86,7	5,7	19,5	74,7	11,5	11,8	76,7	6,4	7,3	86,4	1,1	5,6	93,3	5,3	6,0	88,6
May	1,6	15,1	83,3	3,2	8,1	88,8	17,4	19,0	63,4	8,9	21,8	69,3	0,0	2,8	97,2	2,2	10,7	87,3	0,5	5,1	94,5	1,7	17,6	80,7	9,4	14,7	75,8	2,6	4,2	93,2	1,6	7,5	90,9	0,0	1,3	98,7
June	1,1	7,8	91,1	3,7	3,0	93,4	17,6	15,6	66,7	12,0	12,7	75,1	0,5	1,4	98,1	1,5	7,2	91,1	0,0	2,3	97,7	2,1	13,6	84,1	6,7	16,0	77,3	3,4	3,7	93,0	0,6	6,1	93,3	0,0	2,0	98,0
July	7,5	13,4	79,0	2,4	5,2	92,6	17,1	24,2	58,7	12,6	13,2	74,1	0,5	0,9	98,6	1,7	5,2	93,0	1,4	0,5	98,2	2,6	15,8	81,8	8,2	12,5	79,1	1,6	5,2	93,3	0,0	5,9	94,1	0,0	1,2	98,9
Aug.	5,4	13,4	81,2	1,9	4,2	94,2	17,3	18,2	64,4	15,8	11,3	73,0	0,0	0,9	99,1	0,7	5,3	94,1	0,0	0,0	100,0	3,2	13,9	82,8	6,5	14,1	79,6	1,0	4,5	94,6	0,0	2,2	97,9	0,0	0,0	100,0
Sep.	1,7	12,8	85,6	5,3	8,3	86,4	11,7	19,7	68,6	32,6	12,7	54,7	0,5	0,5	99,1	3,0	6,9	90,1	1,0	2,4	96,7	7,4	11,5	80,9	12,6	15,9	71,7	5,3	9,7	85,0	1,1	3,3	95,6	1,4	2,0	96,7
Oct.	1,1	12,4	86,6	3,6	13,4	83,0	6,8	14,2	79,0	40,7	15,5	43,9	0,0	5,1	94,9	4,4	10,3	85,5	5,1	13,8	81,1	6,4	21,2	72,5	13,8	17,7	68,6	10,0	12,6	77,6	1,6	6,5	91,9	0,6	11,0	88,5
Nov.	1,1	16,1	82,8	3,3	9,7	87,1	3,2	17,6	79,4	41,4	12,3	46,3	0,5	6,2	93,3	3,3	12,6	84,0	6,2	22,9	71,0	9,6	27,6	62,8	18,9	13,8	67,4	8,2	15,6	76,4	1,7	6,1	92,2	3,3	12,0	84,8
Dec.	2,2	11,3	86,6	3,2	9,4	86,6	1,6	9,4	89,1	35,5	18,1	46,5	0,5	5,5	94,0	2,5	12,9	84,7	12,0	30,4	57,6	8,1	28,8	63,2	10,7	18,1	71,2	6,5	19,0	74,4	1,6	7,0	91,4	3,2	22,0	74,9
Year	2,2	12,4	85,4	5,0	8,3	86,8	9,0	15,8	75,3	24,4	15,7	60,0	0,6	4,6	94,8	3,0	10,2	87,0	4,2	13,5	82,1	6,1	21,6	72,3	11,8	15,2	73,1	6,5	11,3	82,4	1,4	6,7	92,0	1,6	9,2	89,2
No. of years		6			10			10			10			7			14			7			13			10			10			6			5	

5. Atmospheric conditions: it was assumed that T =20 C and there are no wind effects.

6. Pump's characteristics: the main caracteristics of the model, using Freon 113 as working liquid, are listed below.

$A_a = 0.25 m^2$	$V_r = 1.2 \ell$	$m_f = 50$ gr
$(mc_p) = 450 \frac{J}{°C}$	$V_d = 0.3 \ell$	$d_r = 0.05$ m
$d_c = 0.07$ m	$d_p = 0.008$ m	$L_r = 0.5$ m
$L_c = 0.5$ m	$L_b = 0.15$ m	$\dot{m}_{cw} = 0.01$ kg/sec
$T_{w,in} = 25$ °C	$\epsilon_c = 0.88$	$\epsilon_r = 0.91$
η_o: from figure 4.9	$d_b = 0.05$ m	$A_r = 0.1 m^2$

7. Adjustement requirements: The user requires twelve adjustments per year.

F.2. CALCULATION OF THE SYSTEM'S ADJUSTMENTS REQUIREMENTS.

1. Time of adjustments

According to the analysis developed in section 3.4, the time between two consecutive adjustments, according to equation 3.50, must be equal to the required time by the sun to travel an angular distance of

$$\Delta\delta = \frac{4 \cdot 23.44}{n}$$

$$= \frac{4 \cdot 23.44}{12}$$

$$= 7.81^{\circ}$$

We assume that the first adjustment takes place on the winter solstice, ie. on the 21st of June. For this day, which is the 172nd day of the year (table A.1), the solar declination, according to equation A.1, is

$$\delta_1 = 23.44 \cdot \sin\frac{360 \cdot (D-81)}{365}$$

$$= 23.44 \cdot \sin\frac{360 \cdot (172-81)}{365}$$

$$= 23.44^{\circ}$$

The second adjustment must be done on the day when the solar declination is

$$\delta_2 = \delta_1 - \Delta\delta$$

$$= 23.44 - 7.81$$

$$= 15.63^{\circ}$$

The number of that day, calculated from equation A.1 is

$$D = 81 + \frac{\text{arc sin}(\delta/23.44)}{360/365}$$

$$= 81 + \frac{\text{arc sin}(15.63/23.44)}{360/365}$$

$$= 221$$

ie. this is the 9th of Austust.

By repeating the above procedure throughout a year, the dates when the adjustments must be done are calculated and

given in table F.3.

2. Concentrator's tilt adjustments.

The tilt adjustments are calculated from equation 3.52. For example, at the first adjustment the tilt must be

$$\beta_1 = \delta_1 - \frac{\Delta\delta}{2} - \varphi$$
$$= 23.44 - \frac{7.81}{2} - (-26)$$
$$= 45.54^\circ$$

Similarly, at the second adjustment the concentrator's tilt is

$$\beta_2 = 15.63 - \frac{7.81}{2} - (-26)$$
$$= 37.72^\circ$$

The values of the collector's tilt for a year, calculated according to the above procedure are given in table F.3

3. Peak radiation conditions.

First the period between the first and second adjustment is examined.

According to the assumptions made in section 3.4, the maximum possible direct radiation reaches the concentrator during the solar noon of the day when the solar declination, according to equation 3.53, is

$$\delta = \varphi + \beta$$

$$= -26 + 45.54$$

$$= 19.54^{\circ}$$

The number of this day is calculated from equation A.1

$$D = 81 + \frac{\text{arc sin}(\delta/23.44)}{360/365}$$

$$= 81 + \frac{\text{arc sin}(19.54/23.44)}{360/365}$$

$$= 206$$

ie. this is the 25th of July. (table A.1)

For the solar noon of this day the azimuth angle (equation A.4) is

$$\cos\theta_z = \cos(\varphi - \delta)$$

$$= \cos(-26 - 19.54)$$

$$= 0.70$$

For the same day the apparent extraterrestrial solar radiation (A) as well as the extinction coefficient (B) are calculated from table 1.1 by interpolation.

$$A = 1088 \ \frac{W}{m^2}$$

$$B = 0.206$$

The pressure of the location in question relative to a standard atmosphere is given by equation 1.3.

$$\frac{P}{P_o} = \exp(-0.0001184 \cdot Y)$$

$$= \exp(-0.0001184 \cdot 1500)$$

$$= 0.8373$$

Finally, the maximum direct solar radiation (equation 1.2) is

$$I_{D,n} = A \cdot \exp\left(-\frac{P}{P_o} \cdot \frac{B}{\cos\theta_z}\right)$$

$$= 1088 \cdot \exp\left(-0.8373 \cdot \frac{0.206}{0.7}\right)$$

$$= 850.4 \ \frac{W}{m^2}$$

By repeating the above procedure for every period between consecutive adjustments the peak radiation conditions throughout the year were calculated. The results are shown in table F.3.

4. Theoretical analysis for peak radiation conditions

4.1 Thermodynamic analysis

For peak radiation conditions the thermodynamic cycle is shown in figure F.1.a:

Specific volumes for points 1, 3:

$$v_1 = \frac{V_1}{m_f}$$

$$= \frac{1.2 \cdot 10^{-3}}{50 \cdot 10^{-3}}$$

$$= 0.024 \ \frac{m^3}{Kg}$$

$$v_3 = \frac{V_3}{m_f}$$

$$= \frac{1.5 \cdot 10^{-3}}{50 \cdot 10^{-3}}$$

$$= 0.03 \ \frac{m^3}{Kg}$$

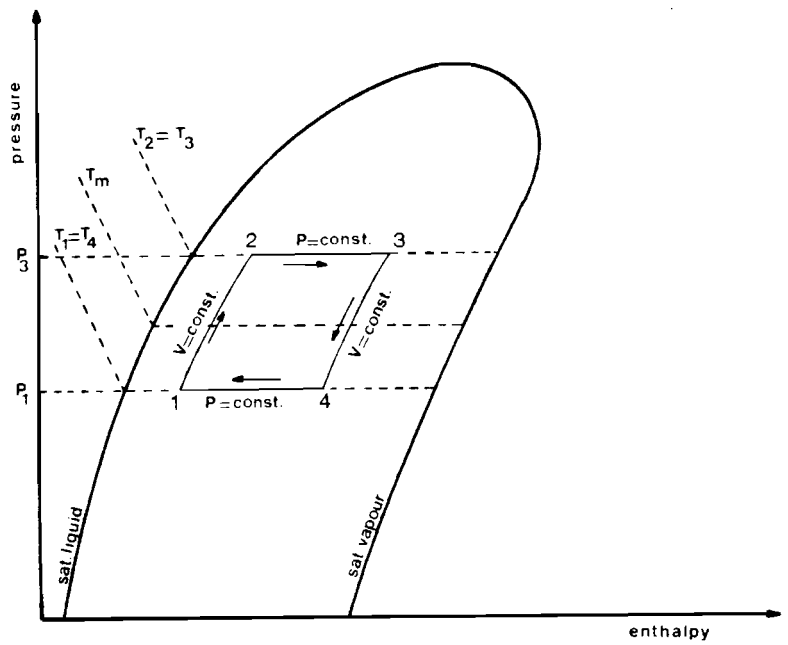

Figure F.1.a Thermodynamic cycle for peak radiation conditions.

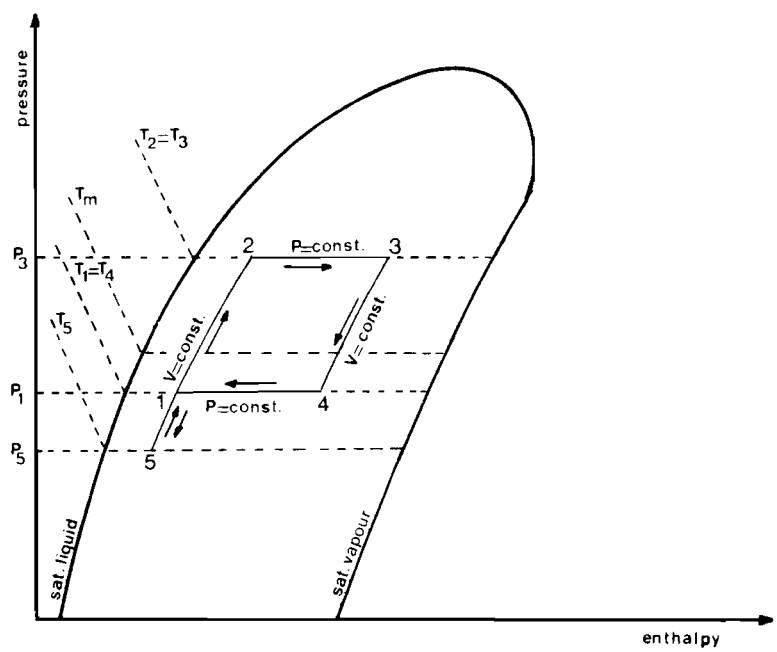

Figure F.1.b Thermodynamic cycle for peak off radiation conditions.

Pressure for points 1, 3:

$$P_1 = P_{at} - H - \Delta P \qquad P_3 = P_{at} + \Delta P$$

$$= 101.4 - 11.9 - 4.8 \qquad = 101.4 + 4.8$$

$$= 84.7 \text{ KPa} \qquad = 106.2 \text{ KPa}$$

Dryness index for points 1, 3:

$$x_1 = \frac{v_1}{v_{g_1}} \qquad x_3 = \frac{v_3}{v_{g_1}}$$

$$= \frac{0.024}{0.164} \qquad = \frac{0.03}{0.13}$$

$$= 0.146 \qquad = 0.231$$

Enthalpy for points 1, 3:

$$h_1 = h_{f_1} + x_1 \cdot (h_{g_1} - h_{f_1})$$

$$= 71.62 + 0.146 \cdot (220.11 - 71.62) = 93.3 \text{ KJ/ Kg}$$

$$h_3 = h_{f_3} + x_3 \cdot (h_{g_3} - h_{f_3})$$

$$= 77.87 + 0.231 \cdot (224.25 - 77.87) = 111.9 \text{ KJ/Kg}$$

Heat added (from equation 3.2):

$$Q_{add} = m[h_3 - h_1 - v_1 \cdot (P_3 - P_1)]$$

$$= \frac{50}{1000}[111.9 - 93.3 - .024 \cdot (106.2 - 84.7)]$$

$$= 904.2 \text{ J}$$

Heat rejected (from equation 3.3):

$$Q_{rej} = -m[h_3 - h_1 - v_3 \cdot (P_3 - P_1)]$$

$$= -\frac{50}{1000}[111.9 - 93.3 - 0.03 \cdot (106.2 - 84.7)]$$

$$= -897.75 \text{ J}$$

Net work (from equation 3.4):

$$W = Q_{add} + Q_{rej}$$

$$= 904.2 - 897.75$$

$$= 6.45 \text{ J}$$

Cycle thermal efficiency (from equation 3.5):

$$\eta_c = \frac{W}{Q_{add}}$$

$$= \frac{6.45}{904.2}$$

$$= 7.13\ 10^{-3}$$

Cycle mean temperature (from equation 3.41):

$$T_m = \frac{T_1 + T_3}{2}$$

$$= \frac{42 + 49}{2}$$

$$= 45.5\ ^{\circ}C$$

4.2 Heat transfer analysis

Losses from the bellows

Convection heat transfer coefficient (from equation 3.30):

$$h_{c,b} = 1.32\left(\frac{T_m - T_a}{L_b}\right)^{1/4}$$

$$= 1.32\left(\frac{45.5-20}{0.15}\right)^{1/4}$$

$$= 4.77 \text{ W/m}^2\ ^{\circ}C$$

Heat losses due to convection (from equation 3.28):

$$Q_{c,b} = A_b \cdot h_{c,b} \cdot (T_m - T_a)$$

$$= 0.025 \cdot 4.77 \cdot (45.5-20)$$

$$= 3.0 \text{ W}$$

Radiation heat transfer coefficient (from equation 3.29):

$$h_{r,b} = F_{b,a} \cdot \sigma \cdot \epsilon_b \frac{T_m^4 - T_a^4}{T_m - T_a}$$

$$= 1 \cdot 5.669 \cdot 10^{-8} \cdot 0.91 \frac{(273+45.5)^4 - (273+20)^4}{45.5-20}$$

$$= 5.8 \text{ W/m}^2\,^{\circ}\text{C}$$

Losses due to radiation (from equation 3.27):

$$Q_{r,b} = A_b \cdot h_{r,b} \cdot (T_m - T_a)$$

$$= 0.025 \cdot 5.8 \cdot (45.5-20)$$

$$= 3.7 \text{ W}$$

Losses from the cooling system.

It is first assumed that the outlet temperature of the cooling water is equal to the inlet temperature. Therefore the mean temperature is 25 C.

For this temperature the properties of water are evaluated:

$\rho = 997$ Kg/m^3 $\qquad$ $c_p = 4174$ J/Kg $^{\circ}$C

$k = 0.6045$ W/m $^{\circ}$C $\qquad$ $\mu = 9.55\ 10^{-4}$ Kg/m sec

$Pr = 6.65$

The Reynolds number (from equation 3.36) is

$$Re = \frac{4 \cdot \dot{m}_{cw}}{n \cdot \pi \cdot \mu \cdot d_p}$$

$$= \frac{4 \cdot 0.01}{4 \cdot \pi \cdot 0.000955 \cdot 0.008}$$

$$= 416.6$$

Heat transfer coefficient (from equation 3.35):

$$h_w = \frac{k \cdot Re \cdot Pr}{4 \cdot L_p} \ln\left[1 - \frac{2.654}{Pr^{0.167} \cdot \left(\frac{Re \cdot Pr \cdot d_p}{L_p}\right)^{0.5}}\right]^{-1}$$

$$= \frac{0.6045 \cdot 416.6 \cdot 6.65}{4 \cdot 0.45} \ln\left[1 - \frac{2.654}{6.65^{0.167} \left(\frac{416.6 \cdot 6.65 \cdot 0.008}{0.45}\right)^{0.5}}\right]^{-1}$$

$$= 300 \text{ W/m}^2\,^{\circ}\text{C}$$

Outlet water temperature (from equation 3.37):

$$n \cdot h_w \cdot A_p \cdot \left(T_m - \frac{T_{w,out} + T_{w,in}}{2}\right) = \dot{m}_{cw} \cdot (c_p)_w \cdot (T_{w,out} - T_{w,in})$$

$$4 \cdot 300 \cdot n \cdot 0.008 \cdot \left(45.5 - \frac{T_{w,out} + 25}{2}\right) = 0.01 \cdot 4174 \cdot (T_{w,out} - 25)$$

$$T_{w,out} = 30.7\,^{\circ}\text{C}$$

which is in very good agreement with the experimentaly observed temperature of approximately 29 $^{\circ}$C.

Thus, we should go back and evaluate properties at the mean temperature of :

$$T_{m,w} = \frac{T_{w,in} + T_{w,out}}{2}$$

$$= \frac{25 + 30.7}{2} = 27.75\,^{\circ}\text{C}$$

By repeating the calculation we finally obtain:

$\rho = 995.3$ Kg/m^3	$c_p = 4174$ J/Kg C
$k = 0.612$ W/m C	$\mu = 0.00088$ Kg/m sec
$Pr = 6.16$	$Re = 452.1$
$h_w = 305.2$ W/m^2 C	$T_{w,out} = 30.8$ C

The itteration makes very little difference in the problem. Therefore the rate of heat transfer by the cooling

water, (from equation 3.37) is:

$$Q_w = m_{cw} \cdot (c_p)_w \cdot (T_{w,out} - T_{w,in})$$

$$= 0.01 \ 4174 \ (30.8 - 25)$$

$$= 242 \ W$$

Losses from the receiver.

In order to simplify the calculations the following assumptions were made:

1. The cover's transmitance is unity.

2. The cover's temperature is constant with time.

Under these assumptions equation 3.42 becomes:

$$(h_{r,c} + h_{c,c}) \cdot (T_c - T_a) = (h_{r,r} + h_{c,r}) \cdot (T_r - T_c) \qquad F.1$$

where the properties of air are evaluated for the mean temperature:

$$T_{m,a} = \frac{T_c + T_a}{2}$$

Equation F.1 can be solved for T_c using an itterative technique. The solution gives:

$$T_c = 33.8 \ ^\circ C$$

Therefore the thermal losses from the receiver are:

Radiation heat transfer coefficient (equation 3.10):

$$h_{r,r} = F_{r-c} \cdot \sigma \cdot \left(\frac{1}{\epsilon_r} + \frac{1}{\epsilon_c} - 1\right)^{-1} \frac{T_m^4 - T_c^4}{T_m - T_c}$$

$$= 1 \cdot 5.669 \cdot 10^{-8} \cdot (0.91^{-1} + 0.88^{-1} - 1)^{-1} \frac{(273+45.5)^4 - (273+33.8)^4}{45.5 - 33.8}$$

$$= 5.54 \ W/m^2 \ ^\circ C$$

Losses due to radiation (equations 3.8):

$$Q_{r,r} = A_r \cdot h_{r,r} \cdot (T_m - T_c)$$

$$= 0.1 \cdot 5.54 \cdot (45.5 - 33.8)$$

$$= 6.4 \text{ W}$$

Convection heat transfer coefficient (equation 3.11):

$$h_{c,r} = \frac{k}{r_c - r_r} 0.55 \cdot [Pr \cdot g \cdot \beta \cdot (r_c - r_r)^3 \frac{T_m - T_c}{\nu^2}]^{1/4}$$

$$= \frac{0.027}{0.035 - 0.025} 0.55 \cdot [0.7 \cdot 9.8 \cdot 0.003 \cdot (0.035 - 0.025)^3 \frac{45.5 - 33.8}{(1.7 \cdot 10^{-5})^2}]^{1/4}$$

$$= 5.0 \text{ W/m}^2 \text{ °C}$$

Lossed due to convection (equation 3.9):

$$Q_{c,r} = A_r \cdot h_{c,r} \cdot (T_m - T_c)$$

$$= 0.1 \cdot 5.0 \cdot (45.5 - 33.8)$$

$$= 5.8 \text{ W}$$

5. Cooling water adjustment requirements.

Let us examine the period between the first and second adjustment. Equation 3.47.a gives the necessary time for the cooling process for peak radiation conditions

$$t_{cool} = \frac{(mc_p) \cdot (T_3 - T_1) + [Q_{rej}]}{[Q_w + Q_l] - Q_{abs,r}}$$

$$= \frac{450 \cdot (49 - 42) + 897.75}{242 + 18.9 - 97.8}$$

$$= 24.8 \text{ sec}$$

By applying the above formula for every period between consecutive adjustments the cooling water requirements for the year were calculated, and are shown in table F.3. To ensure further the trouble free operation of the pump, an adjusted value of the volume of cooling water, as shown in table F.3, will be used in subsequent calculations.

n	D	$\beta(^0)$	$I_{D,n}(W/m^2)$	$Q_{abs,r}(W)$	$t_{cool}(s)$	adj $t_{cool}(s)$
1	172	45.54	850.4	97.8	24.8	25
2	221	37.71	895.4	103	25.6	26
3	244	29.90	950.7	109.3	26.7	27
4	264	22.10	996.2	114.6	27.7	28
5	283	14.28	1038.2	119.4	28.6	29
6	306	6.46	1072	123.3	29.4	30
7	355	6.46	1089	125.2	29.8	30
8	39	14.28	1095.9	125.9	30	30
9	62	22.10	1042.2	119.9	28.7	29
10	81	29.90	998.3	114.8	27.7	28
11	101	37.72	938.7	108	26.5	27
12	123	45.54	877.7	100.9	25.3	26

Table F.3 System's adjustment requirements

F.3 CALCULATION OF THE PUMP'S DAILY CAPACITY FOR THE 15th OF JANUARY.

1. Radiation requirements.

The mean daily hours of sunshine expressed as percentage of the possible hours of sunshine, (see table F.2) is 62%. Therefore, equation 1.2, applicable only for clear days, can no longer be used in order to predict the direct solar radiation. A more suitable method for the prediction of the available solar radiation seems to be the Liu-Jordan method, which is based on average radiation data.

From table F.1 we have:

$$H_T = 24034 \text{ MJ/m}^2 \text{ day}$$

$$H_d = 8561 \text{ MJ/m}^2 \text{ day}$$

Since the radiation data are based on horizontal surfuce, the direct radiation impinging on the collector is

$$I_a = H_D \frac{\cos\theta}{\cos\theta_z} \qquad \text{F.2}$$

For the 15th of January (D=15 from table A.1) the solar declination is given from equation A.1:

$$\delta = 23.44 \sin\frac{360\ (D-\ 81)}{365}$$

$$= 23.44 \cdot \sin\frac{360(15-81)}{365}$$

$$= -21.26$$

The sunset angle is given from equation A.3:

$$\omega_s = \text{arc cos}(-\tan\varphi \cdot \tan\delta\ )$$

$$= \text{arc cos}(-\tan(-26) \cdot \tan(-21.26)$$

$$= 101^0$$

The ratio of the hourly diffuse to the daily diffuse (r_d), and of the hourly total to the daily total (r_T) are given from figures **B.2** and **B.1** respectively. The results are computed in table F.4. The same table gives the mean hourly values of the angle of incidence (θ), (calculated from equation A.5), the vertical solar swing (θ_{xy}), (calculated from equation A.6), the azimuth angle (θ_z) (equation A.4), the collector's optical efficiency (from figure 4.9), the direct radiation impinging on the concentrator (I_a) (calculated from equation F.2), and the heat absorbed by the receiver ($Q_{abs,r}$) (calculated from equation 3.45)

2. Theoretical analysis.

Let us examine for example the case when the absorbed radiation by the receiver is

$$Q_{abs,r} = 67.2\ w$$

Hours from s.n.	0.5	1.5	2.5	3.5
r_T	0.130	0.118	0.102	0.077
H_T (KJ/hr/m^2)	3125	2832	2452	1851
r_d	0.118	0.111	0.098	0.080
H_d (KJ/hr/m^2)	1010	950	839	684
H_D (KJ/hr/m^2)	2115	1882	1613	1167
θ (^{0})	7.24	21.14	35.11	49.01
θ_{xy} (^{0})	1.89	3.31	6.59	11.15
η_o	0.456	0.453	0.447	0.40
$\cos\theta_z$	0.989	0.933	0.823	0.669
I_a (W)	147.3	130.7	111.3	79.5
$Q_{abs,r}$ (W)	67.2	59.2	49.8	31.8

Table F.4 Radiation absorbed by the receiver

The thermodynamic cycle is shown in figure F.1.b, where the temperature T_5 is unknown. However it can be caclulated by solving equation 3.47.a using an itterative technique as shown in table F.5.

T_5	Q_{rej}	$(mc_p)\cdot\Delta T$	Q_w	Q_l	t_{cool}
39	1090	4500	224	17.4	32.09
40	1020	4050	230	17.8	28.07
39.5	1055	4275	226	17.6	30.04

Table F.5 Evaluation of the temperature T_5

After the temperature T_5 and the time of the cooling process have been established, the pump's performance was evaluated as follows:

Time of the heating process (from equation 3.47.a)

$$t_{heat} = \frac{(mc_p)\cdot\Delta T + Q_{add}}{Q_{abs,r} + Q_l}$$

$$= \frac{4275 + 1061.5}{67.2 - 17.6}$$

$$= 107.6 \text{ sec}$$

Cycle's time (from equation 3.48)

$$t_c = t_{heat} + t_{cool}$$

$$= 107.6 + 30$$

$$= 137.6 \text{ sec}$$

Pumped water flow rate (from equation 3.49)

$$\dot{V}_d = \frac{V_d}{t_c}$$

$$= \frac{300}{137.6}$$

$$= 2.18 \text{ ml/sec}$$

Pump's efficiency (from equation 3.50)

$$\eta_p = \frac{\rho\cdot g\cdot H\cdot V_d}{I_a}$$

$$= \frac{1000\ \ 9.8\ \ 1.2\ \ 2.18\ \ 10^{-3}}{0.1\ \ 147.3}$$

$$= 1.74\ \ 10^{-4}$$

By repeating the above procedure for different values of the absorbed radiation, the results as computed in table F.6

are obtained.

Hours from s.n.		0.5	1.5	2.5	3.5
I_a	(W)	147.3	130.7	111.3	79.5
$Q_{abs,r}$	(W)	67.2	59.2	49.8	31.8
$\dot{V}_d$	(ml/sec)	2.18	1.84	1.42	0.56
η_p		1.74	1.66	1.50	0.83

Table F.6 Pump's performance for the 15th of January

3. Pump's daily capacity.

Using the values for the pumped water flow rate from table F.6, the following table F.7 that gives the pump's daily capacity is obtained. A graphical represantation of this table is shown in figure 4.28.

Solar time	Pumped water (lt)
9 am	2.02
10	7.13
11	13.75
12	21.60
1 pm	27.38
2	34.0
3	39.11
4	41.13

Table F.7 Pump's daily capacity.

F.4 CALCULATION OF THE PUMP'S DAILY CAPACITY FOR THE 15th OF JUNE

The procedure to calculate the pump's daily capacity for the 15th of June is identical to the one developed to predict the pump's performance for the 15th of January, and explained in the previous sections. Therefore no analytical calculations will be presented. All the results are tabulated in table F.8

$\delta = 23.3^0$

$\omega_s = 77.9^0$

$H_T = 14124$ MJ/day/m^2

$H_d = 2868$ MJ/day/m

Hours from s.n.	0.5	1.5	2.5	3.5
r_T	0.158	0.140	0.109	0.069
H_T (KJ/hr/m^2)	2232	1977	1540	975
r_d	0.147	0.134	0.110	0.076
H_d (KJ/hr/m^2)	422	384	315	218
H_D (KJ/hr/m^2)	1810	1593	1225	757
θ (^{0})	7.93	21.26	35.02	48.76
θ_{xy} (^{0})	3.94	5.45	8.96	15.74
η_o	0.452	0.449	0.442	0.272
$\cos\theta_z$	0.645	0.589	0.482	0.329
$Q_{abs,r}$ (W)	87.2	78.6	63.6	28.6
V_d (ml/sec)	3.69	3.31	2.65	1.00
η_p	2.25	2.22	2.16	4.11

Table F.8 Pump's performance for the 15th of June.

APPENDIX G

RESULTS OF THE PRELIMINARY TESTS

		Q_{in}=310W		Q_{in}=365W		Q_{in}=420W		Q_{in}=485W	
m_f(gr)	$\dot{V}_d$(ml)	λ	$\dot{V}_d(\frac{ml}{s})$	λ	$\dot{V}_d$	λ	$\dot{V}_d$	λ	$\dot{V}_d$
35	400	0.44	4.08	0.48	4.35	0.55	4.71	0.68	5.56
	350	0.46	4.00	0.52	4.27	0.59	4.55	0.72	5.22
	300	0.49	3.83	0.58	4.17	0.65	4.48	0.77	4.84
	250	0.54	3.70	0.64	4.03	0.73	4.17	0.88	4.39
50	400	0.42	4.21	0.45	4.44	0.52	4.88	0.63	5.71
	350	0.44	4.08	0.49	4.38	0.55	4.67	0.66	5.38
	300	0.48	3.92	0.53	4.29	0.59	4.55	0.70	5.00
	250	0.53	3.79	0.58	4.17	0.66	4.31	0.80	4.55
100	400	0.47	3.88	0.54	4.21	0.64	4.60	0.75	5.33
	350	0.49	3.68	0.57	4.12	0.68	4.38	0.80	5.00
	300	0.52	3.57	0.63	4.00	0.74	4.29	0.87	4.62
	250	0.57	3.48	0.68	3.85	0.81	3.97	0.96	4.17
200	400	0.62	3.74	0.70	4.00	0.84	4.21	1.00	4.71
	350	0.65	3.57	0.74	3.89	0.90	4.12		
	300	0.69	3.44	0.80	3.75	0.97	4.00		
	250	0.74	3.31	0.88	3.57				

Table G.1 Experimental values of the water volume flow rate ($\dot{V}_d$) and the utilization ratio (λ) versus mass of working fluid (m_f) (Freon 113 - Water head 0.5m)

		Q_{in}=260W		Q_{in}=310W		Q_{in}=365W	
m_f(gr)	V_d(ml)	λ	$\dot{V}_d(\frac{ml}{s})$	λ	$\dot{V}_d$	λ	$\dot{V}_d$
35	400	0.55	2.27	0.60	2.85	0.67	3.57
	350	0.58	2.25	0.64	2.79	0.72	3.48
	300	0.64	2.22	0.72	2.71	0.81	3.35
	250	0.72	2.18	0.80	2.58	0.92	3.02
50	400	0.53	2.35	0.58	2.93	0.65	3.68
	350	0.56	2.33	0.61	2.88	0.69	3.64
	300	0.60	2.31	0.67	2.81	0.77	3.53
	250	0.68	2.27	0.75	2.67	0.88	3.13
100	400	0.61	2.22	0.67	2.77	0.76	3.48
	350	0.64	2.19	0.71	2.71	0.81	3.33
	300	0.72	2.14	0.78	2.58	0.90	3.16
	250	0.80	2.08	0.88	2.46		
200	400	0.78	2.05	0.86	2.62	0.98	3.33
	350	0.83	2.03	0.91	2.57		
	300	0.90	2.00	0.98	2.44		
	250	1.00	1.92				

Table 6.2 Experimental values of the water volume flow rate ($\dot{V}_d$) and the utilization ratio (λ) versus mass of working fluid (m_f) (Freon 113 - Water head 1.2m)

		Q_{in}=365W		Q_{in}=420W		Q_{in}=485W		Q_{in}=555W	
m_f(gr)	V_d(ml)	λ	$\dot{V}_d(\frac{ml}{s})$	λ	$\dot{V}_d$	λ	$\dot{V}_d$	λ	$\dot{V}_d$
35	400	0.27	3.70	0.31	4.44	0.38	5.33	0.46	5.97
	350	0.30	3.57	0.34	4.27	0.40	5.00	0.49	5.65
	300	0.34	3.41	0.39	4.00	0.44	4.62	0.54	5.17
	250	0.39	3.21	0.51	4.03	0.62	4.55		
50	400	0.26	4.00	0.30	4.71	0.37	5.61	0.43	6.30
	350	0.29	3.89	0.33	4.55	0.38	5.38	0.46	5.93
	300	0.33	3.66	0.37	4.29	0.42	5.00	0.50	5.45
	250	0.38	3.33	0.42	3.85	0.48	4.55	0.58	4.81
100	400	0.29	3.54	0.33	4.35	0.40	5.13	0.49	5.71
	350	0.31	3.43	0.36	4.12	0.43	4.79	0.53	5.30
	300	0.35	3.33	0.40	3.85	0.47	4.41	0.58	4.84
	250	0.40	3.01	0.46	3.42	0.54	3.85	0.66	4.17
200	400	0.31	3.39	0.36	4.00	0.43	4.71	0.51	5.33
	350	0.34	3.24	0.39	3.80	0.46	4.38	0.56	4.93
	300	0.38	3.06	0.43	3.53	0.51	4.00	0.62	4.41
	250	0.44	2.84	0.50	3.13	0.58	3.57	0.70	3.85

Table G.3 Experimental values of the water volume flow rate ($\dot{V}_d$) and the utilization ratio (λ) versus mass of working fluid (m_f) (Methanol - Water head 0.5m)

		Q_{in}=365W		Q_{in}=420W		Q_{in}=485W		Q_{in}=555W	
m_f(gr)	V_d(ml)	λ	$\dot{V}_d(\frac{ml}{s})$	λ	$\dot{V}_d$	λ	$\dot{V}_d$	λ	$\dot{V}_d$
35	400	0.37	2.67	0.45	3.41	0.52	4.12	0.61	5.04
	350	0.40	2.46	0.48	3.08	0.57	3.98	0.68	4.85
	300	0.44	2.32	0.54	2.82	0.65	3.77	0.75	4.37
	250	0.51	2.07	0.64	2.44	0.74	3.36	0.88	3.92
50	400	0.36	2.96	0.43	3.64	0.50	4.44	0.58	5.33
	350	0.39	2.76	0.46	3.33	0.54	4.27	0.63	5.00
	300	0.43	2.50	0.52	3.00	0.61	4.00	0.70	4.62
	250	0.50	2.17	0.61	2.63	0.70	3.57	0.81	4.17
100	400	0.39	2.42	0.47	3.14	0.55	3.87	0.65	4.88
	350	0.42	2.31	0.50	2.87	0.61	3.74	0.71	4.61
	300	0.46	2.17	0.57	2.55	0.69	3.51	0.80	4.17
	250	0.53	1.94	0.67	2.29	0.79	3.18	0.96	3.68
200	400	0.44	2.35	0.51	2.90	0.61	3.64	0.73	4.46
	350	0.47	2.19	0.56	2.65	0.68	3.50	0.80	4.12
	300	0.52	2.02	0.63	2.40	0.77	3.26	0.91	3.75
	250	0.58	1.79	0.74	2.12	0.90	2.94		

Table G.4 Experimental values of the water volume flow rate ($\dot{V}_d$) and the utilization ratio (λ) versus mass of working fluid (m_f) (Methanol - Water head 1.2m)

		Q_{in}=420W		Q_{in}=485W		Q_{in}=555W		Q_{in}=630W	
m_f(gr)	V_d(ml)	λ	$\dot{V}_d(\frac{ml}{s})$	λ	$\dot{V}_d$	λ	$\dot{V}_d$	λ	$\dot{V}_d$
35	400	0.19	4.55	0.20	5.33	0.21	6.25	0.24	6.75
	350	0.21	4.22	0.22	5.00	0.24	5.90	0.26	6.14
	300	0.24	3.85	0.25	4.62	0.27	5.32	0.29	5.55
	250	0.28	3.38	0.29	3.97	0.30	4.58	0.32	4.81
50	400	0.18	4.60	0.19	5.48	0.20	6.35	0.23	7.02
	350	0.19	4.38	0.21	5.22	0.20	6.03	0.25	6.36
	300	0.22	4.00	0.24	4.76	0.25	5.45	0.28	5.77
	250	0.26	3.47	0.28	4.17	0.30	4.72	0.32	5.00
100	400	0.19	4.44	0.20	5.25	0.22	6.08	0.24	6.57
	350	0.21	4.12	0.22	4.91	0.24	5.78	0.26	5.93
	300	0.24	3.75	0.26	4.53	0.27	5.21	0.29	5.38
	250	0.28	3.33	0.29	3.85	0.31	4.45	0.33	4.66
200	400	0.20	4.21	0.21	5.00	0.24	5.88	0.25	6.15
	350	0.22	3.89	0.24	4.67	0.26	5.38	0.27	5.65
	300	0.25	3.53	0.27	4.11	0.29	4.84	0.31	5.08
	250	0.29	3.13	0.30	3.57	0.34	4.17	0.36	4.31

Table G.1 Experimental values of the water volume flow rate ($\dot{V}_d$) and the utilization ratio (λ) versus mass of working fluid (m_f) (**Cyclohexane** – Water head 0.5m)

		Q_{in}=420W		Q_{in}=485W		Q_{in}=555W		Q_{in}=630W	
m_f(gr)	V_d(ml)	λ	$\dot{V}_d(\frac{ml}{s})$	λ	$\dot{V}_d$	λ	$\dot{V}_d$	λ	$\dot{V}_d$
35	400	0.25	3.81	0.27	4.21	0.29	5.00	0.31	5.97
	350	0.28	3.61	0.30	4.02	0.31	4.67	0.33	5.56
	300	0.32	3.26	0.34	3.66	0.36	4.26	0.38	4.97
	250	0.38	2.78	0.40	3.25	0.42	3.76	0.45	4.31
50	400	0.24	3.92	0.26	4.25	0.28	5.26	0.30	6.15
	350	0.27	3.68	0.29	4.12	0.30	4.86	0.33	5.83
	300	0.30	3.33	0.33	3.75	0.35	4.48	0.38	5.28
	250	0.36	2.87	0.38	3.33	0.40	3.85	0.44	4.55
100	400	0.26	3.74	0.28	4.12	0.30	4.88	0.32	5.80
	350	0.29	3.50	0.31	3.93	0.32	4.55	0.34	5.38
	300	0.33	3.16	0.35	3.57	0.37	4.05	0.40	4.84
	250	0.39	2.72	0.41	3.16	0.44	3.52	0.46	4.17
200	400	0.26	3.64	0.28	3.92	0.30	4.76	0.33	5.72
	350	0.29	3.09	0.32	3.77	0.34	4.43	0.36	5.27
	300	0.33	3.09	0.36	3.49	0.39	3.92	0.41	4.61
	250	0.40	2.66	0.42	3.08	0.46	3.41	0.48	4.06

Table G.1 Experimental values of the water volume flow rate ($\dot{V}_d$) and the utilization ratio (λ) versus mass of working fluid (m_f) (Cyclohexane - Water head 1.2m)

APPENDIX H

COLLECTOR'S OPTICAL EFFICIENCY

H.1. Measurement of radiation intensity.

The measurement of the radiation intensity incidence on the reflector was done in the following manner.
The radiation intensity for normal incidence was measured at 54 positions at the aperture of the concentrator as shown in figure H.1.

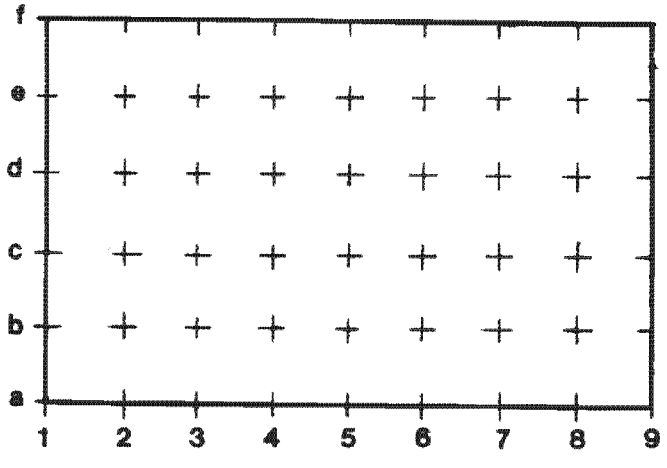

Figure H.1 Measurement of radiation at the collector's aperture

Table H.1 shows the output values of the solarimeter. The mean radiation intensity was approximated as the average value of the intensities at the various positions:

mean irradiation =7.72 mV

	a	b	c	d	e	f
1	1.62	1.69	1.78	1.78	1.89	1.71
2	2.77	3.05	3.21	3.13	3.03	2.72
3	4.32	5.04	5.59	6.16	6.06	5.09
4	6.43	8.27	9.27	10.36	10.25	8.58
5	8.88	11.4	12.8	14.38	13.35	11.65
6	9.41	10.86	12.87	14.46	13.24	12.07
7	8.13	9.31	10.72	11.78	11.02	10.16
8	5.25	5.32	5.91	6.13	5.14	6.04
9	3.04	3.08	2.93	2.98	2.86	3.02

Table H.1 Values of radiation intensity at the collector's aperture

The solarimeter conversion factor is specified by the manufacturer

$$1 \text{ KW/m}^2 = 11.8 \text{ mV}$$

Thus the radiation intensity was calculated as:

$$I_n = 654.2 \text{ W/m}^2$$

H.2. Receiver's heat capacity

The procedure to evaluate the heat capacity of the receiver and cooling system has already been described in section 4.2. The energy balance equation for the system (receiver and cooling system)+(hot water) gives

$$\Delta U = 0$$

$$(mc_p)\cdot\Delta T + (mc_p)_w\cdot\Delta T_w = 0 \qquad \text{H.1}$$

$$(mc_p) = (mc_p)_w \frac{\Delta T_w}{\Delta T}$$

The values of the variables involved in the above equation were evaluated to be:

$$(mc_p)_w = 2097 \text{ J/°C} \qquad \Delta T_w = 1.76 \text{ °C}$$

$$\Delta T = 8.24 \text{ °C}$$

Therefore, according to equation H.1, the heat capacity of the receiver and cooling system is

$$(mc_p) \simeq 450 \text{ J/°C}$$

H.3. Optical efficiency

The procedure to evaluate the collector's optical efficiency was described in section 4.2. Assuming that the heat losses are negligible, the energy absorbed by the receiver is utilized to increase the system's internal energy.

$$Q_{abs,r} = (mc_p)\cdot\Delta T + (mc_p)_w\cdot\Delta T_w$$
$$= [(mc_p) + (mc_p)_w]\cdot\Delta T \qquad \text{H.2}$$

Therefore the optical efficiency is

$$\eta_o = \frac{[(mc_p) + (mc_p)_w]\cdot\Delta T}{t\cdot A_a\cdot I_{D,n}\cdot\cos\theta} \qquad \text{H.3}$$

The results of the tests are given in table H.2.

θ_{xy} (°)	T (°C)	t (s)	η_o
0	2.83	60	0.46
5	2.76	60	0.45
10	2.67	60	0.44
15	1.67	60	0.28
20	1.10	60	0.19
30	0.72	90	0.09
40	0.21	90	0.03

Table H.2 Collector's optical efficiency.

APPENDIX I

RESULTS OF THE FINAL TESTS

		Q_{in}=120W		Q_{in}=105W		Q_{in}=85W		Q_{in}=70W	
H (m)	λ	$\dot{V}_d$ (ml/s)	$\eta_{th} \cdot 10^4$	$\dot{V}_d$	η_{th}	$\dot{V}_d$	η_{th}	$\dot{V}_d$	η_{th}
0	0.70	2.07		1.66		1.22		0.69	
	0.63	2.14		1.74		1.25		0.70	
	0.57	2.22		1.82		1.30		0.71	
	0.50	2.34		1.86		1.35		0.73	
	0.43	2.46		1.96		1.42		0.77	
1.75	0.70	2.00	2.86	1.64	2.68	1.20	2.42	0.68	1.67
	0.63	2.09	2.99	1.71	2.79	1.21	2.44	0.69	1.69
	0.57	2.16	3.09	1.77	2.89	1.26	2.54	0.70	1.72
	0.50	2.27	3.24	1.83	2.99	1.32	2.66	0.72	1.76
	0.43	2.40	3.43	1.90	3.10	1.41	2.84	0.75	1.83
2.75	0.70	1.94	4.36	1.58	4.06	1.17	3.71	0.67	2.58
	0.63	2.02	4.53	1.67	4.29	1.20	3.80	0.68	2.62
	0.57	2.08	4.67	1.71	4.39	1.22	3.87	0.69	2.66
	0.50	2.19	4.92	1.77	4.54	1.27	4.03	0.71	2.73
	0.43	2.31	5.19	1.85	4.75	1.39	4.41	0.73	2.81
3.45	0.70	1.77	4.99	1.42	4.57	1.09	4.33	0.66	3.19
	0.63	1.86	5.24	1.54	4.96	1.11	4.42	0.67	3.24
	0.57	1.94	5.47	1.60	5.15	1.15	4.57	0.68	3.28
	0.50					1.22	4.85	0.69	3.33
4.15	0.70	1.56	5.29	1.33	5.15	1.05	5.02	0.64	3.72
	0.63	1.62	5.49	1.38	5.35	1.09	5.21	0.65	3.78
	0.57	*	*	*	*	1.13	5.41	0.66	3.83

* see extension table I.2

Table I.1 $\dot{V}_d$ -H diagram for Methanol

Q_{in}(W)	λ	H_{max}(m)	$\dot{V}_d$ (ml/s)	$\eta_{th} 10^4$
120	0.43	2.80	2.28	5.21
	0.50	3.20	2.12	5.54
	0.57	3.70	1.94	5.86
	0.63	4.30	1.54	5.40
	0.70	4.70	1.45	5.56
105	0.43	3.0	1.78	4.36
	0.50	3.40	1.66	4.61
	0.57	3.90	1.52	4.84
	0.63	4.40	1.26	4.53
	0.70	4.80	1.22	4.78
85	0.43	3.20	1.29	3.37
	0.50	3.60	1.17	3.44
	0.57	4.10	1.05	3.52
	0.63	4.60	1.03	3.87
	0.70	5.0	0.95	3.88
70	0.43	3.40	0.70	1.94
	0.50	3.80	0.67	2.08
	0.57	4.30	0.64	2.25
	0.63	4.75	0.61	2.37
	0.70	5.20	0.58	2.46

Table I.2 Extension of table I.1

		Q_{in}=120W		Q_{in}=105W		Q_{in}=85W		Q_{in}=70W	
H(m)	λ	$\dot{v}_d$ (ml/s)	$\eta_{th} \cdot 10^4$	$\dot{v}_d$	η_{th}	$\dot{v}_d$	η_{th}	$\dot{v}_d$	η_{th}
0	1.0	2.46		3.13		3.90		4.41	
	0.9	2.65		3.24		4.10		4.76	
	0.8	2.86		3.55		4.54		5.30	
	0.7	3.02		3.78		4.87		5.83	
0.5	1.0	2.34	1.64	3.00	1.73	3.75	1.75	4.29	1.75
	0.9	2.53	1.77	3.16	1.82	4.01	1.87	4.70	1.92
	0.8	2.79	1.95	3.47	2.00	4.46	2.08	5.24	2.14
	0.7	2.93	2.05	3.71	2.14	4.76	2.22	5.76	2.35
1.0	1.0	2.21	3.10	2.86	3.30	3.53	3.29	4.16	3.40
	0.9	2.44	3.42	3.06	3.53	3.92	3.66	4.60	3.76
	0.8	2.68	3.75	3.38	3.90	4.32	4.03		
	0.7	2.85	3.99						
1.5	1.0	2.07	4.35	2.70	4.67	3.36	4.70	*	*
	0.9	2.32	4.87	2.91	5.03	*	*	*	*

* see extension table I.4

Table I.3 $\dot{v}_d$-H diagram for Freon 113 (experimental values)

Q_{in}(W)	λ	H_{max}(m)	$\dot{v}_d$ (ml/s)	$\eta_{th} \cdot 10^4$
120	0.7	0.7	3.21	5.62
	0.8	0.9	3.79	5.16
	0.9	1.1	4.02	4.48
	1.0	1.3	4.14	3.90
105	0.7	0.8	3.40	4.55
	0.8	1.1	4.36	4.25
	0.9	1.3	4.57	3.77
	1.0	1.5	4.70	3.36
85	0.7	0.9	3.74	3.60
	0.8	1.2	4.54	3.28
	0.9	1.5	5.03	2.91
	1.0	1.7	5.10	2.60
70	0.7	1.1	3.99	2.85
	0.8	1.3	4.55	2.50
	0.9	1.6	5.04	2.25
	1.0	1.8	4.79	1.90

Table I.4 Extension of table I.3